Physics Opportunities at an Electron-Ion Collider

Nuclear Imaging at the Electron-Ion Collider

Wenbin Zhao

Lawrence Berkeley National Laboratory

University of California, Berkeley

27. February, 2025

Collaborators: **Heikki Mäntysaari, Farid Salazar, Björn Schenke, and Chun Shen**

Miami, Florida International University, Modesto Maidique Campus

Small x Diffractive vector meson production in DIS

High energy factorization:

1. $\gamma^* \to q\bar{q}$ splitting,
   wave function $\Psi^{\gamma}(r, Q^2, z)$
2. $q\bar{q}$ dipole scatters elastically N(r, x, b)
3. $q\bar{q} \to J/\Psi$, wave function $\Psi^{V}(r, Q^2, z)$

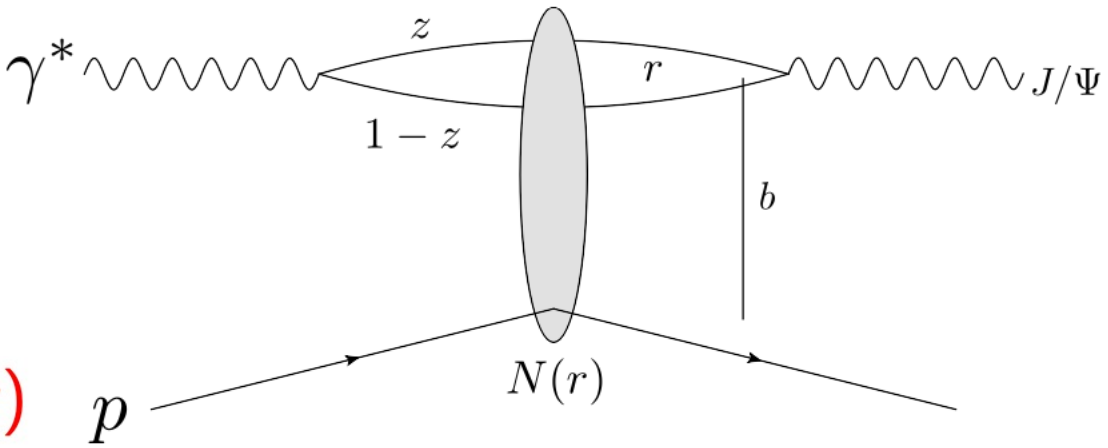

Diffractive scattering amplitude

$$\mathcal{A}^{\gamma^* p \to Vp} \sim \int \mathrm{d}^2 b \mathrm{d}z \mathrm{d}^2 r \Psi^{\gamma *} \Psi^{V}(r, z, Q^2) \mathbf{e}^{-\mathbf{i}\mathbf{b}\cdot\mathbf{\Delta}} N(r, x, b)$$

Impact parameter, b, is the Fourier conjugate of the momentum transfer, $\Delta \approx \sqrt{-t}$

N(r, x, b) dipole-target scattering amplitude.

Miettinen, Pumplin, PRD 18, 1978; Caldwell, Kowalski, 0909.1254; Mäntysaari, Schenke, 1603.04349; Mäntysaari, 2001.10705

Small x Dipole-target scattering amplitude (CGC)

- The dipole amplitude N can be calculated from Wilson line V(x)

$$N\left(\mathbf{b}=\frac{\mathbf{x}+\mathbf{y}}{2},\mathbf{r}=\mathbf{x}-\mathbf{y},x_{\mathbb{P}}\right)=1-\frac{1}{N_c}\,\mathrm{Tr}\,\left(V(\mathbf{x})V^{\dagger}(\mathbf{y})\right), \quad V(\mathbf{x})=P\exp\left(-ig\int dx^{-}\frac{\rho(x^{-},\mathbf{x})}{\nabla^2+m^2}\right)$$

- Using MV model for Gaussian distribution of color charge ρ:

$$\langle\rho^a(\mathbf{b}_\perp)\rho^b(\mathbf{x}_\perp)\rangle = g^2\mu^2(x,\mathbf{b}_\perp)\delta^{ab}\delta^{(2)}(\mathbf{b}_\perp-\mathbf{x}_\perp)$$

Q_s: saturation scale, Q_s is determined from IP-Sat parametrization, $Q_s/g^2\mu$ is a free parameter,.

- Or, equivalently, factorize $\mu(x,\mathbf{b}_\perp)\sim T(\mathbf{b}_\perp)\mu(x)$

N(r, x, b) accesses to the spatial structure of the target ($T_{p/A}$).

- **Diffractive scattering amplitude is roughly proportional to Fourier transform of the spatial structure function of target ($T_{p/A}$).**

Schenke , etc.al. PhysRevLett.108.252301 , PhysRevC.86.034908, Mäntysaari, Schenke, 1603.04349;

Coherent and incoherent processes

- **Coherent** $\sigma_{\text{coherent}} \sim |\langle \mathcal{A} \rangle_\Omega|^2$

Target stays intact, (Iinitial state> = Ifinal state>)
Probes the average shape of the target.

- **Incoherent** $\sigma_{\text{incoherent}} \sim \langle |\mathcal{A}|^2 \rangle_\Omega - |\langle \mathcal{A} \rangle_\Omega|^2$

Target breaks apart, (|initial state> ≠ |final state>)

Probes the variance of event-by-event initial state fluctuations in target structure.

- Theoretically: no net color transfer.
- Experimental signature: rapidity gap.

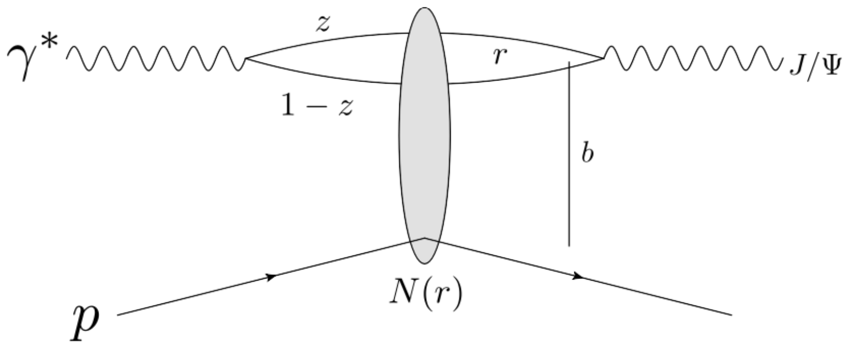

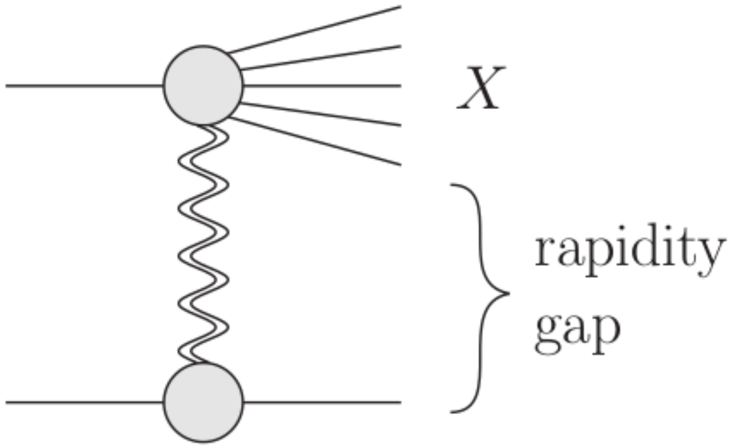

Miettinen, Pumplin, PRD 18, 1978; Caldwell, Kowalski, 0909.1254; Mäntysaari, Schenke, 1603.04349; Mäntysaari, 2001.10705

Proton geometry fluctuations

- Proton's event-by-event fluctuating density profile:

$$T_p(\mathbf{b}_\perp) = \frac{1}{N_q}\sum_{i=1}^{N_q} p_i T_q(\mathbf{b}_\perp - \mathbf{b}_{\perp,i}), \quad P(\ln p_i) = \frac{1}{\sqrt{2\pi}\sigma}\exp\left[-\frac{\ln^2 p_i}{2\sigma^2}\right].$$

- The density profile of each spot is:

$$T_q(\vec{b}) = \frac{1}{2\pi B_q} e^{-b^2/(2B_q)}$$

- The spot positions $\overrightarrow{b_i}$ are sampled from:

$$P(b_i) = \frac{1}{2\pi B_{qc}} e^{-b_i^2/(2B_{qc})}$$

Schenke , etc.al. PhysRevLett.108.252301 ,
PhysRevC.86.034908, Mäntysaari, Schenke, 1603.04349;

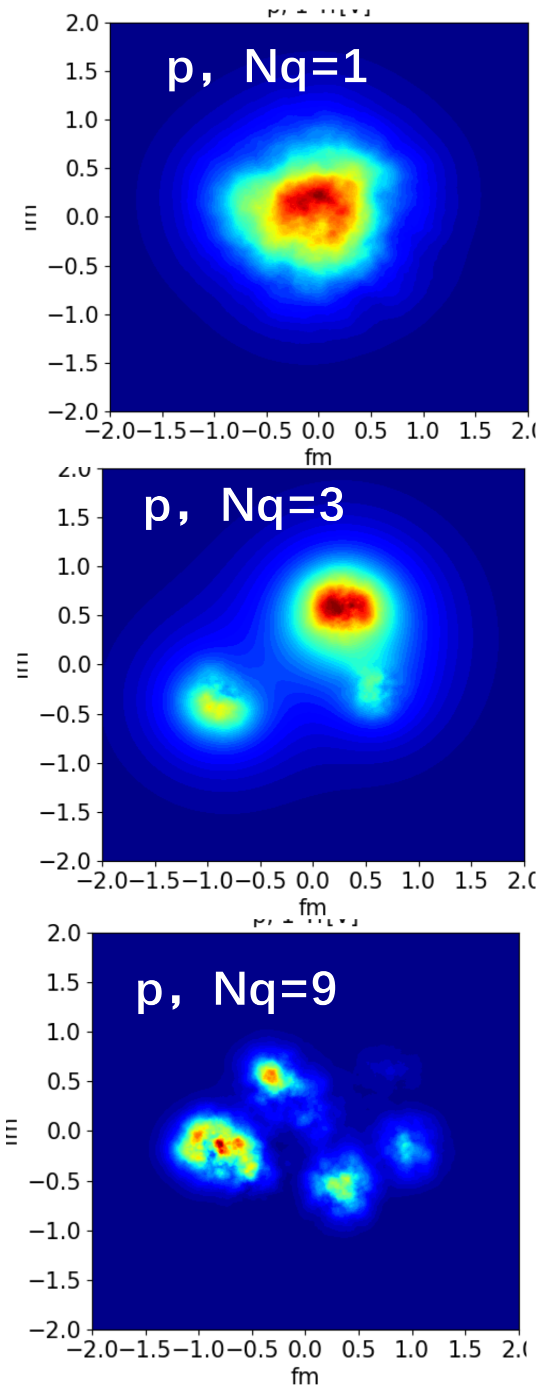

Model parameters and the Exp. Data ($\gamma^* + p \rightarrow J/\psi + p^*$)

Parameterize proton shape (T_p)

- Number of hot spots N_q
- Proton size B_{qc}
- Hot spot size B_q
- Hot spot density fluctuations σ
- Min. distance between hot spots $d_{q,min}$
- Overall color charge density: $Qs(x)/g^2\mu$
- Infrared regulator m

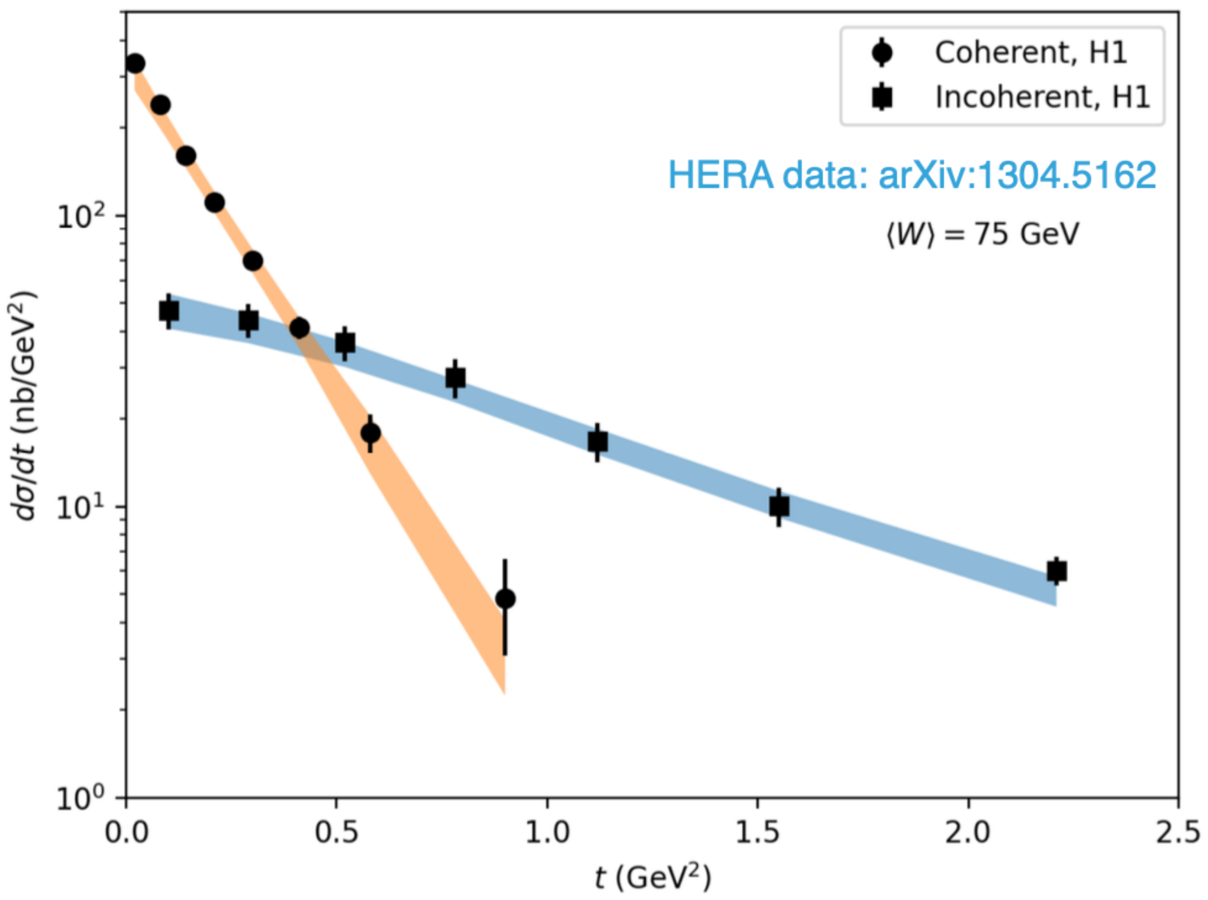

- 7D parameter space; generated 1000 training points for the model emulator

H.Mantysaari, B.Schenke, C. Shen and W. Zhao, Phys. Lett. B 833 (2022), 137348.

Posterior Distribution

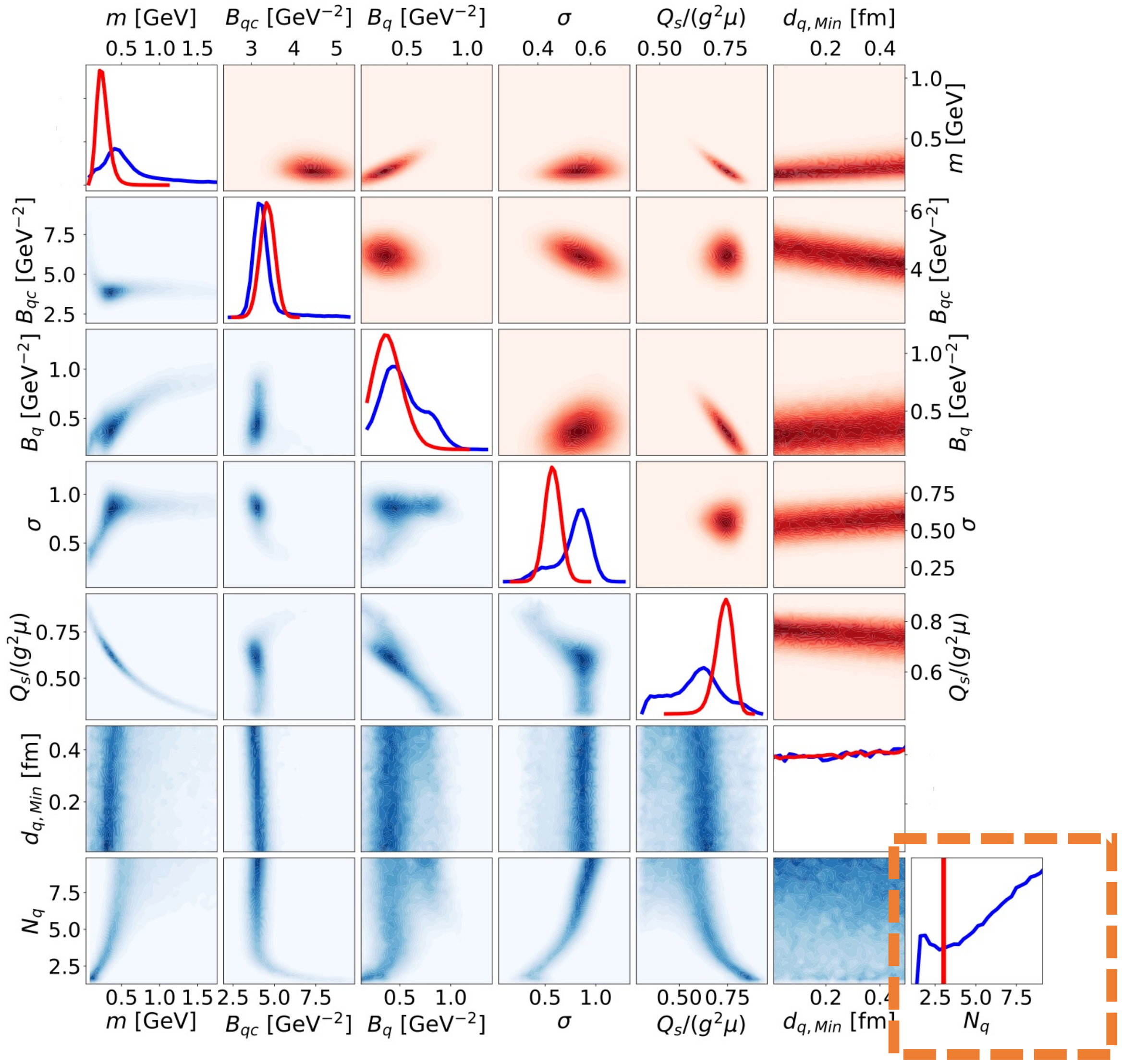

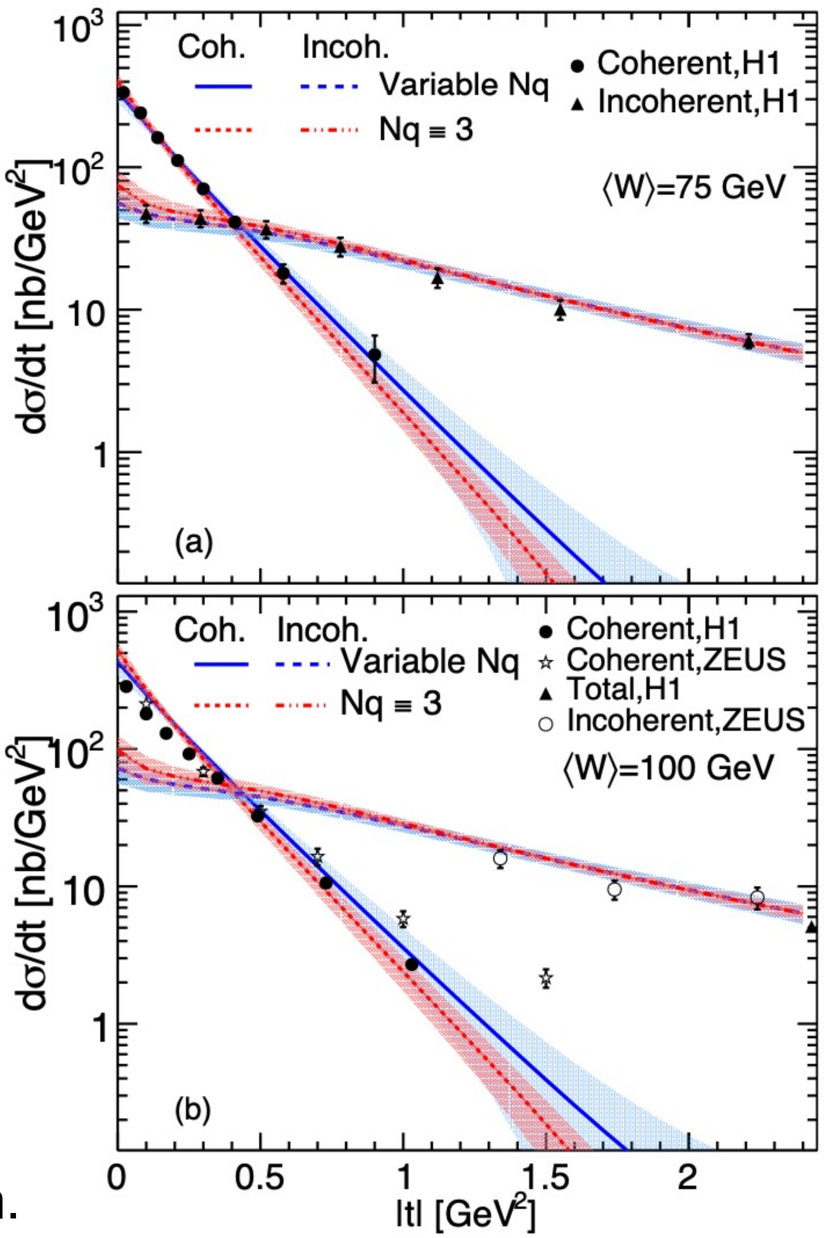

- The 2D RMS proton radius $R_{rms} = \sqrt{2(B_{qc} + B_q)} \sim$ 0.6 fm.

H.Mantysaari, B.Schenke, C. Shen and W. Zhao, Phys. Lett. B 833 (2022), 137348.

Probing protons at different resolutions

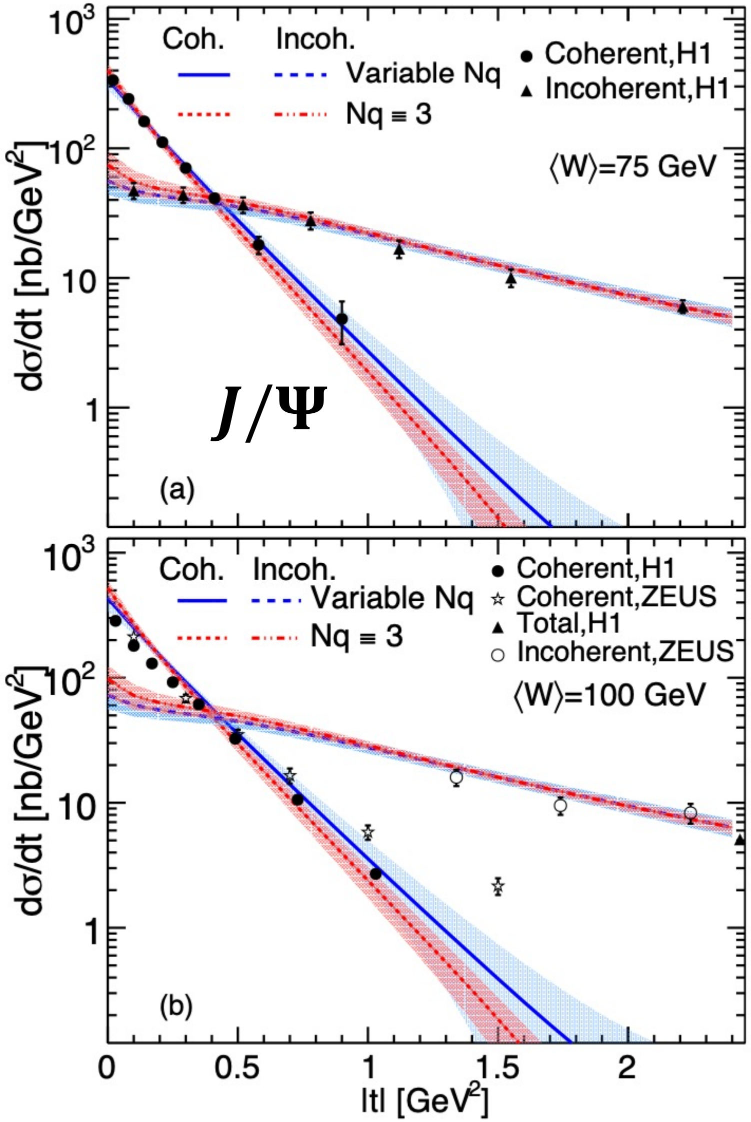

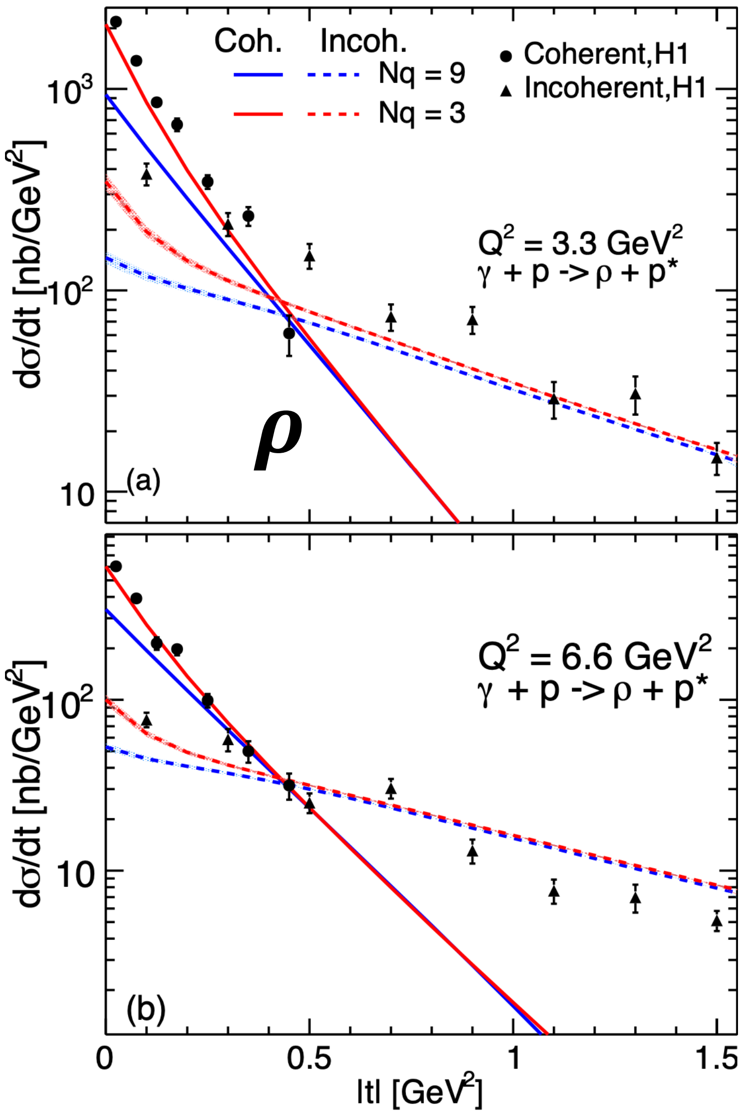

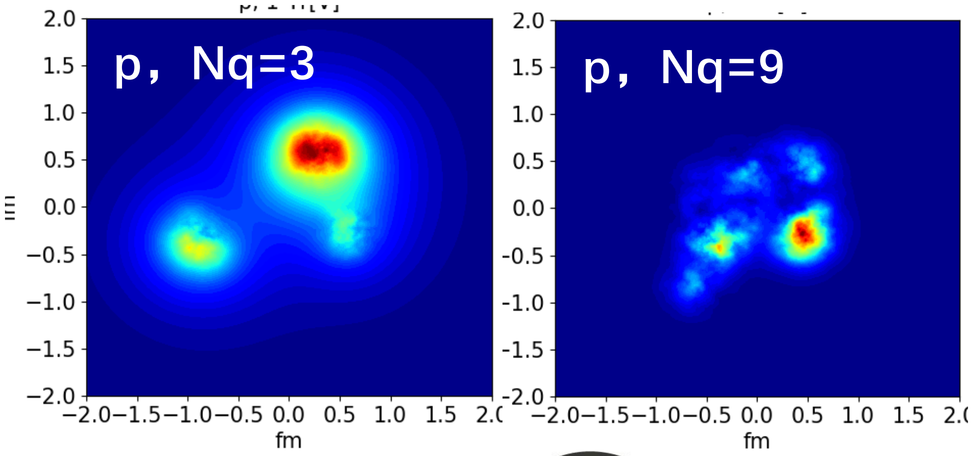

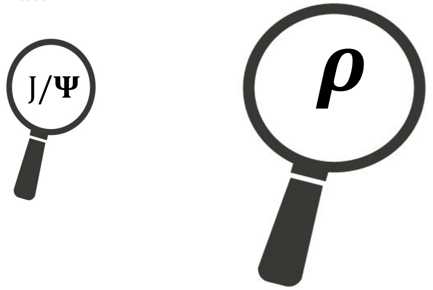

- The ρ mesons probe proton fluctuations at large length scales.
- Large differences observed for ρ productions between Nq=3 and Nq=9 MAPs.
- Larger Q^2, smaller difference.

H. Mantysaari, B.Schenke, C. Shen and W. Zhao, Phys. Lett. B 833 (2022), 137348, and in progress.

Accessing nuclear deformation at small x

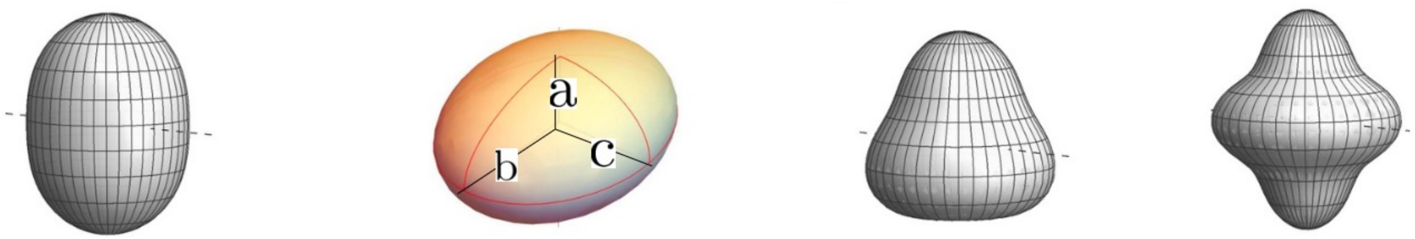

Nuclear structure

Generalized Woods-Saxon profile

$$\rho(r,\Theta,\Phi) \propto \frac{1}{1+\exp\left(\left[r-R(\Theta,\Phi)\right]/a\right)}\ , \quad R(\Theta,\Phi) = R_0\left[1+\beta_2\left(\cos\gamma Y_{20}(\Theta)+\sin\gamma Y_{22}(\Theta,\Phi)\right)+\beta_3 Y_{30}(\Theta)+\beta_4 Y_{40}(\Theta)\right]$$

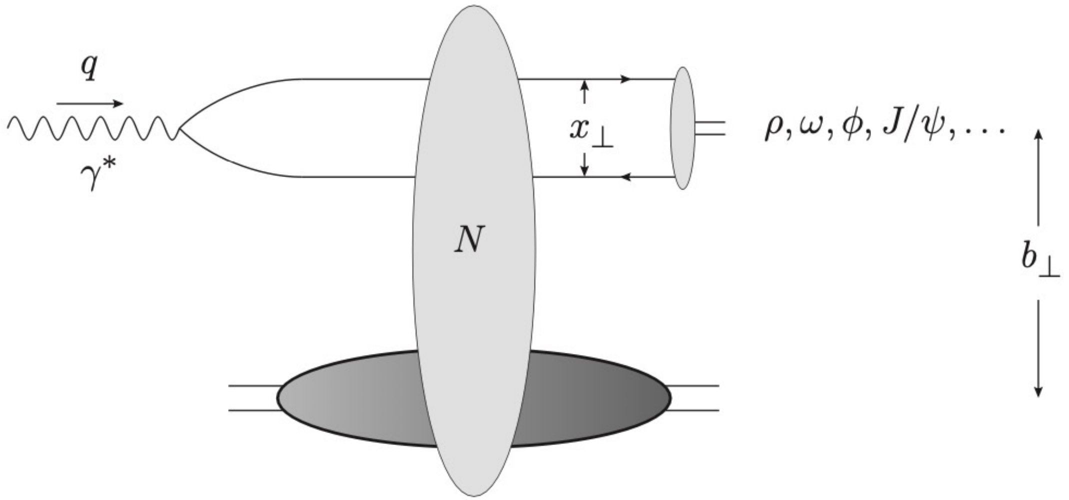

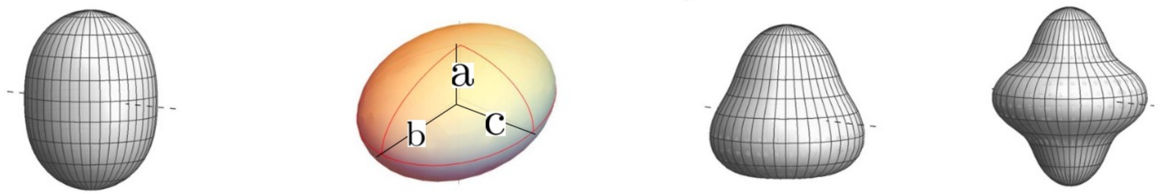

Taken from Giuliano' s slide

- Sample nucleon positions based on the Wood—Saxon distribution.
- Different deformation parameters controls the geometric deformation at different length scale.

γ^* + U → J/ψ + U*

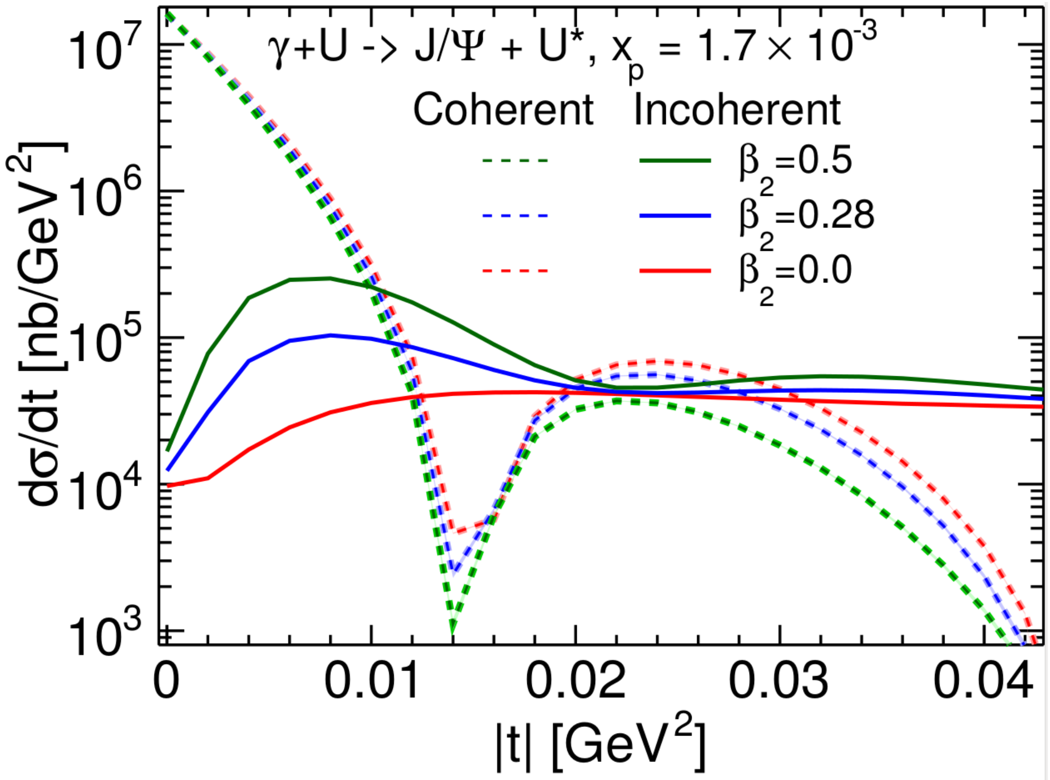

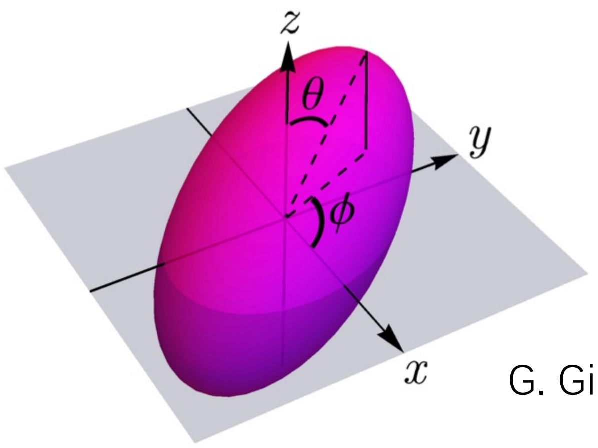

G. Giacalone, arXiv: 2004.14463

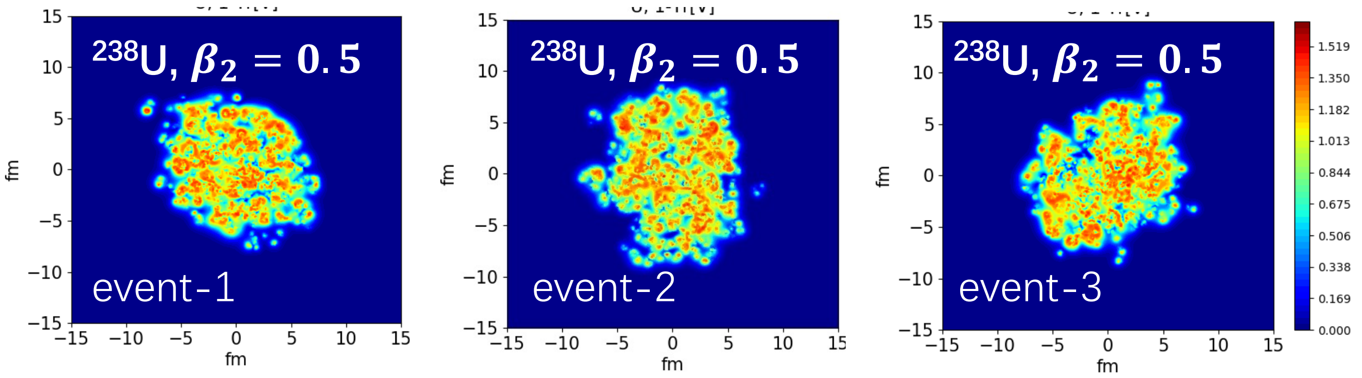

- With $\beta > 0$, the configurations projected onto x-y plane have great fluctuations.
- β_2 quadrupole deformation of the nucleus affects incoherent cross section at small|t|(large length scales) and provides direct information on the nuclear structure at small x.

H.Mantysaari, B.Schenke, C. Shen and W. Zhao, PhysRevLett.131.062301.

JIMWLK evolution to smaller x

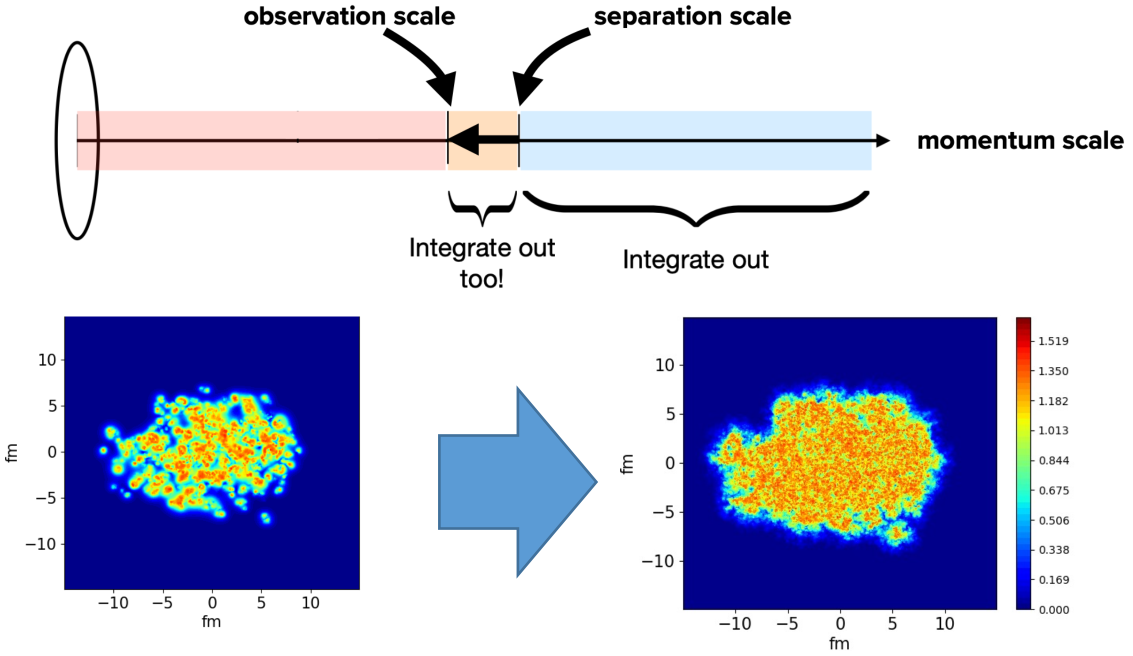

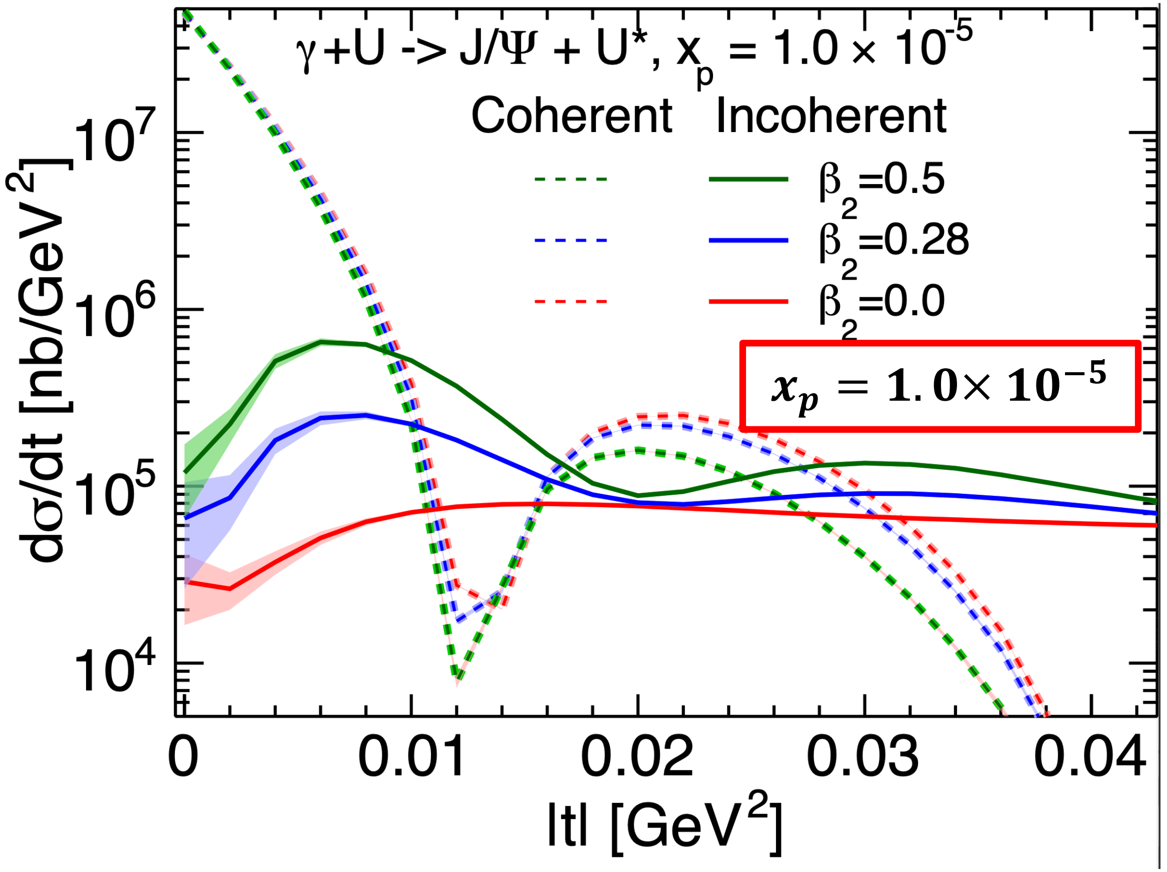

- Energy evolution doesn't wash out this effects.

H.Mantysaari, B.Schenke, C. Shen and W. Zhao PhysRevLett.131.062301.
H.Mantysaari, B.Schenke PRD, 98, 034013.
T. Lappi and H. Mantysaari, EPJC 73, 2307 (2013).
Yuri V. Kovchegov, QUANTUM CHROMODYNAMICS A T HIGH ENERGY

Multi-scale imaging: Nuclear deformations

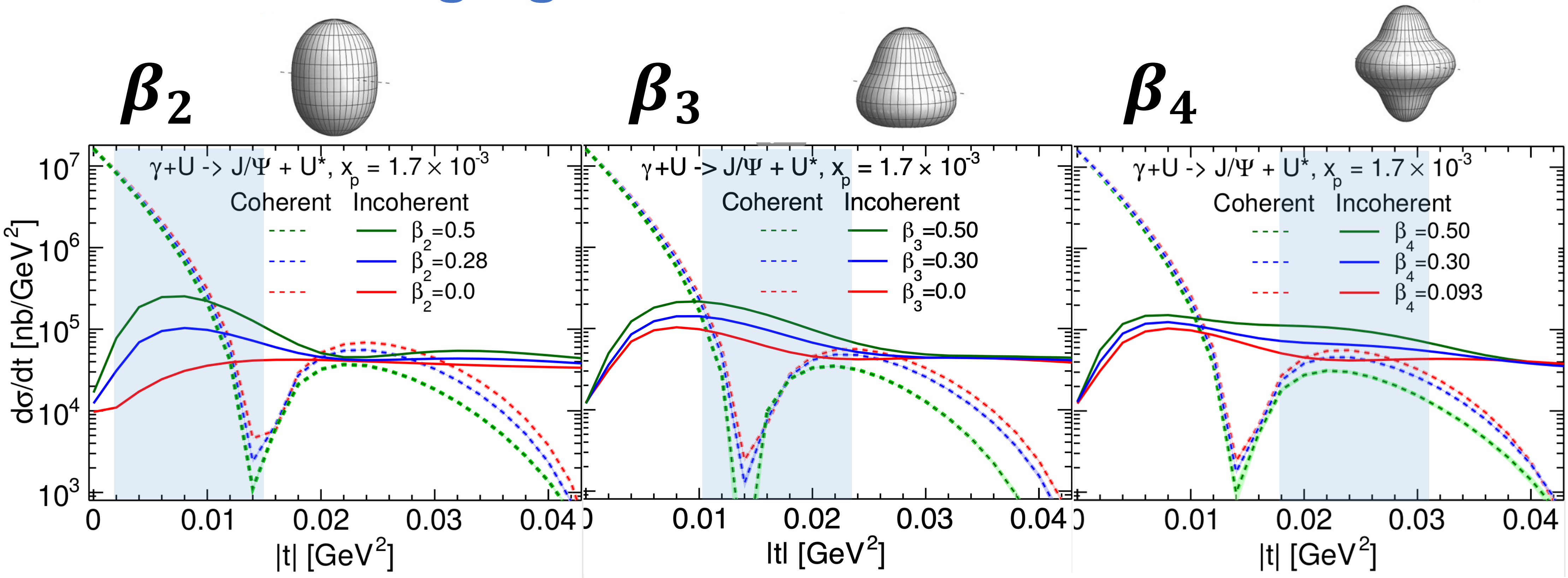

- β_2 , β_3 and β_4 manifest themselves at different |t| regions (different length scales).
- Using AI/ML technology to extract them. **Nobuo Sato, Tuesday**

H.Mantysaari, B.Schenke, C. Shen and W. Zhao, PhysRevLett.131.062301.

Probing isobar, Ru/Zr

system	R_0 [fm]	a_0 [fm]	β_2	β_3	β_4
case1 (Ru+Ru)	5.09	0.46	0.16	0.0	0.0
case2 (Ru+Ru)	5.09	0.46	0.16	0.20	0.0
case3 (Ru+Ru)	5.09	0.46	0.06	0.20	0.0
case4 (Ru+Ru)	5.09	0.52	0.06	0.20	0.0
case5 (Zr+Zr)	5.02	0.52	0.06	0.20	0.0

$$R(\Theta,\Phi) = R_0\left[1 + \underline{\beta_2}\left(\cos\underline{\gamma} Y_{20}(\Theta) + \sin\gamma Y_{22}(\Theta,\Phi)\right) + \underline{\beta_3} Y_{30}(\Theta) + \underline{\beta_4} Y_{40}(\Theta)\right]$$

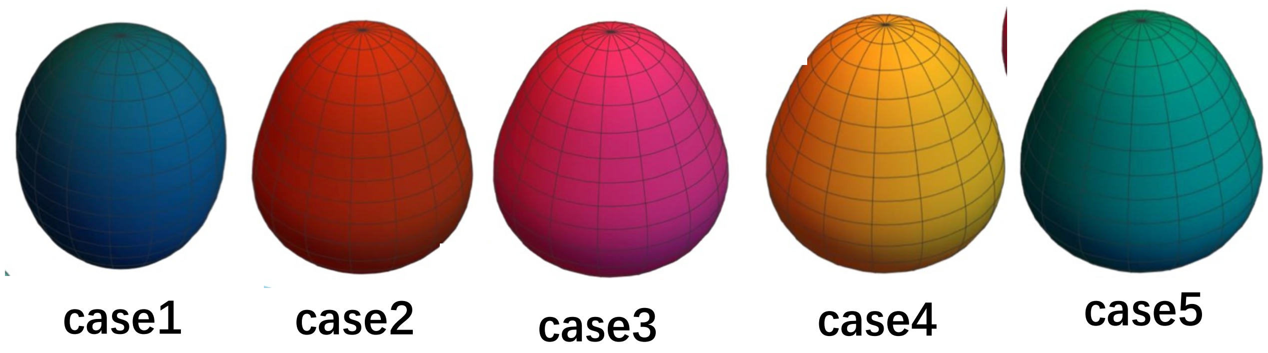

Taken from W. M. Serenone's slide.

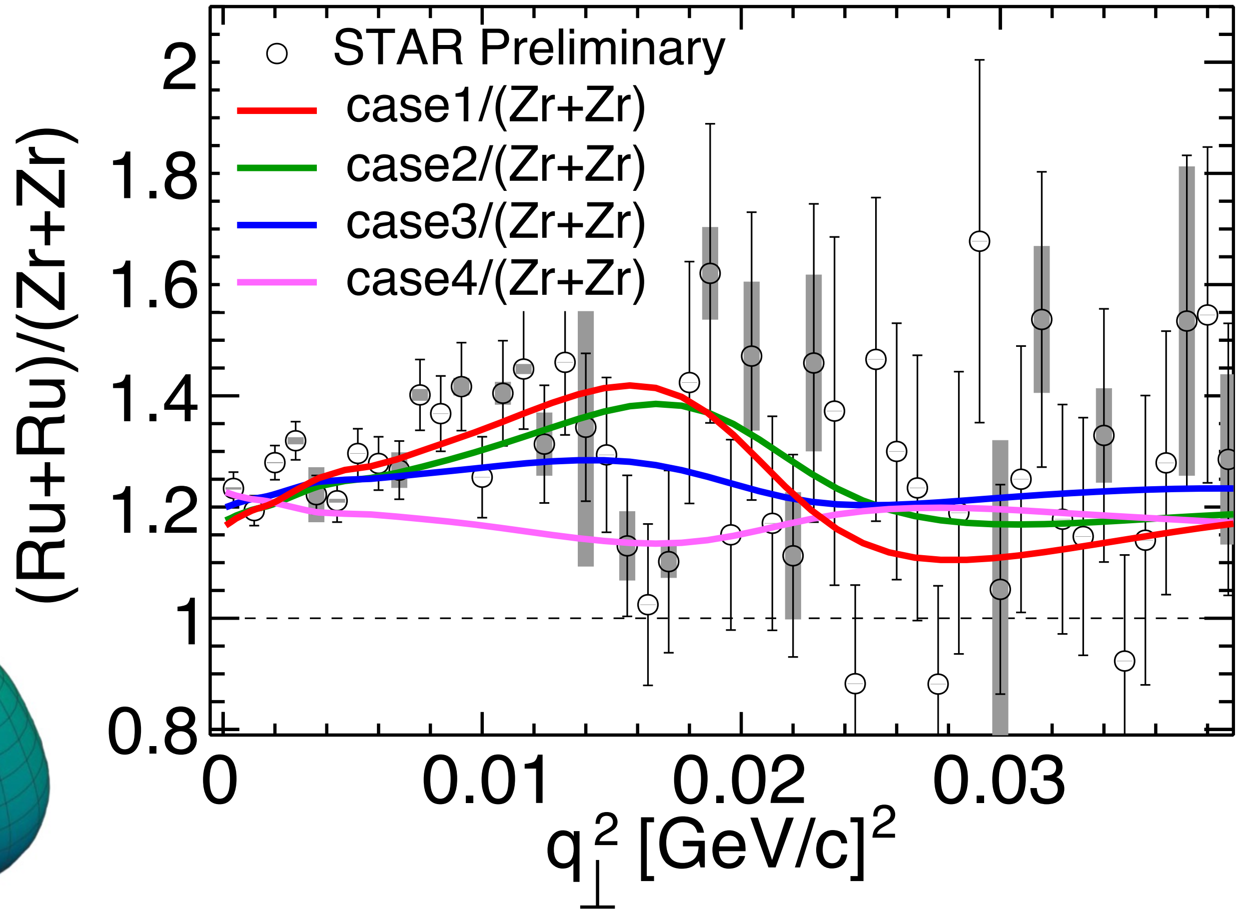

- The vector meson production in isobar UPCs is sensitive to the nuclear structures.
- “By eyes”, the ``full’’ Ru/Zr (case1/case5) is closest to data.

H.Mantysaari, F. Salazar, B.Schenke, C. Shen and W. Zhao PhysRevC.109.024908.

"X-ray vision" for atoms.

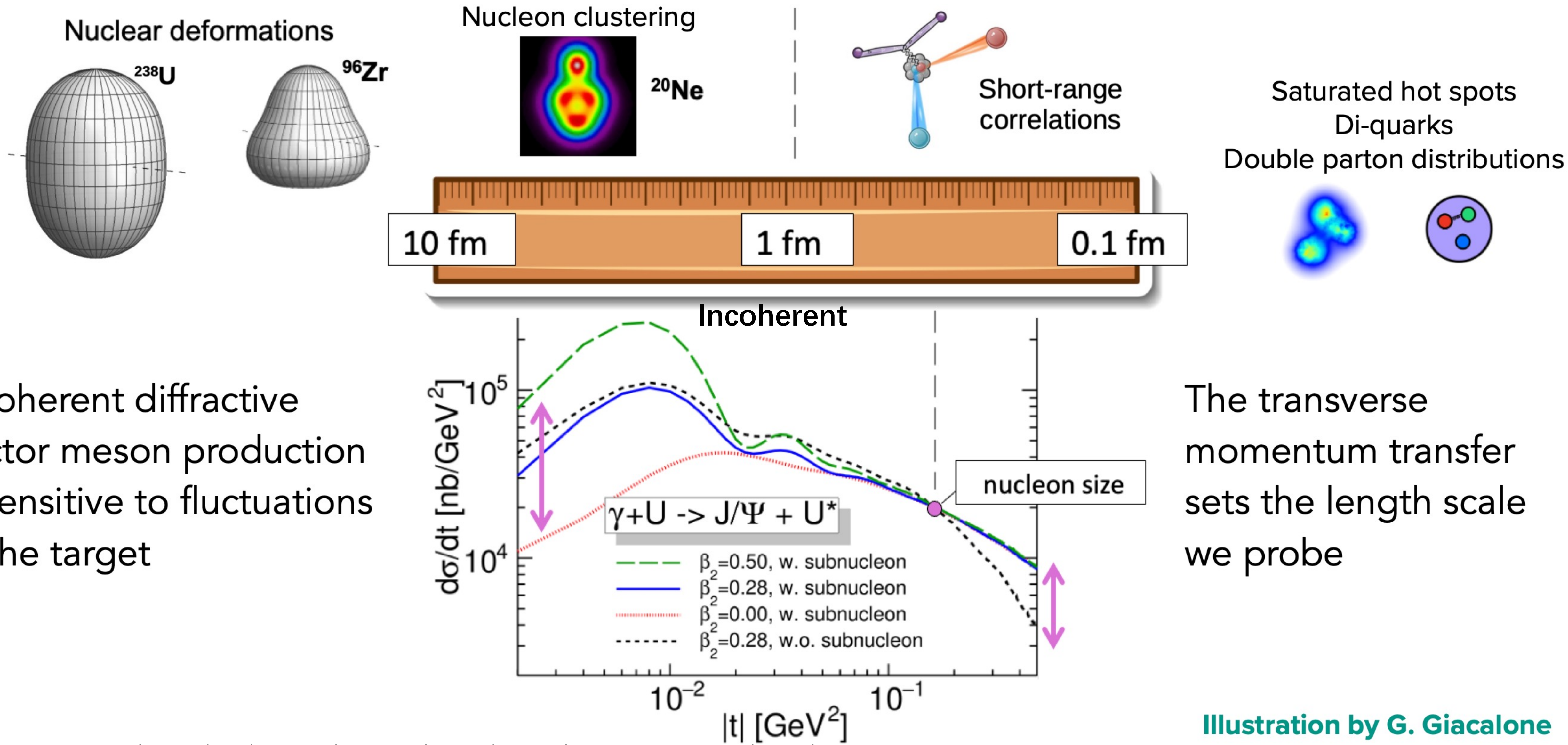

Incoherent diffractive vector meson production is sensitive to fluctuations in the target

The transverse momentum transfer sets the length scale we probe

Illustration by G. Giacalone

H.Mantysaari, B.Schenke, C. Shen and W. Zhao, Phys. Lett. B 833 (2022), 137348.
H.Mantysaari, B.Schenke, C. Shen and W. Zhao, PhysRevLett.131.062301.

Polarized Deuteron

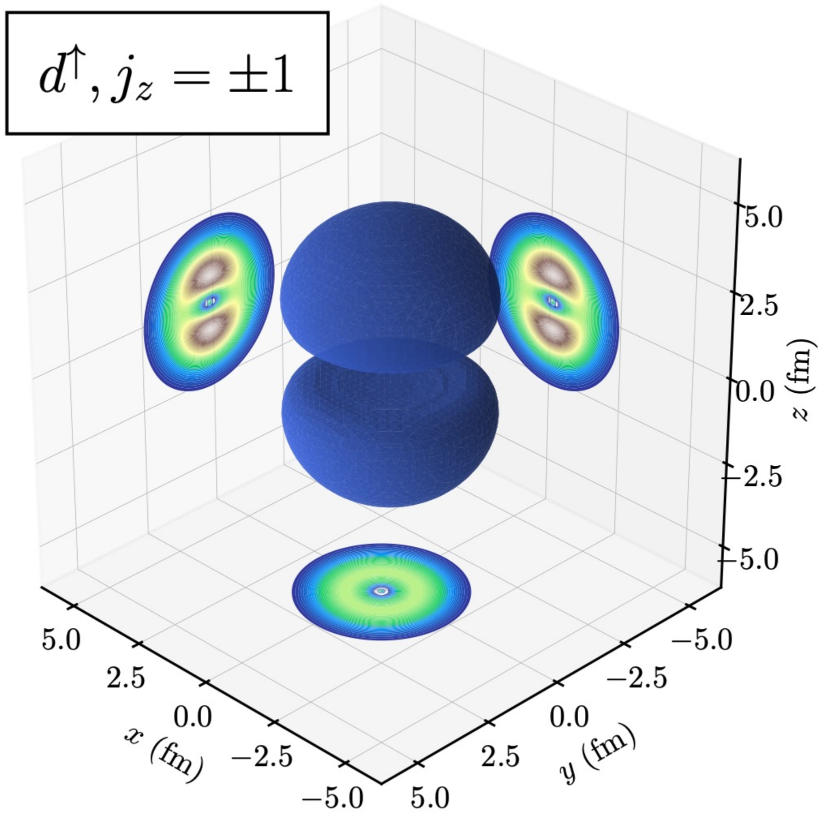

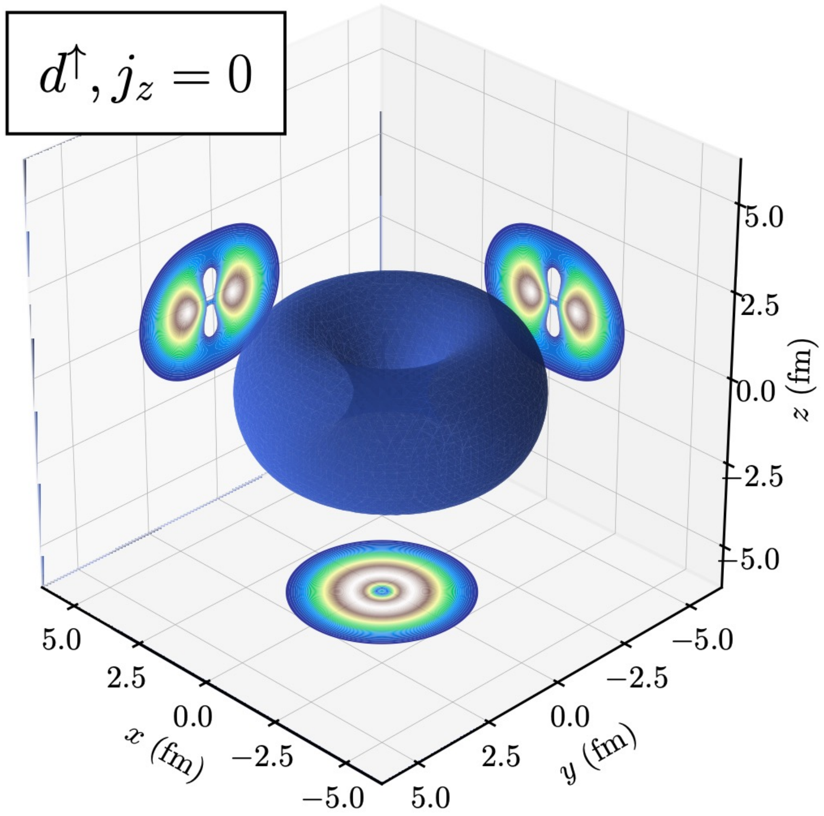

Spatial imaging of polarized deuterons

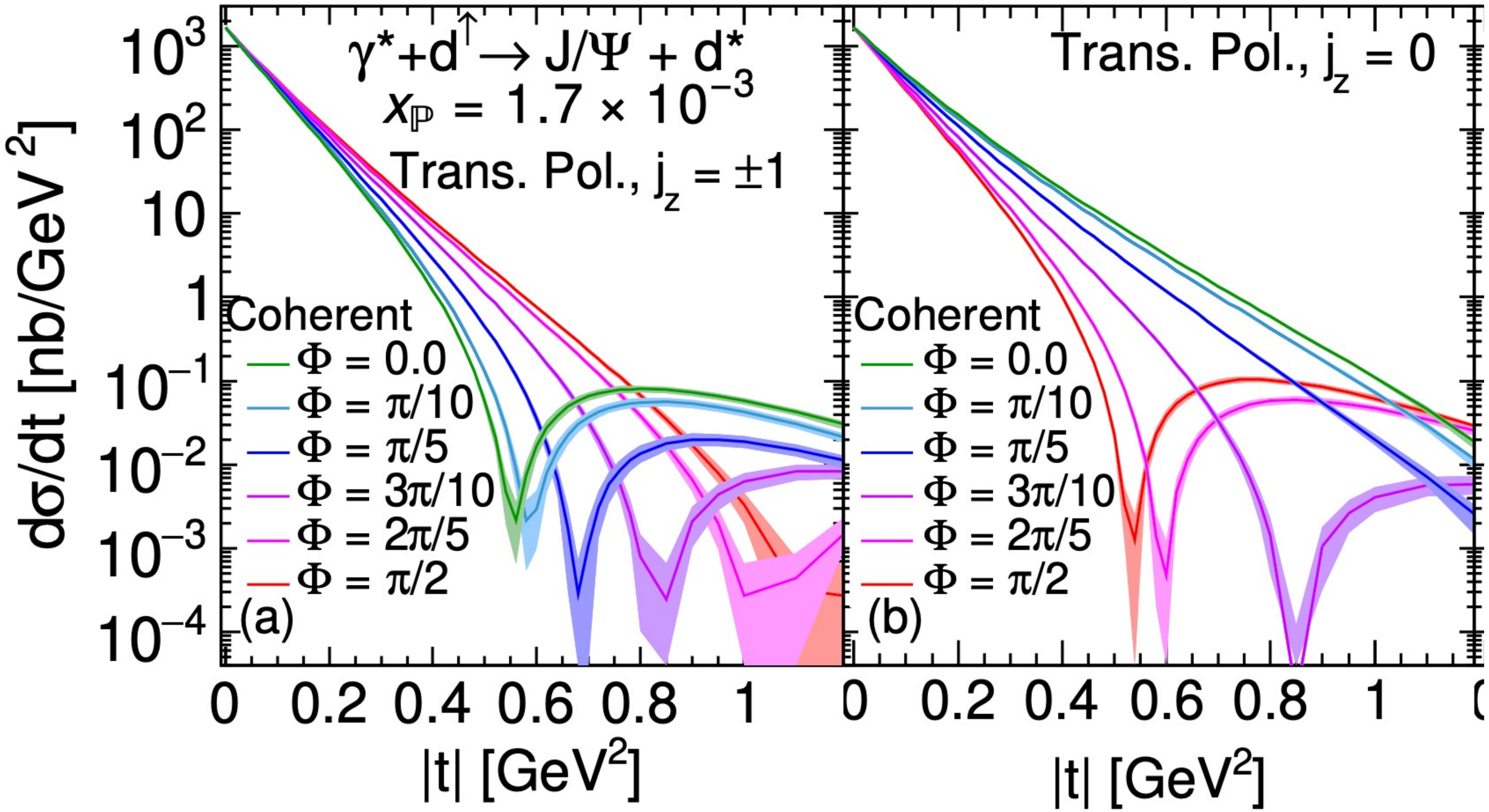

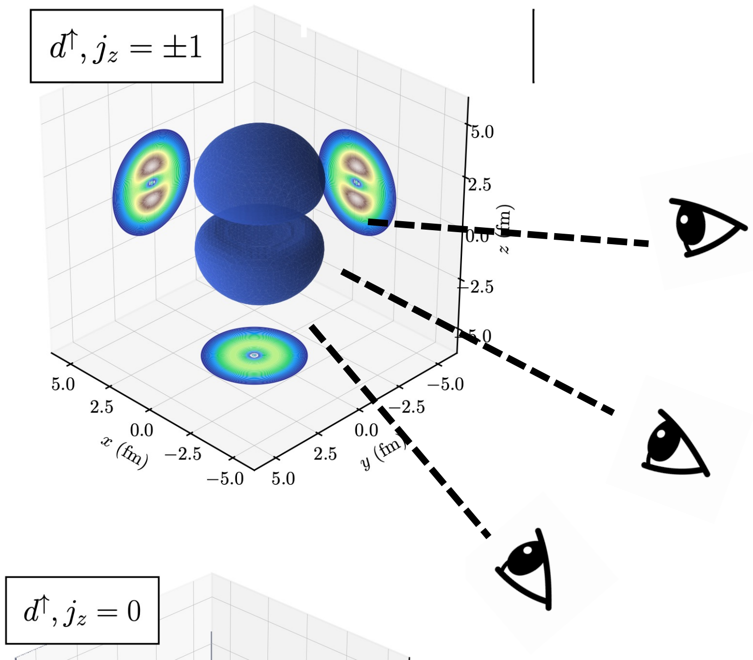

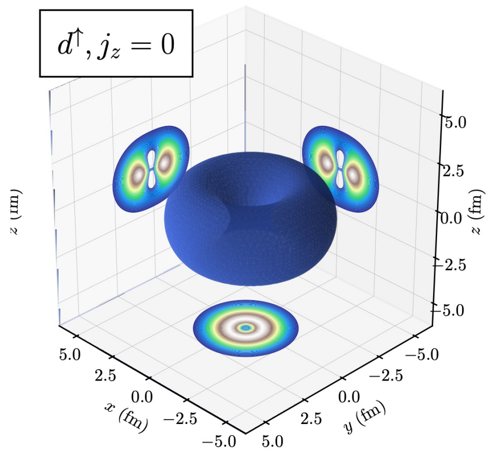

Φ: the angle relative to polarized direction.

- Clear angular dependence of the vector meson production.
- Transverse polarized case, $j_z = \pm 1$ has the opposite angular dependence with $j_z = 0$.

H.Mantysaari, F. Salazar, B.Schenke, C. Shen and W. Zhao, physletb.2024.139053.

Spatial imaging of polarized deuterons

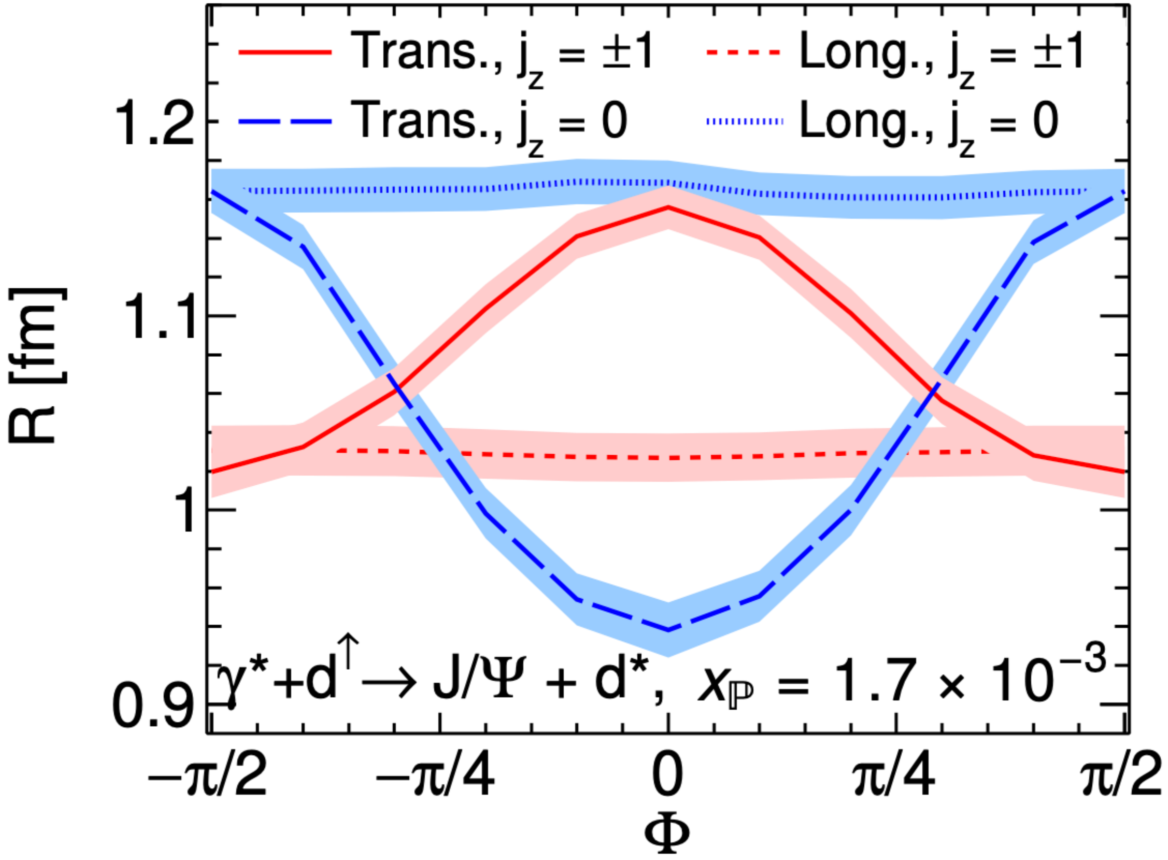

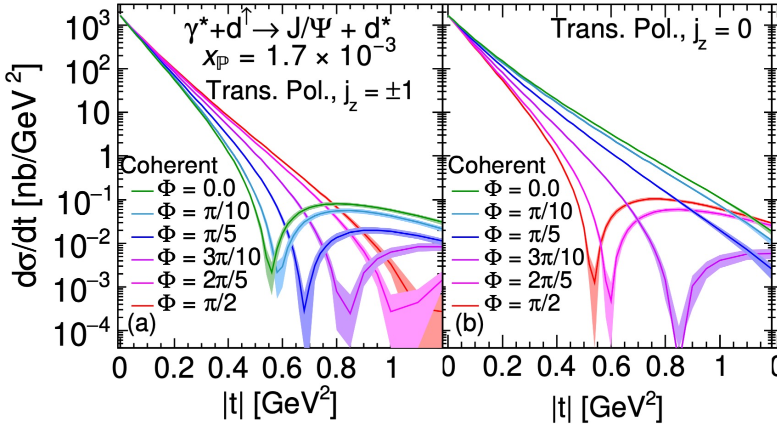

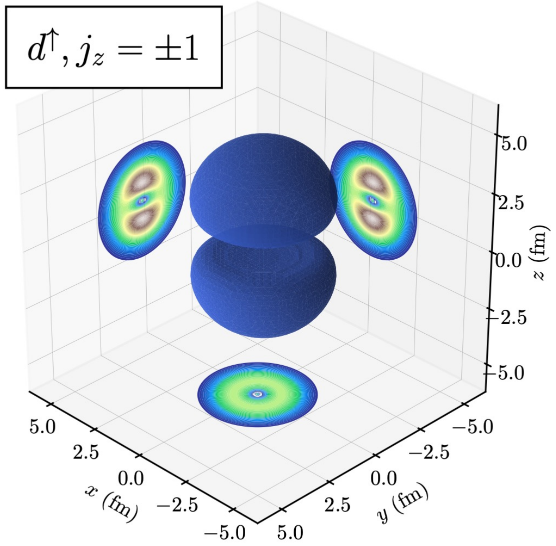

$$d\sigma/dt \sim e^{-B_D|t|}$$

$$R = \sqrt{2B_D}.$$

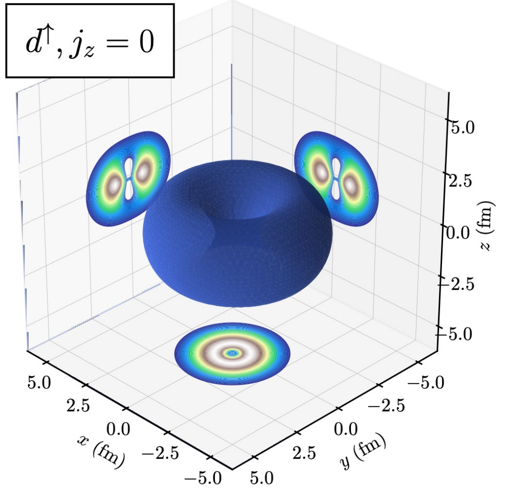

- Help to construct the 3D nucleon density profile of the polarized light nuclei.

H.Mantysaari, F. Salazar, B.Schenke, C. Shen and W. Zhao, physletb.2024.139053.

Probe Saturation Signal in $e + d^{\uparrow}$

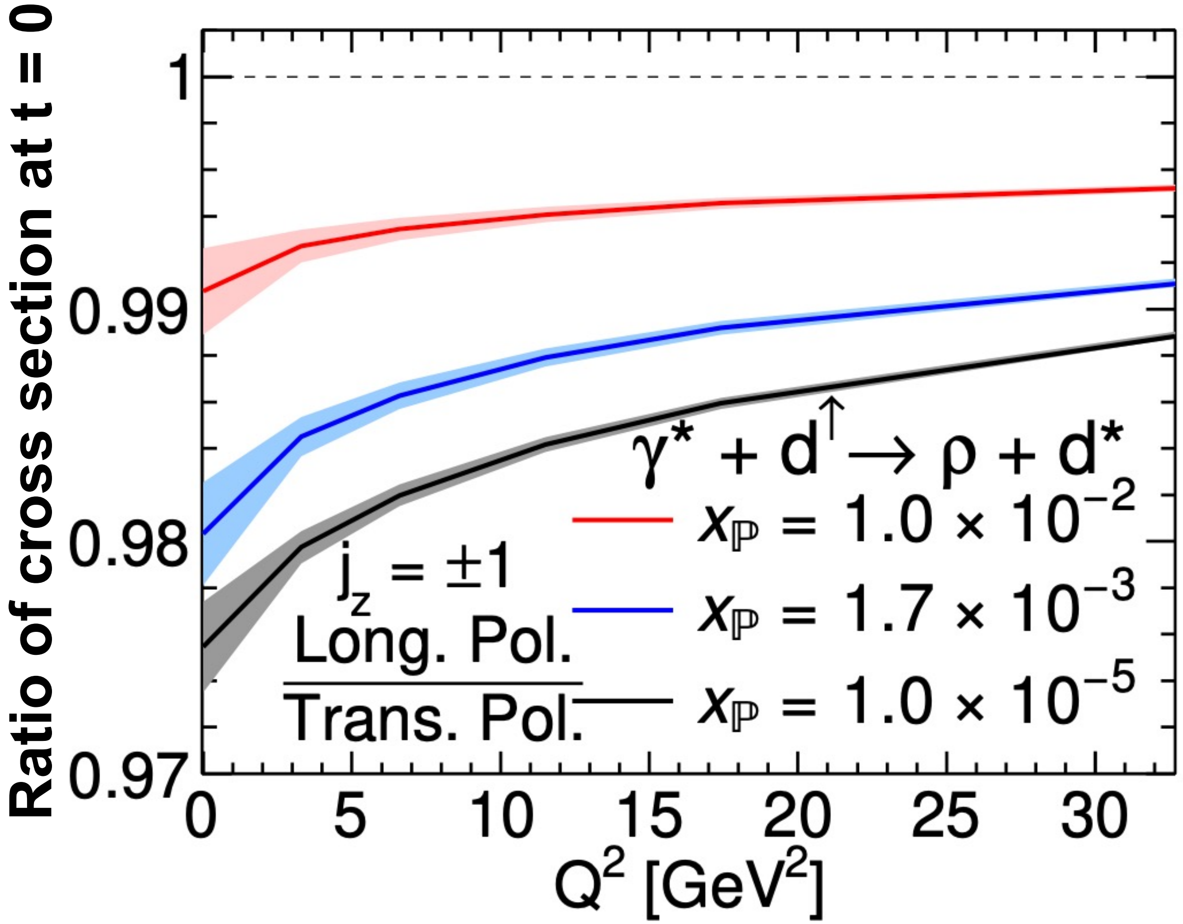

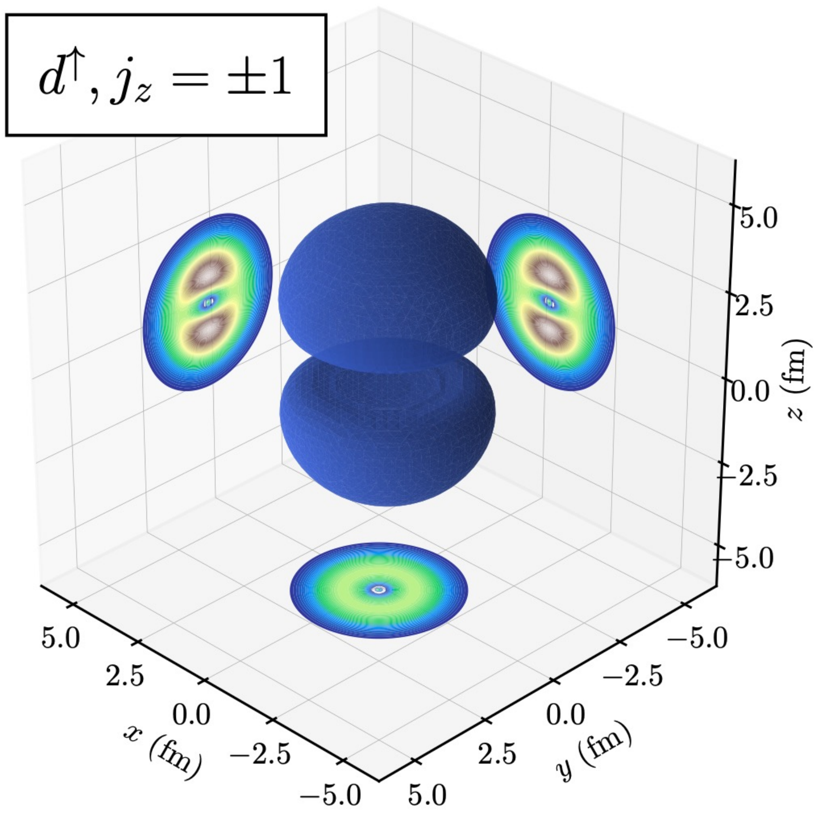

- Longitudinal-to-transverse ratio is below one.
- Smaller Q^2, the smaller ratio; Smaller x, smaller ratio.

H.Mantysaari, F. Salazar, B.Schenke, C. Shen and W. Zhao, physletb.2024.139053.

Energy Evolution of Initial Conditions

Energy evolution of initial state

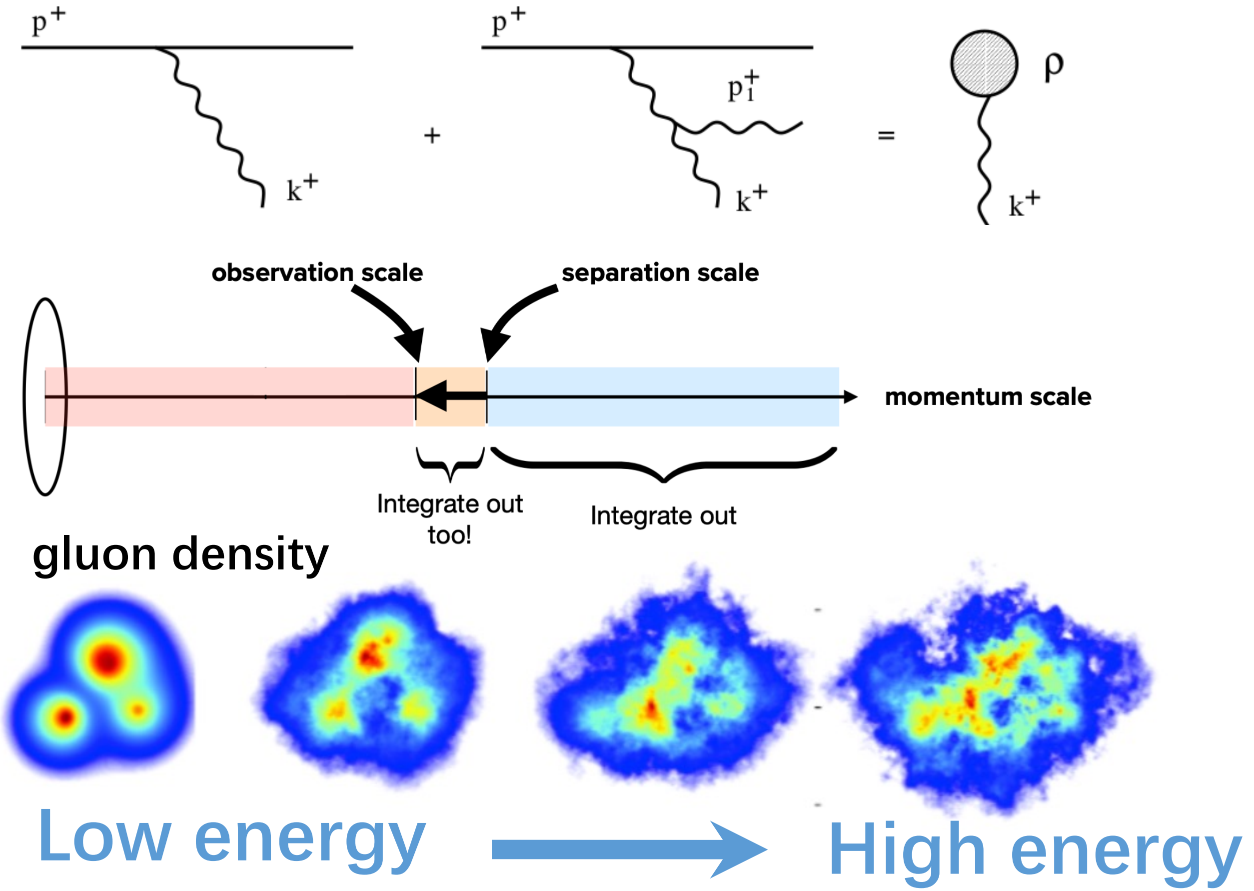

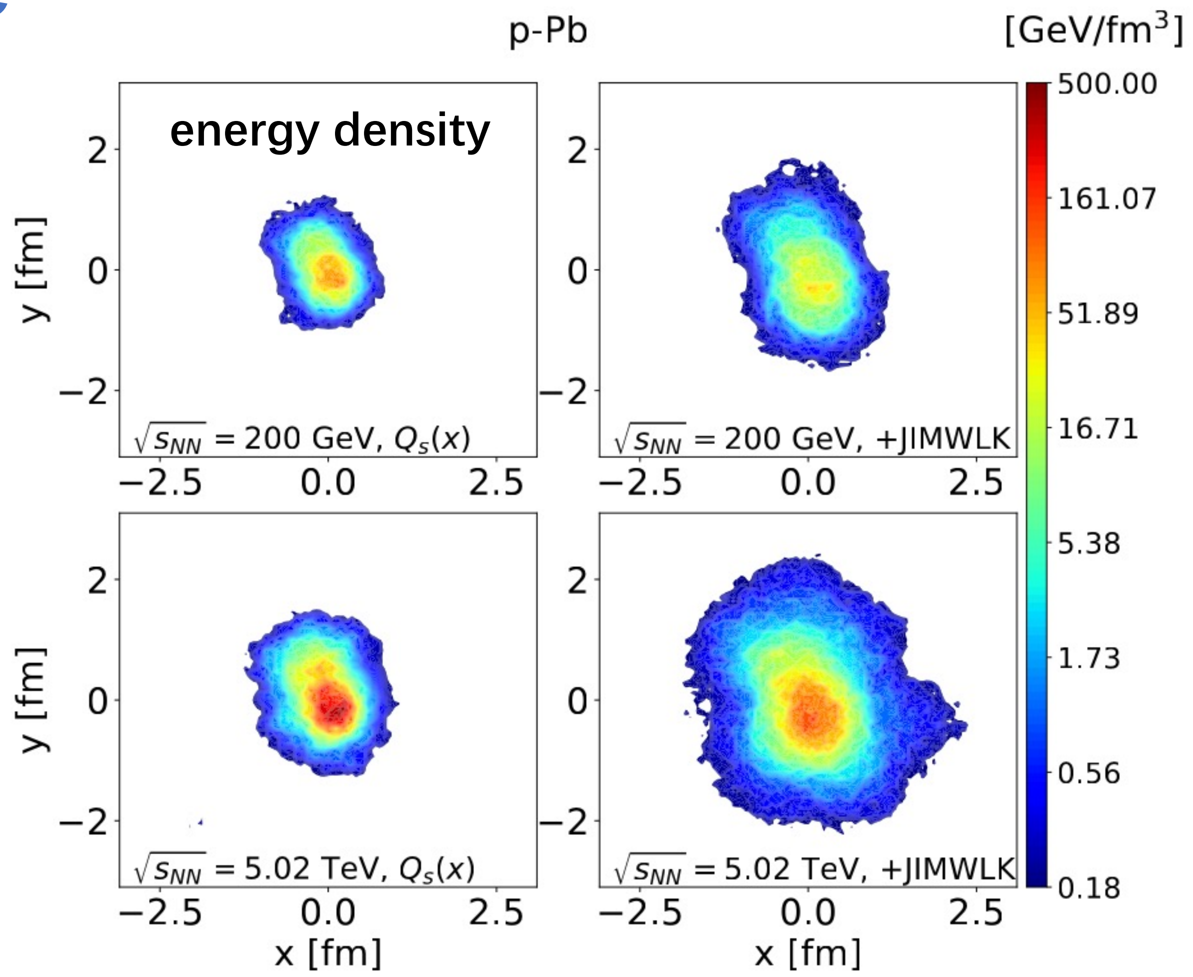

- JIMWLK energy evolution of the initial state increases its size.

H. Mäntysaari and B. Schenke, Phys.Rev. D98 (2018) 034013.
H. Mäntysaari, B. Schenke, C, Shen and WBZ, [arXiv:2502.05138 [nucl-th]].

Energy evolution of initial conditions

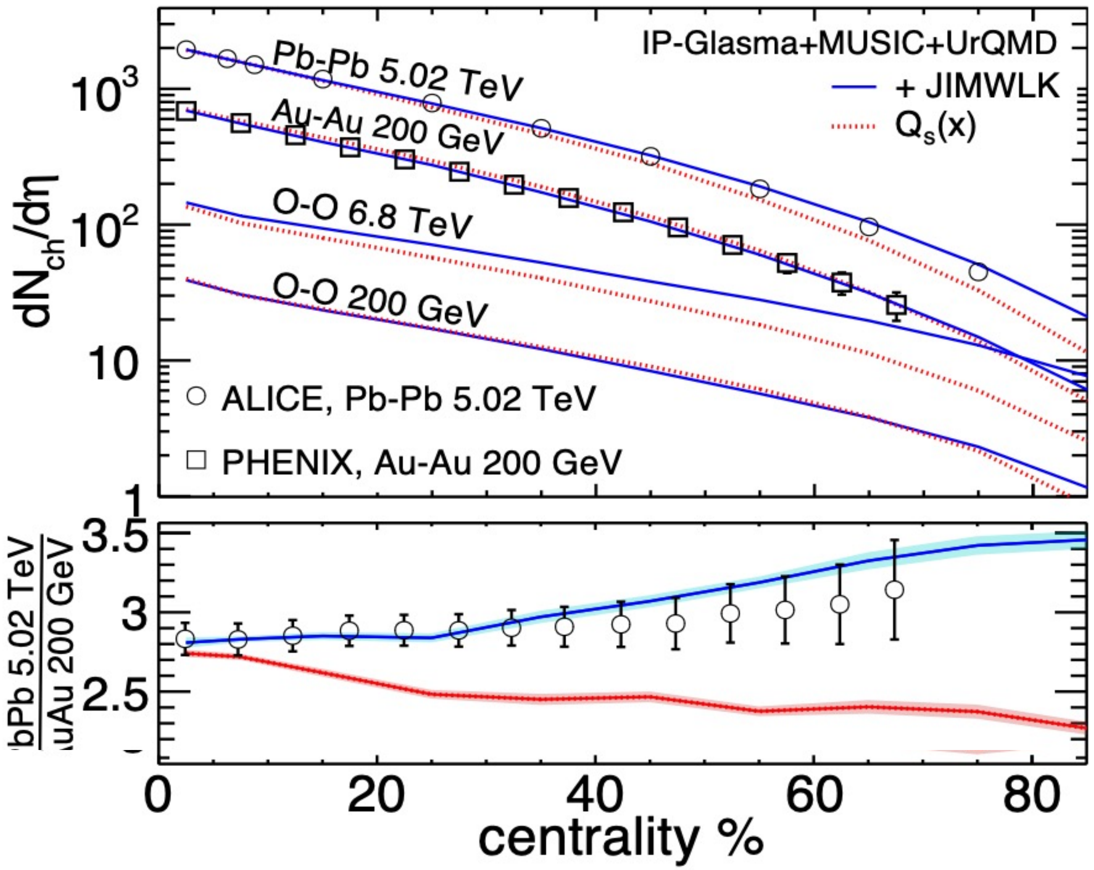

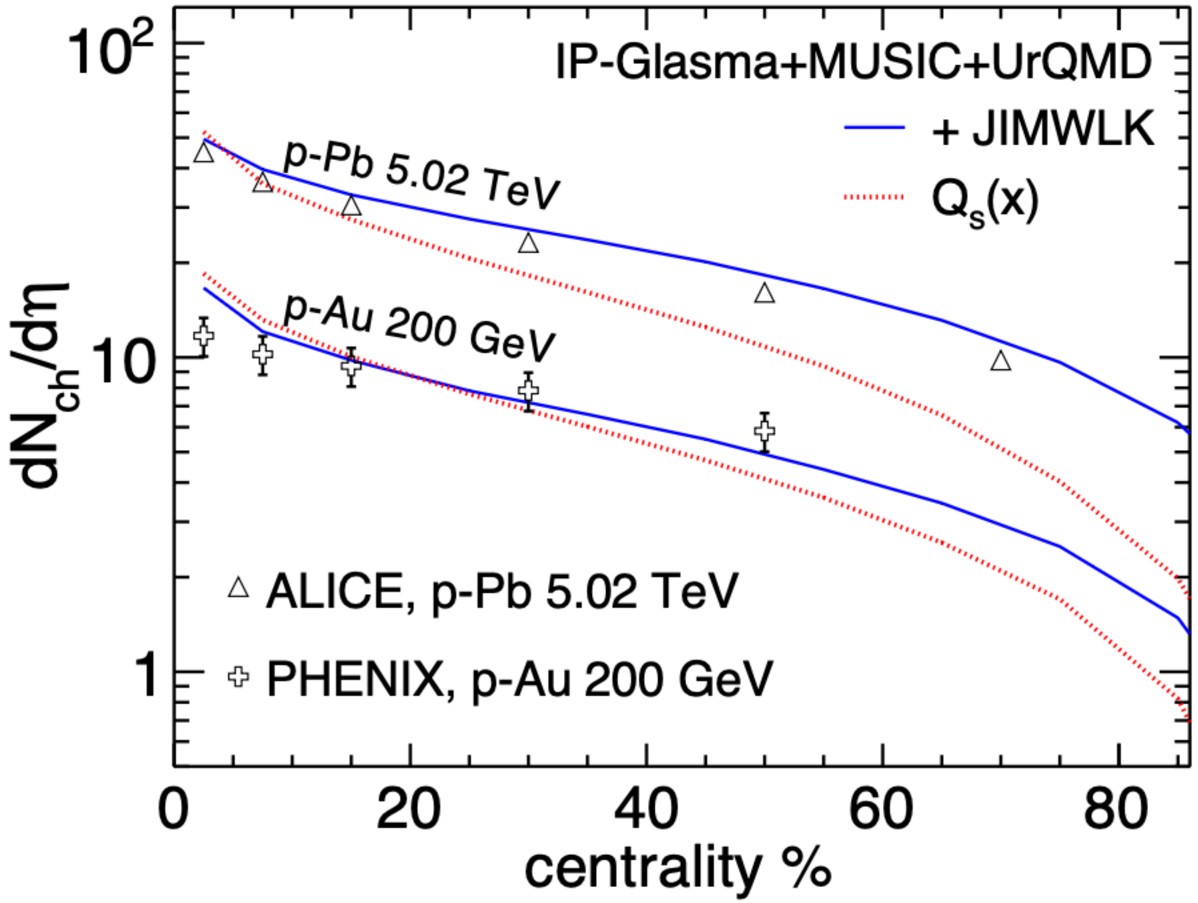

+ JIMWLK: CGC (fit HERA data) + JIMWLK + Hydrodynamics

$Q_s(x)$: CGC (change the $Q_s(x)$ only) + Hydrodynamics

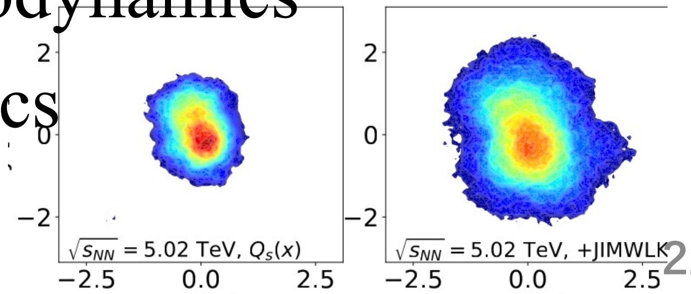

H.Mantysaari, B.Schenke, C. Shen and W. Zhao [arXiv:2502.05138 [nucl-th]].

Energy evolution of initial conditions

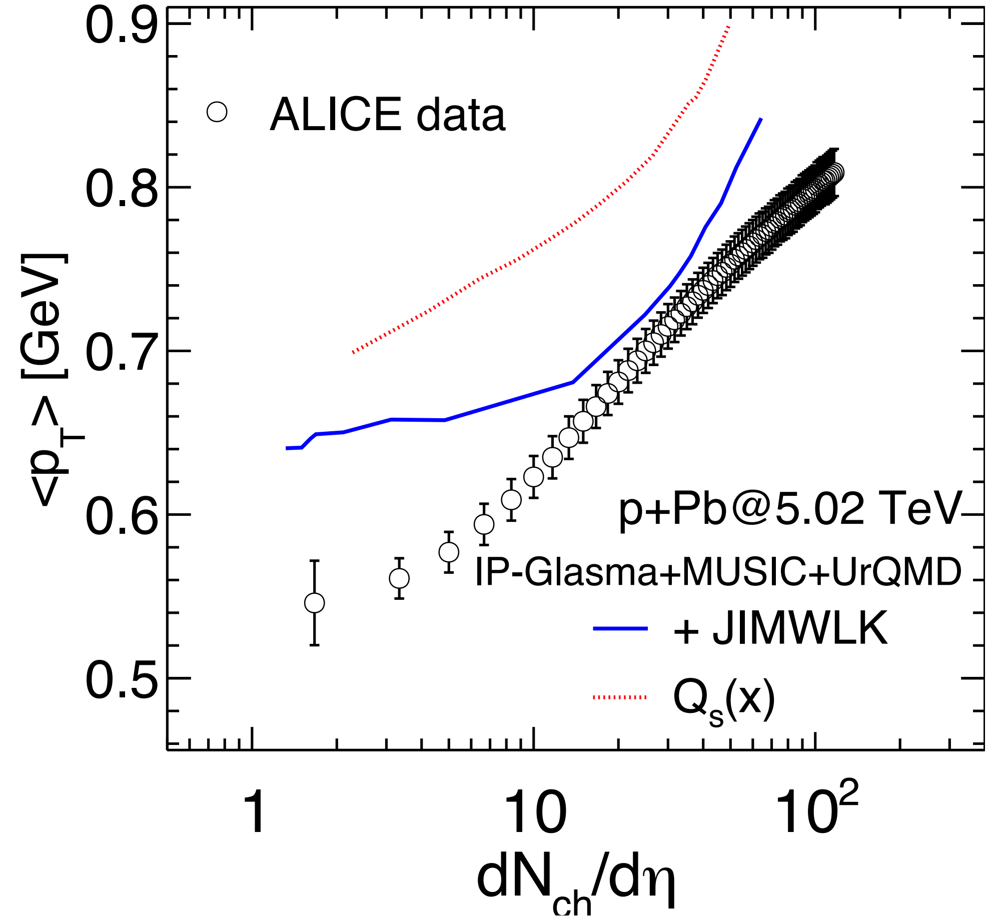

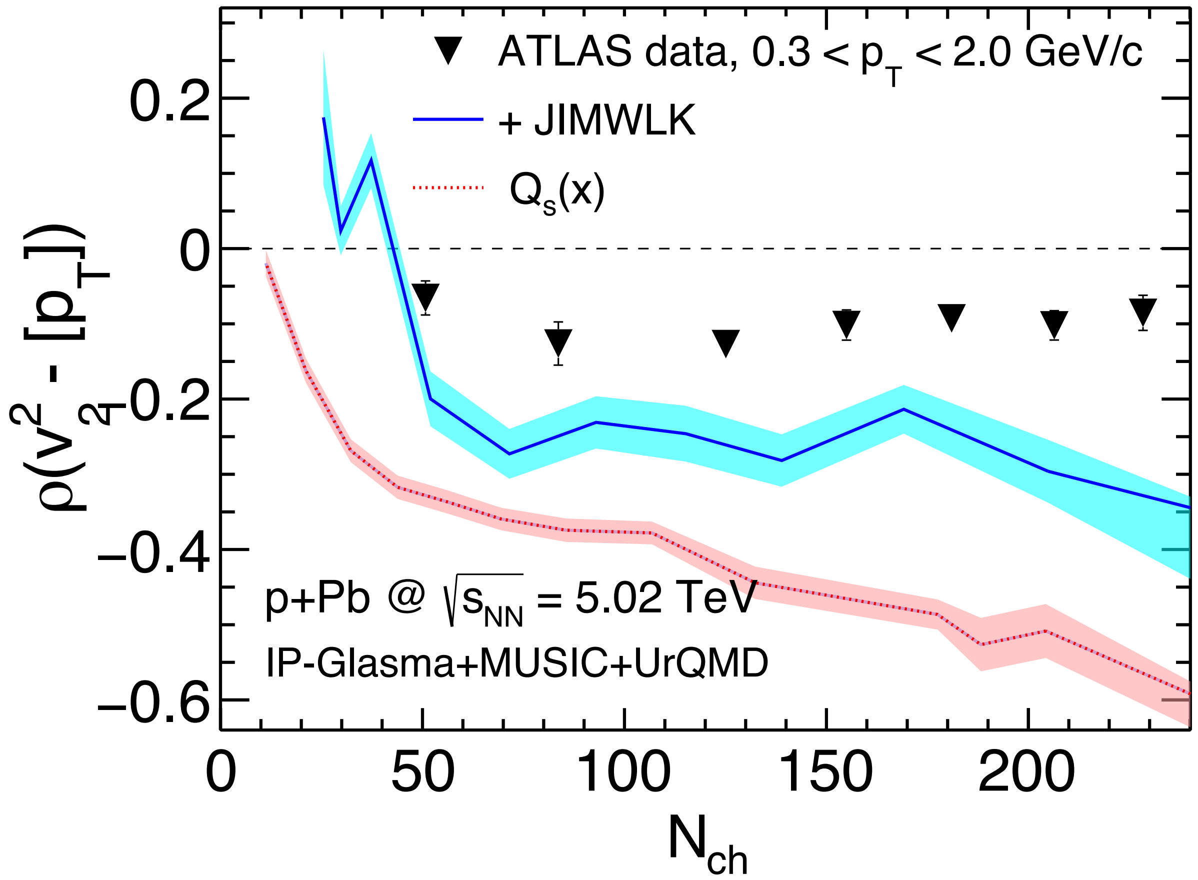

+ JIMWLK: CGC (fit HERA data) + JIMWLK + Hydrodynamics

$Q_s(x)$: CGC (change the $Q_s(x)$ only) + Hydrodynamics

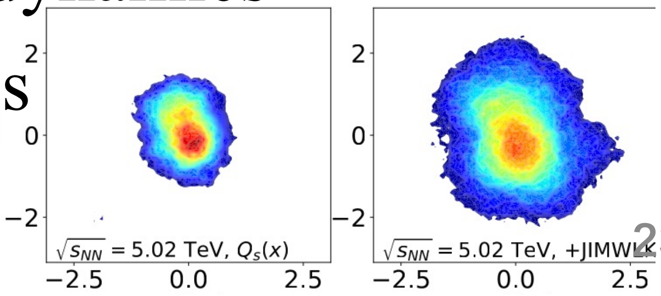

H.Mantysaari, B.Schenke, C. Shen and W. Zhao [arXiv:2502.05138 [nucl-th]].

Take Home Messages (Connection between HIC and EIC)

- Both diffractive vector meson production in the EIC and collectivity in heavy-ion collisions probe the initial gluon distributions inside nucleus.
- In heavy-ion collisions, the initial state is one of biggest model uncertainties.
- Diffractive vector meson productions in EIC provide the complementary constrain of the initial gluon distributions of nucleus.

Summary

- Diffractive vector meson production provides the “X-ray vision” for atoms.
- **On going work**: Global analysis of HERA diffractive data + RHIC and LHC flow data with the energy evolution initial conditions.

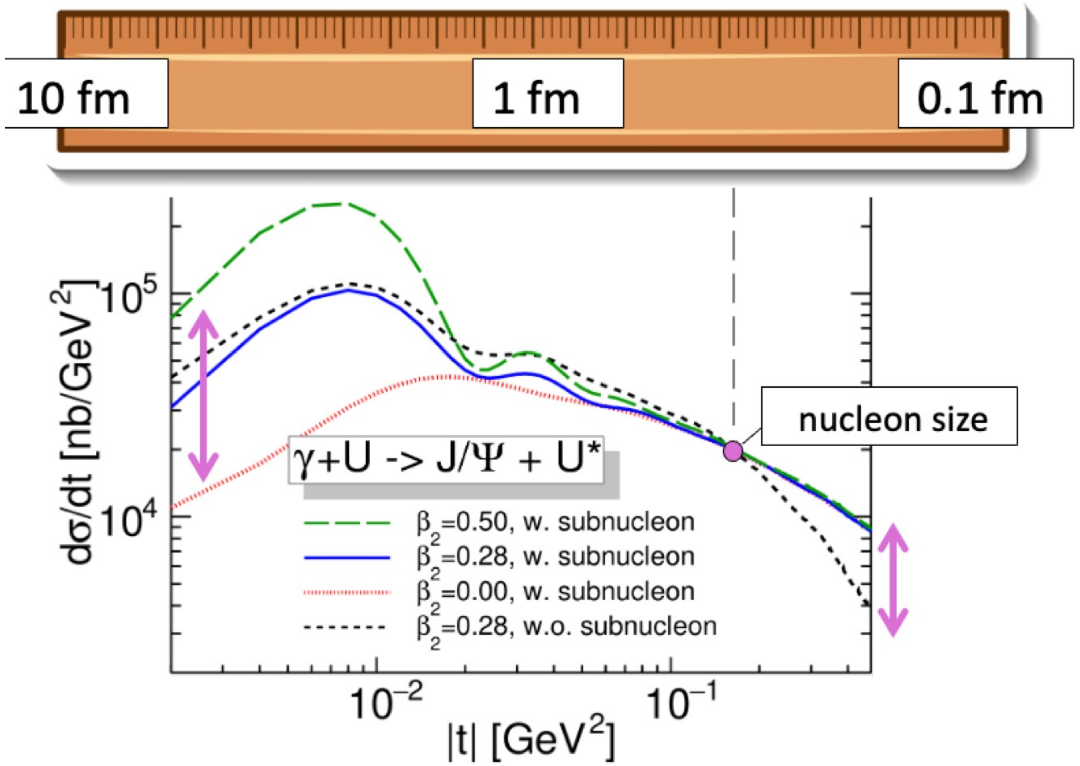

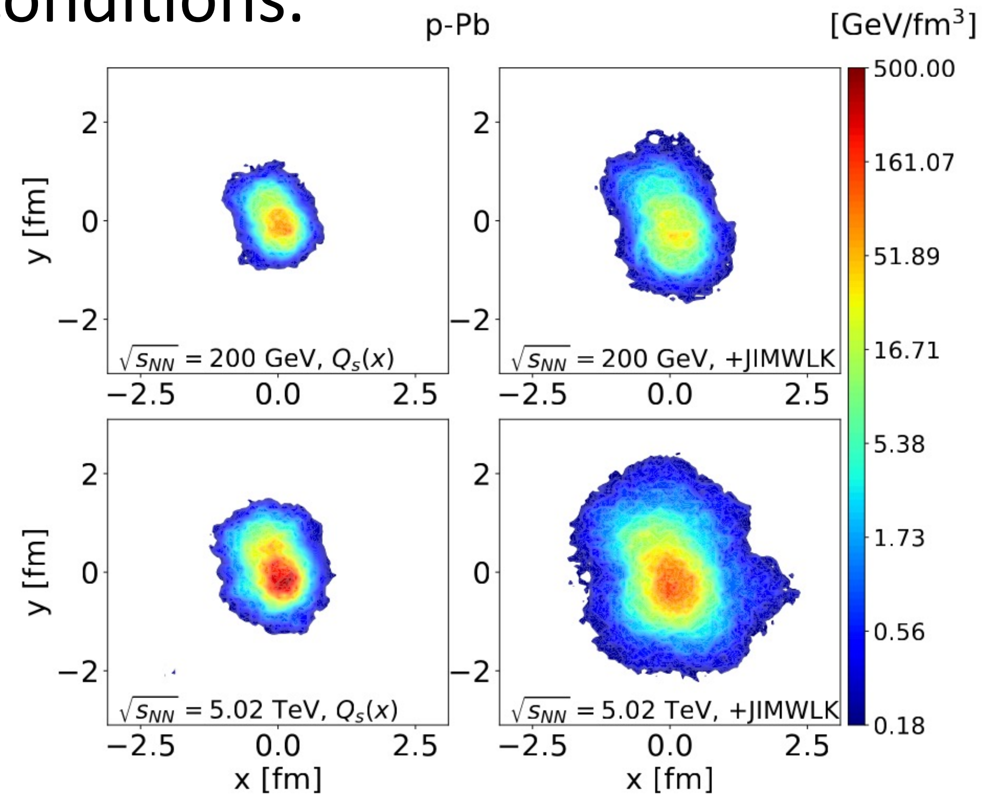

Thanks for Your Attentions!

Back Up

Probing Nuclear Deformations in UPCs

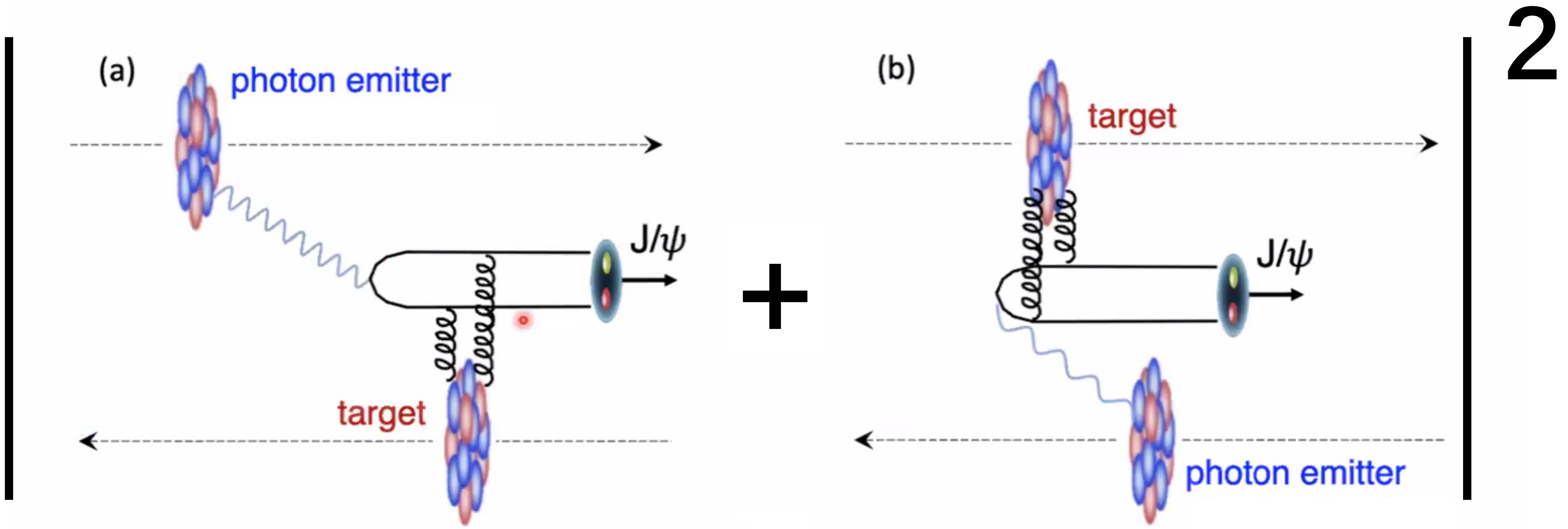

Plot is from J. D. Brandemburg's slide.

Interference Measurement in Au+Au and U+U

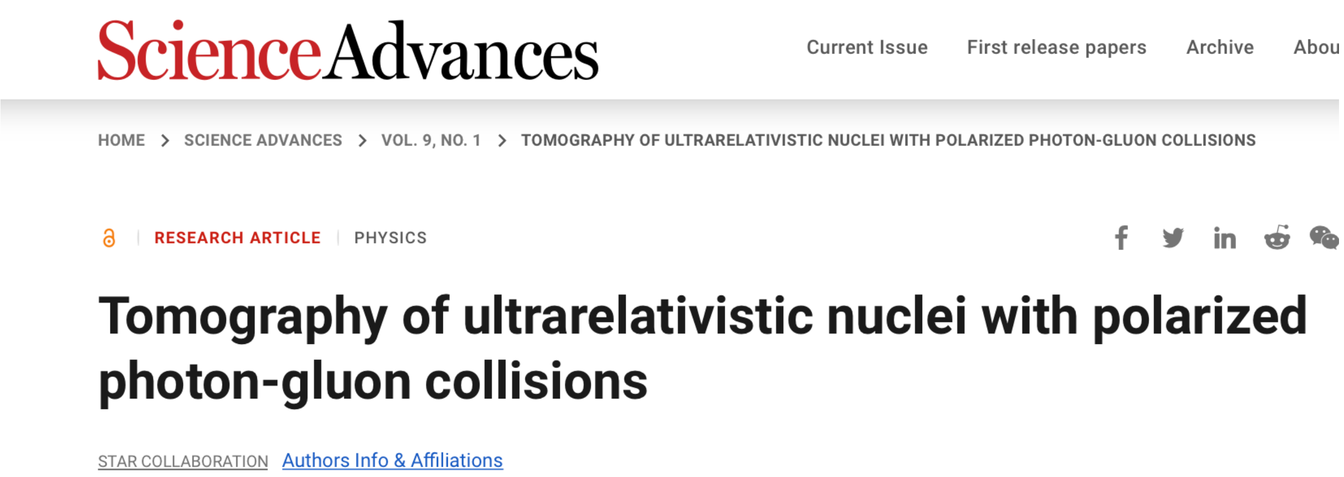
ScienceAdvances

Current Issue First release papers Archive Abou

HOME > SCIENCE ADVANCES > VOL. 9, NO. 1 > TOMOGRAPHY OF ULTRARELATIVISTIC NUCLEI WITH POLARIZED PHOTON-GLUON COLLISIONS

RESEARCH ARTICLE | PHYSICS

Tomography of ultrarelativistic nuclei with polarized photon-gluon collisions

STAR COLLABORATION Authors Info & Affiliations

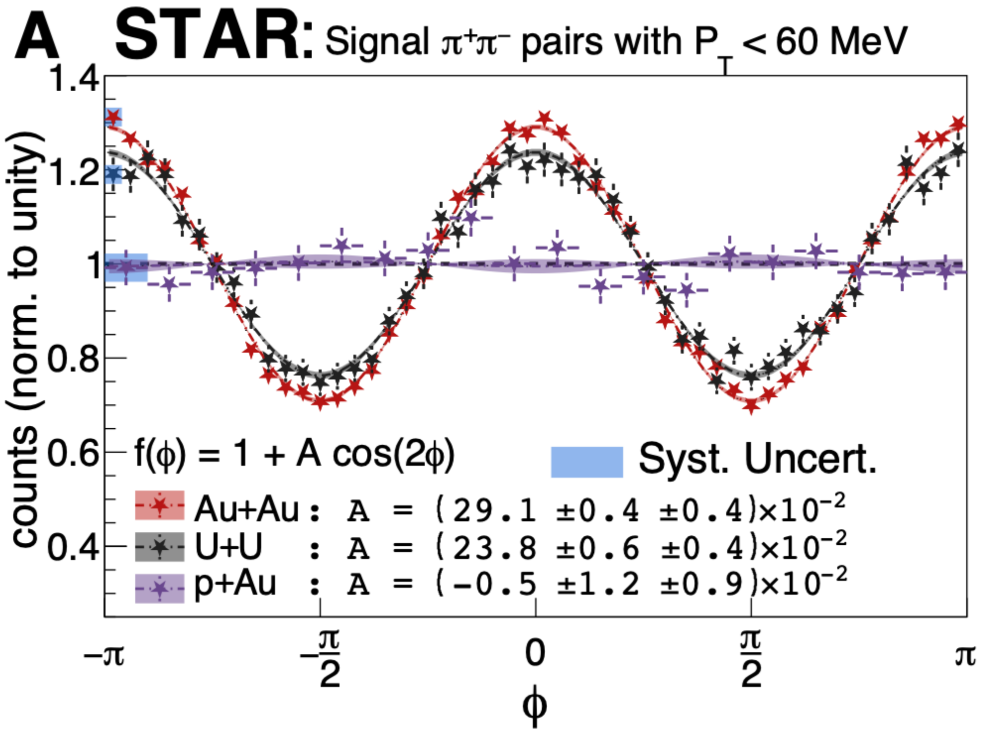

- Beautiful interference pattern observed in UPCs by STAR people.
- The interference effect is sensitive to the nuclear geometry.

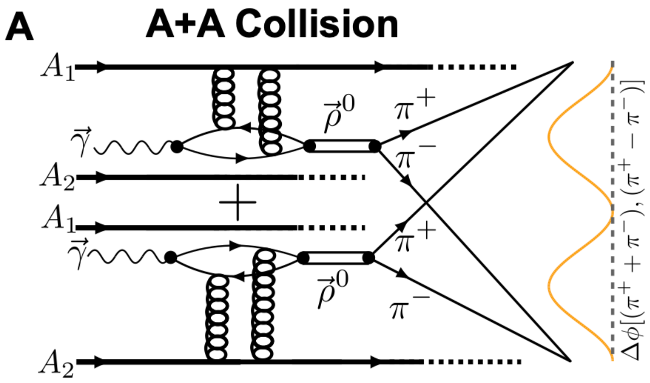

STAR Sci. Adv. 9 (2023) no.1, eabq3903.

Double-slit interference in UPCs

$$\frac{\mathrm{d}\sigma^{\rho\to\pi^+\pi^-}}{\mathrm{d}^2\mathbf{P}_\perp \mathrm{d}q_\perp \mathrm{d}y_1 \mathrm{d}y_2} =$$

$$\frac{1}{2(2\pi)^3}\frac{P_\perp^2}{(Q^2-M_V^2)^2+M_V^2\Gamma^2} f_{\rho\pi\pi}^2 \left\{ \int \mathrm{d}\phi_{\mathbf{q}_\perp} B_\perp \mathrm{d}B_\perp \langle \mathcal{M}^i(y,\mathbf{q}_\perp,\mathbf{B}_\perp)\mathcal{M}^{\dagger,j}(y,\mathbf{q}_\perp,\mathbf{B}_\perp)\rangle_\Omega P_\perp^i P_\perp^j \Theta(|\mathbf{B}_\perp| - B_{\min,\Omega}) \right\}.$$

- The amplitude:

$$\mathcal{M}^i(x_1,x_2,\boldsymbol{q}_\perp,\boldsymbol{B}_\perp) = \int \mathrm{d}^2\boldsymbol{b}_\perp e^{-i\boldsymbol{q}_\perp\cdot\boldsymbol{b}_\perp}\left[\widetilde{\mathcal{A}}(\boldsymbol{b}_\perp)_{A_1,x_1}\widetilde{\mathcal{F}}^i_{A_2}(x_2,\boldsymbol{b}_\perp-\boldsymbol{B}_\perp)+\widetilde{\mathcal{A}}(\boldsymbol{b}_\perp-\boldsymbol{B}_\perp)_{A_2,x_2}\widetilde{\mathcal{F}}^i_{A_1}(x_1,\boldsymbol{b}_\perp)\right]$$

- Subscripts A_1 and A_2 refer to the colliding nuclei. x_1 and x_2: Bjorken x, b: impact parameter of the photon-nucleus collision, B: impact parameter of the nucleus-nucleus collision.
- The function $\widetilde{\mathcal{F}}^j_A($ is the photon flux.
- Diffractive scattering amplitude

$$A^{\gamma^* p\to Vp} \sim \int \mathrm{d}^2 b\mathrm{d}z\mathrm{d}^2 r \Psi^{\gamma *}\Psi^V(r,z,Q^2)\mathrm{e}^{-\mathrm{i}b\cdot\Delta}N(r,x,b)$$

H. Xing, C. Zhang, J. Zhou and Y. J. Zhou, JHEP 10(2020), 064.
J. D. Brandenburg, Z. Xu, W. Zha, C. Zhang, J. Zhou and Y. Zhou, PhysRevD.106.074008.
H.Mantysaari, F. Salazar, B.Schenke, C. Shen and W. Zhao, PhysRevC.109.024908.

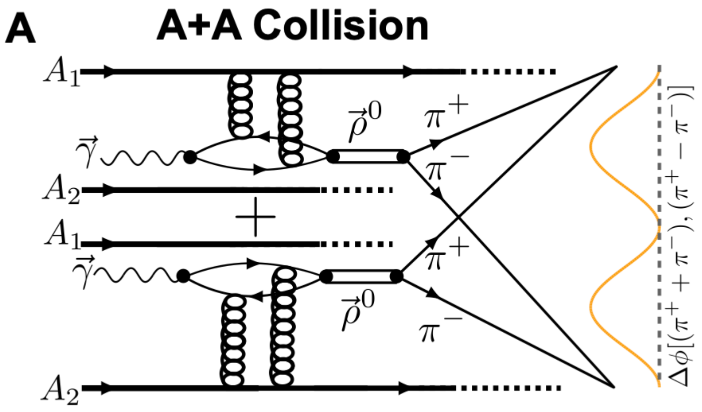

Interference in Au+Au and U+U

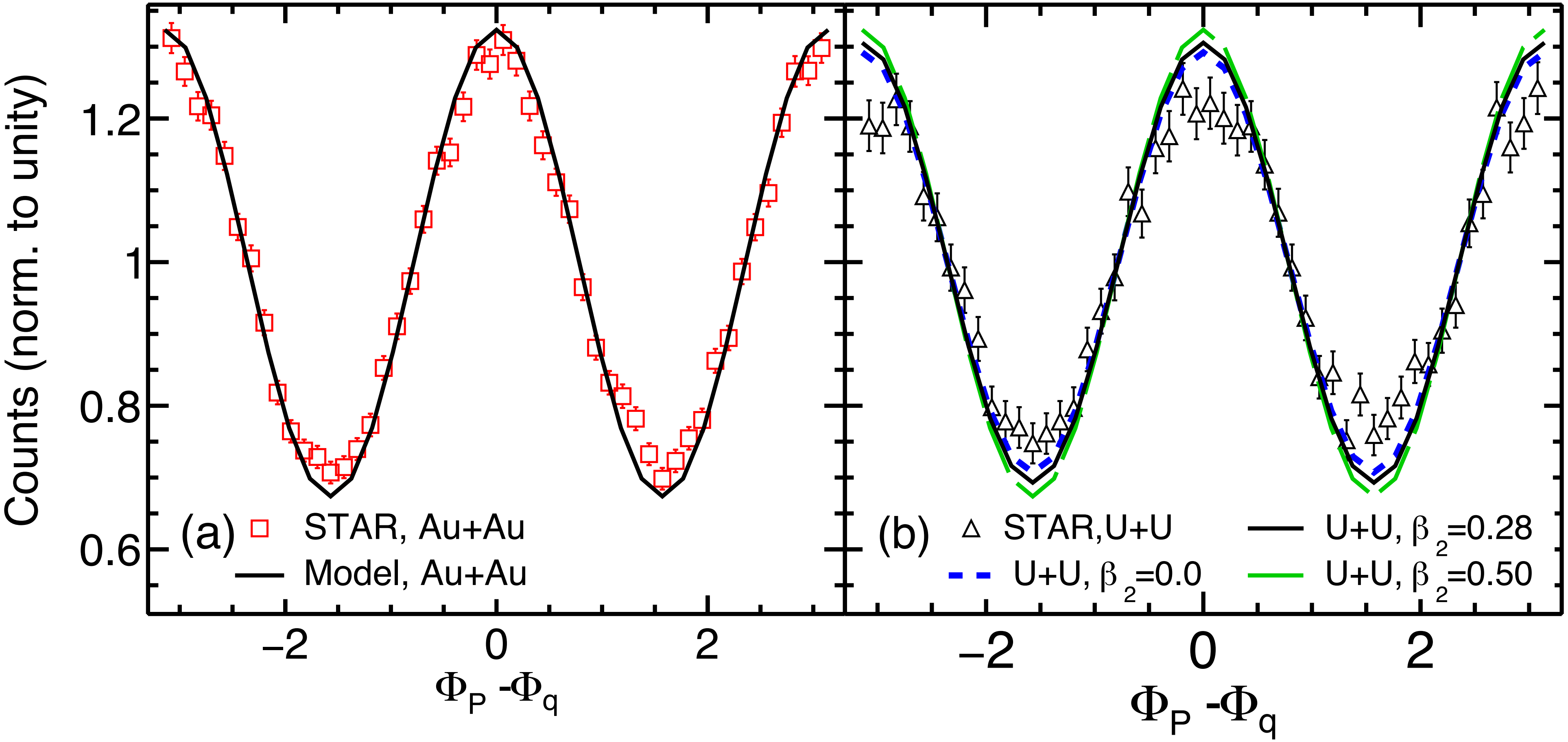

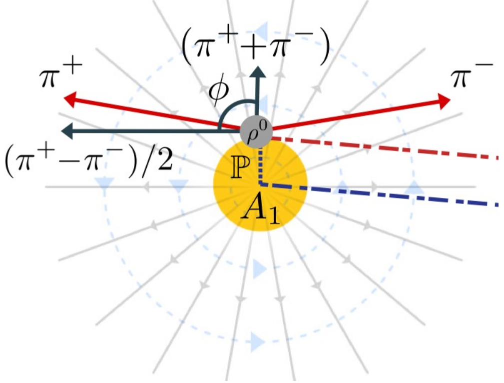

- Our model nicely reproduces the $\cos(2\Delta\Phi)$ modulation.
- In U+U, larger β_2 leads to slightly more pronounced $\cos(2\Delta\Phi)$ modulation.

H.Mantysaari, F. Salazar, B.Schenke, C. Shen and W. Zhao, PhysRevC.109.024908.
STAR Sci. Adv. 9 (2023) no.1, eabq3903.

Interference in Au+Au and U+U

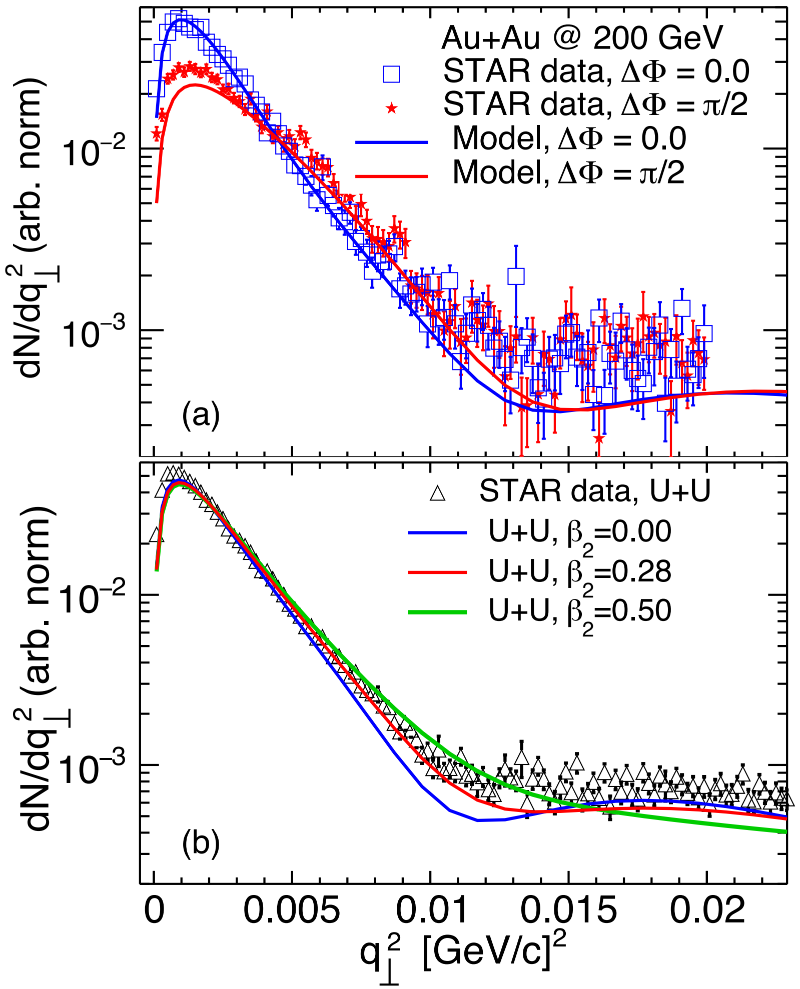

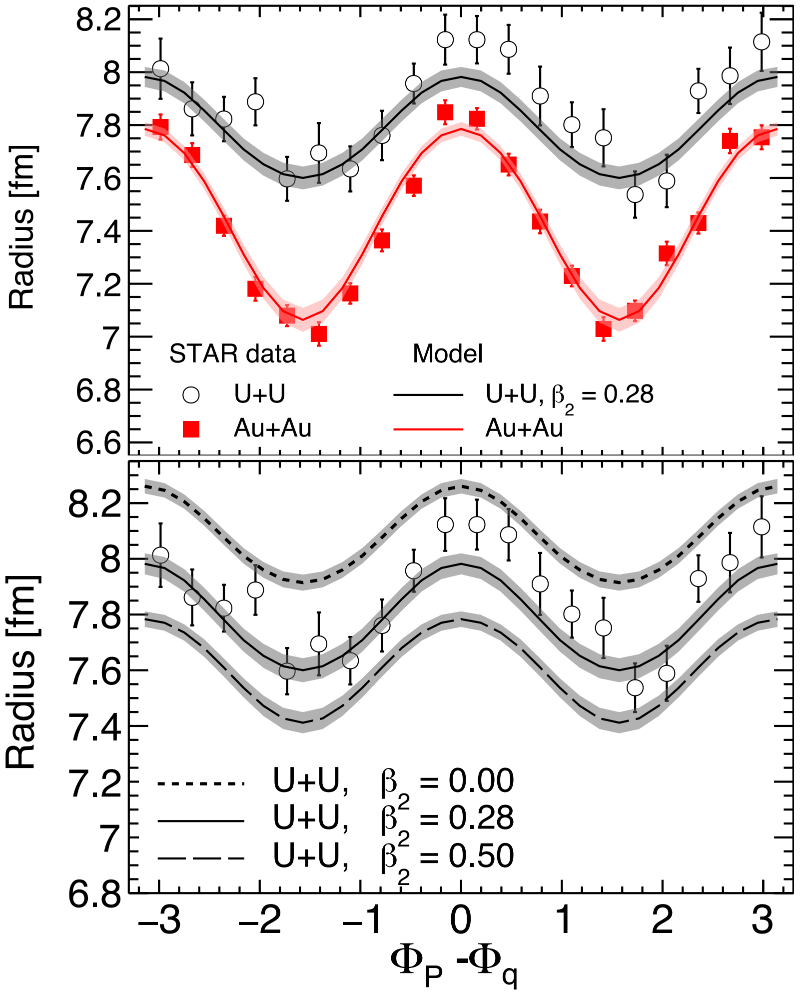

$$\frac{d\sigma^{\gamma^*+A\rightarrow VM+A^*}}{dt} \sim e^{-R\,|t|}$$

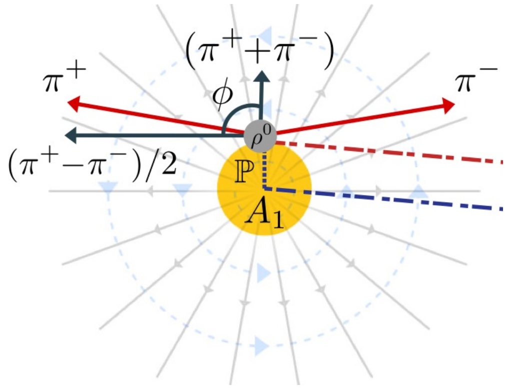

- In U+U, larger β_2 leads to flatter spectra (smaller radius). Larger β_2 has larger incoherent at low $q_\perp^2$, leads to the flatter $dN/dq_\perp^2$. Also the initial photon kT is more important.

H.Mantysaari, F. Salazar, B.Schenke, C. Shen and W. Zhao, PhysRevC.109.024908.
STAR Sci. Adv. 9 (2023) no.1, eabq3903.

Probing isobar, Ru/Zr

system	R_0 [fm]	a_0 [fm]	β_2	β_3	β_4
case1 (Ru+Ru)	5.09	0.46	0.16	0.0	0.0
case2 (Ru+Ru)	5.09	0.46	0.16	0.20	0.0
case3 (Ru+Ru)	5.09	0.46	0.06	0.20	0.0
case4 (Ru+Ru)	5.09	0.52	0.06	0.20	0.0
case5 (Zr+Zr)	5.02	0.52	0.06	0.20	0.0

$$R(\Theta,\Phi) = R_0\left[1 + \beta_2\left(\cos\gamma Y_{20}(\Theta) + \sin\gamma Y_{22}(\Theta,\Phi)\right) + \beta_3 Y_{30}(\Theta) + \beta_4 Y_{40}(\Theta)\right]$$

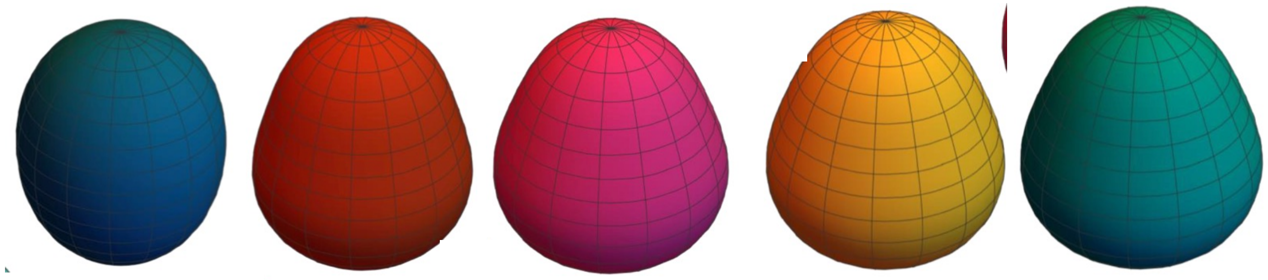

Taken from W. M. Serenone's slide.

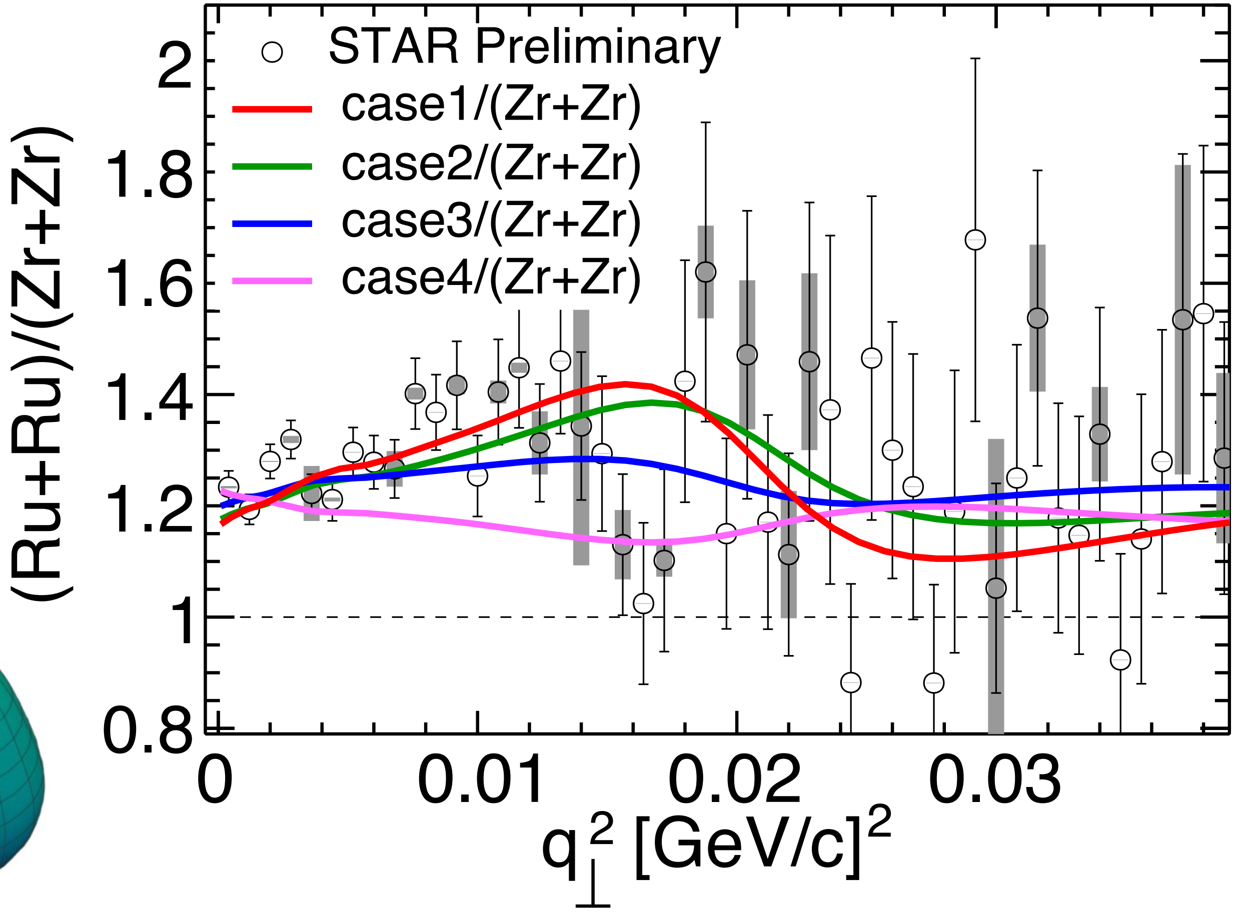

- The vector meson production in isobar UPCs is sensitive to the nuclear structures.
- "By eyes", the ``full'' Ru/Zr (case1/case5) is closest to data.

H.Mantysaari, F. Salazar, B.Schenke, C. Shen and W. Zhao PhysRevC.109.024908.

Collective flow in Polarized deuterons + Nuclei

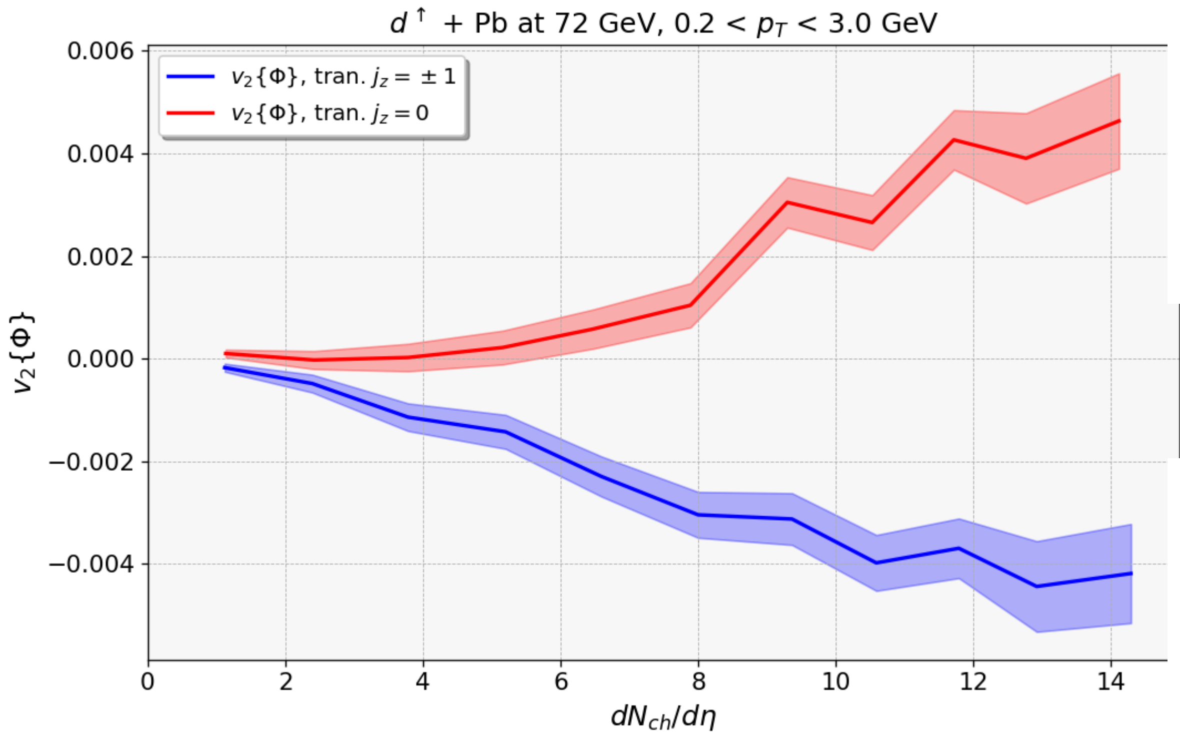

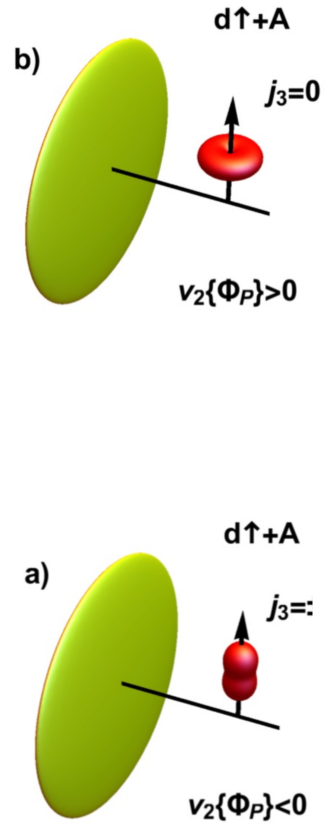

$$\vec{\epsilon}_n = -\frac{\int \rho d\rho d\alpha e^{in\alpha}\rho^n f(\vec{\rho})}{\int \rho d\rho d\alpha \rho^n f(\vec{\rho})}$$

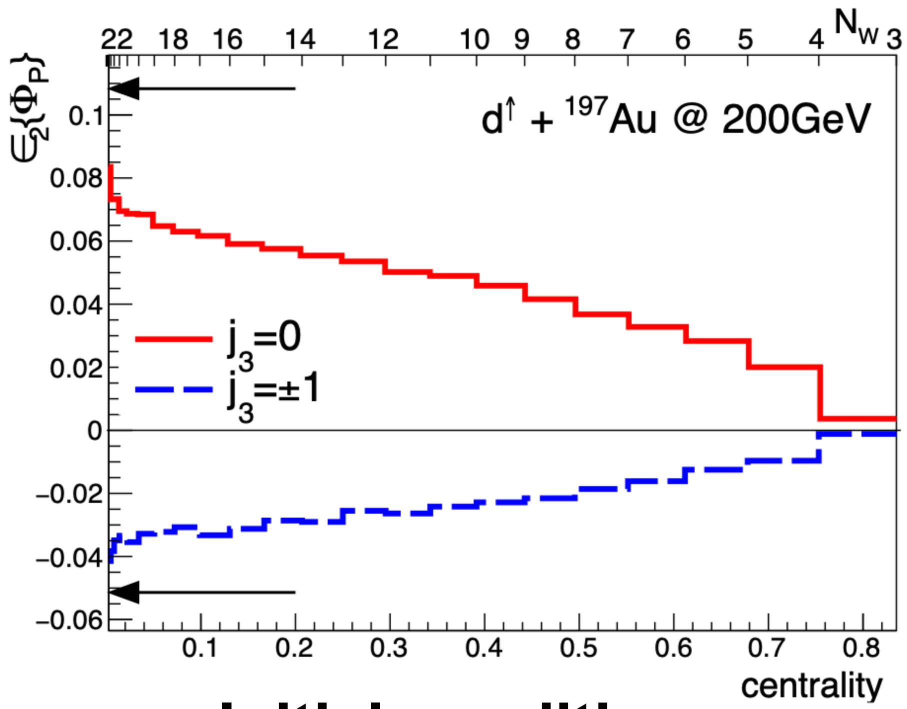

3+1D hydrodynamic simulations.

Initial conditions

- Opposite sign of $v_2\{\Phi\}$ between $j_z = \pm 1$ and $j_z = 0$ in $d^\uparrow + Pb$.
- Could be tested in the coming LHCb measurement.

H.Mantysaari, B.Schenke, C. Shen and W. Zhao in progress.
LHCb: PoS SPIN2023, 036 (2024).

P. Bozek and W. Broniowski, PhysRevLett.121.202301

JIMWLK evolution to smaller x

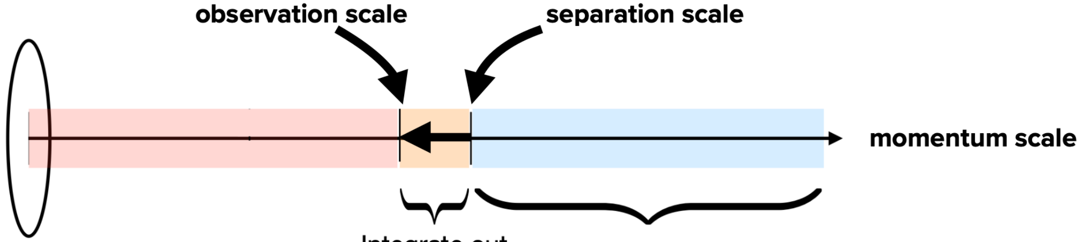

$$\langle\langle\mathcal{O}\rangle\rangle = \int [\mathcal{D}\rho]\, W_{\Lambda^+_{\rm cut}}[\rho]\, \frac{\int^{\Lambda^+_{\rm cut}} [\mathcal{D}A]\, \mathcal{O} e^{iS[A,\rho]}}{\int^{\Lambda^+_{\rm cut}} [\mathcal{D}A]\, e^{iS[A,\rho]}}$$

CGC average for ρ

Path integral in the presence of ρ

$W_{\Lambda^+_{\rm cut}}[\rho]$ Non-perturbative Weight functional for distribution of sources

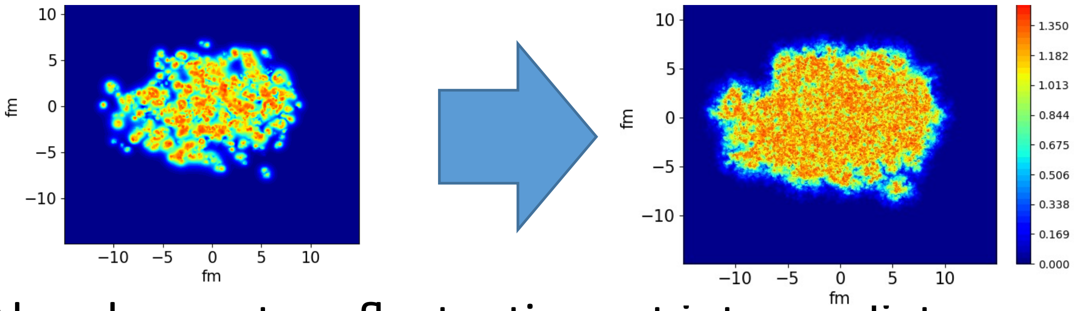

Absorb quantum fluctuations at intermediate x as the color sources of smaller x.

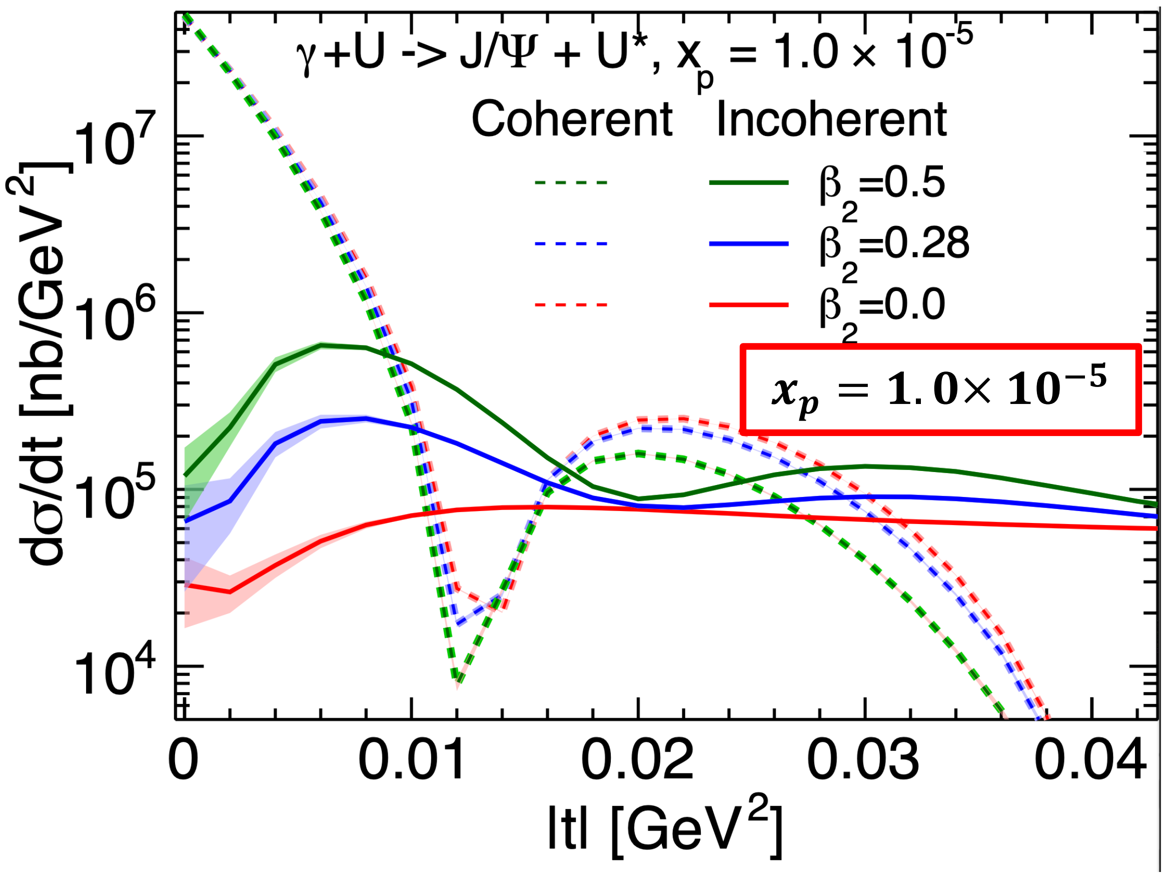

- JIMWLK evolution doesn't wash out this effects.

H.Mantysaari, B.Schenke, C. Shen and W. Zhao PhysRevLett.131.062301
H.Mantysaari, B.Schenke PRD, 98, 034013.
T. Lappi and H. Mantysaari, EPJC 73, 2307 (2013).
Yuri V. Kovchegov, QUANTUM CHROMODYNAMICS A T HIGH ENERGY

Proton & hotspot sizes at high energy

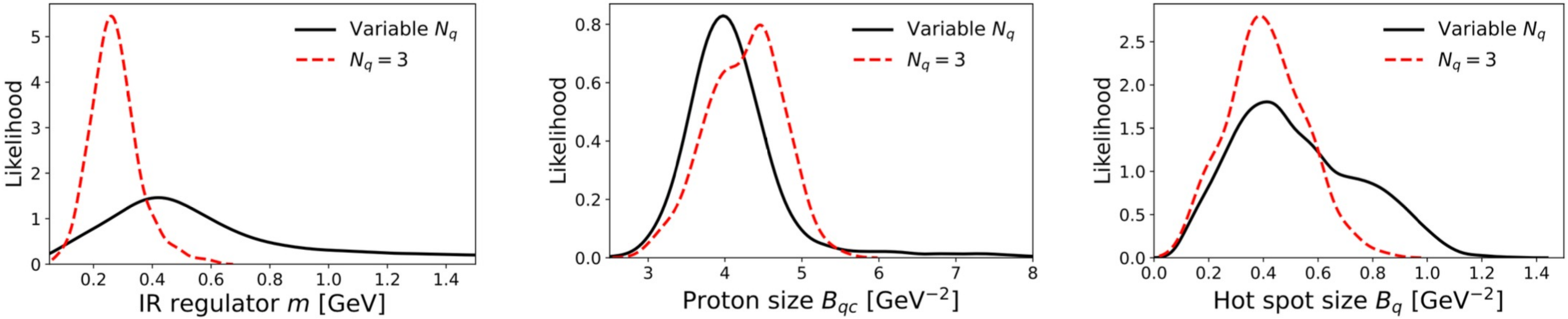

- Some parameters are well constrained .
- The 2D RMS proton radius $R_{rms} = \sqrt{2(B_{qc} + B_q)} \sim 0.6$ fm by fitting the J/Ψ t-spectra at HERA.

H.Mantysaari, B.Schenke, C. Shen and W. Zhao, Phys. Lett. B 833 (2022), 137348.
H.Mantysaari, B.Schenke, C. Shen and W. Zhao, [arXiv:2208.00396 [hep-ph]].

Degeneracy in the number of hot spots

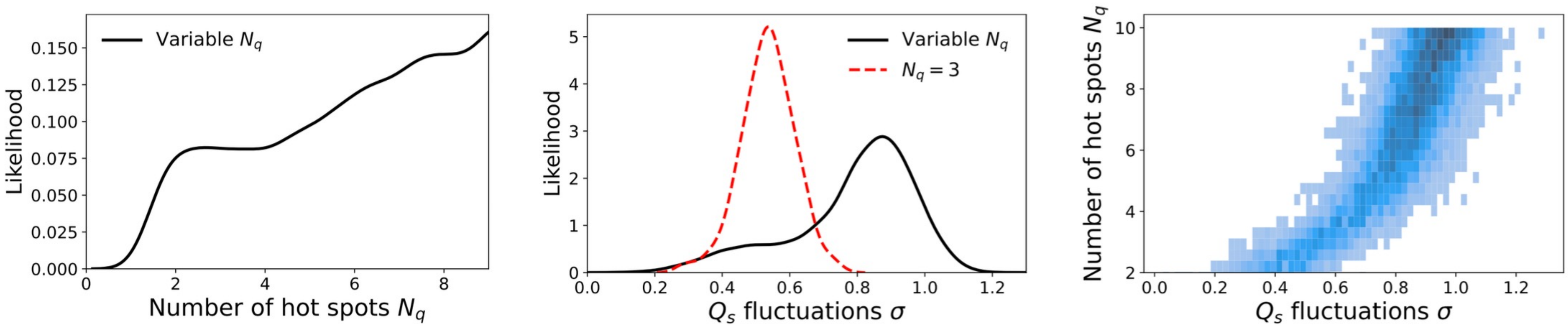

- The likelihood of number of hot spots Nq increases monotonously.
- Large Nq partially compensated by large Qs fluctuations, $\sigma \propto \sqrt{N_q}$, "number of effective hot spots" < Nq

- **Proton's event-by-event fluctuating density profile:**

$$T_p(\mathbf{b}_\perp) = \frac{1}{N_q}\sum_{i=1}^{N_q} p_i T_q(\mathbf{b}_\perp - \mathbf{b}_{\perp,i}), \quad P(\ln p_i) = \frac{1}{\sqrt{2\pi}\sigma}\exp\left[-\frac{\ln^2 p_i}{2\sigma^2}\right].$$

H. Mantysaari, B.Schenke, C. Shen and W. Zhao, Phys. Lett. B 833 (2022), 137348.

MAP of fixed Nq=3 and Nq=9

Parameter	Description	$N_q = 9$	$N_q = 3$
m [GeV]	Infrared regulator	0.780	0.246
B_{qc} [GeV^{-2}]	Proton size	3.98	4.45
B_q [GeV^{-2}]	Hot spot size	0.594	0.346
σ	Magnitude of Q_s fluctuations	0.932	0.563
$Q_s/(g^2\mu)$	$Q_s \Rightarrow$ color charge density	0.492	0.747
$d_{q,\mathrm{Min}}$ [fm]	Min hot spot distance	0.265	0.254
N_q	Number of hot spots	3	9
S	Hydro normalization	0.1135	0.235

- The Nq=3 and Nq=9 have the different configurations at large length scales.
- “See” them by the different probes.

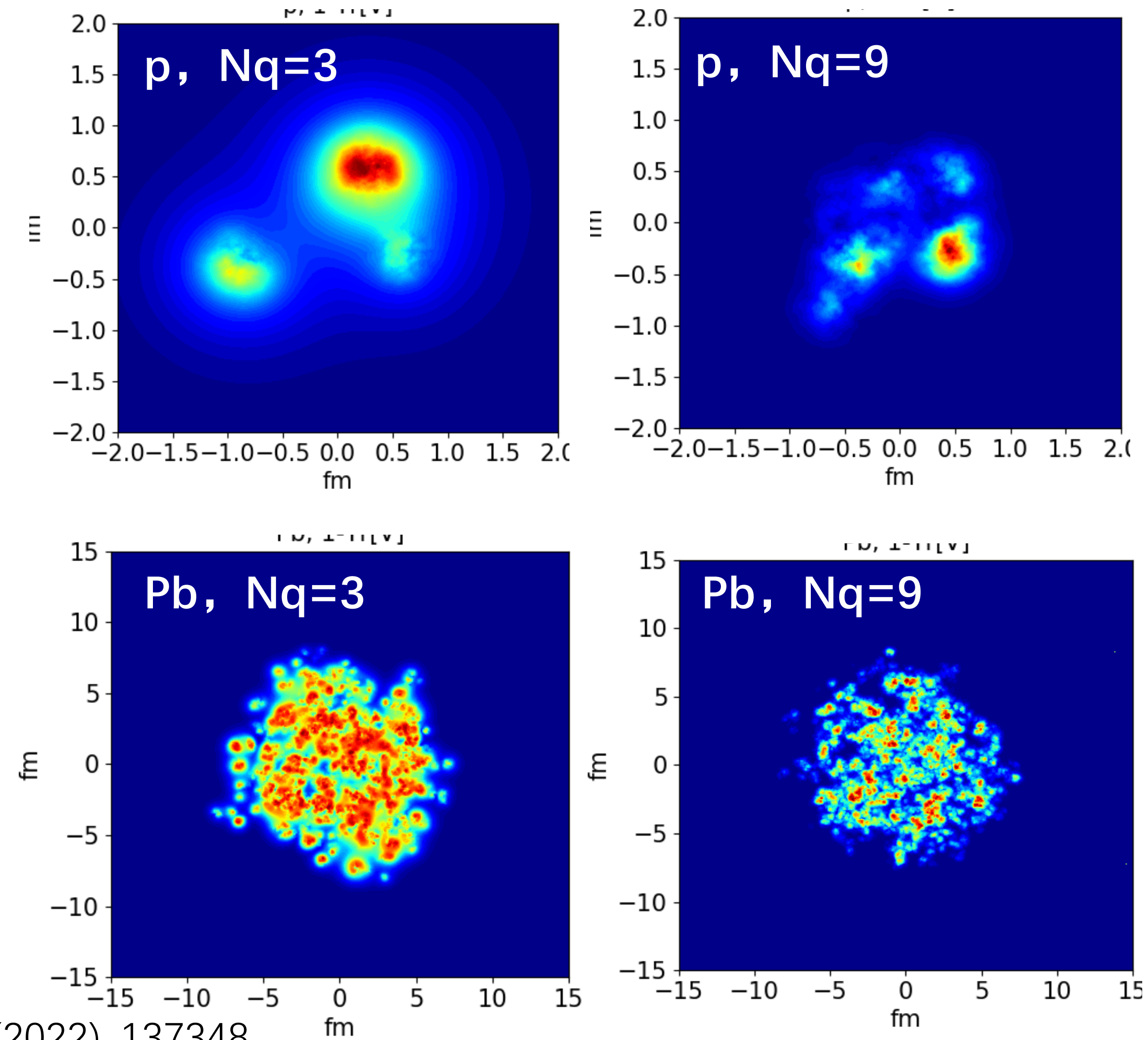

H. Mantysaari, B.Schenke, C. Shen and W. Zhao, Phys. Lett. B 833 (2022), 137348.
H. Mantysaari, B.Schenke, C. Shen and W. Zhao, [arXiv:2208.00396 [hep-ph]].

Probing protons at different resolutions

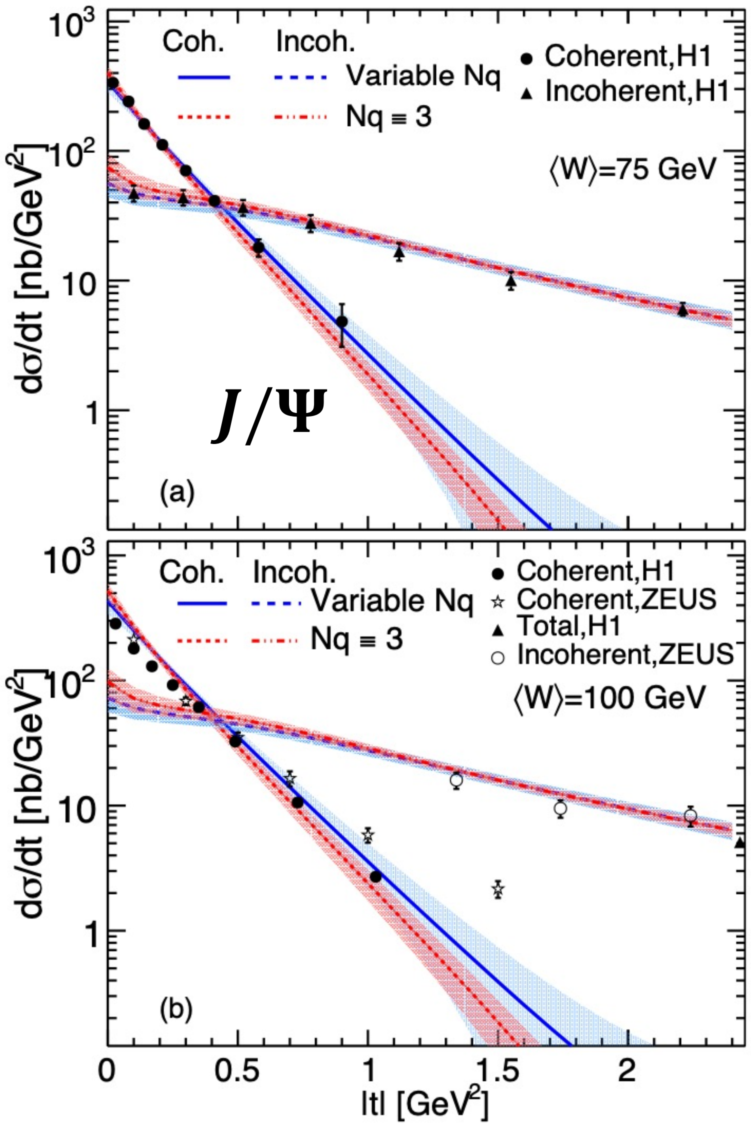

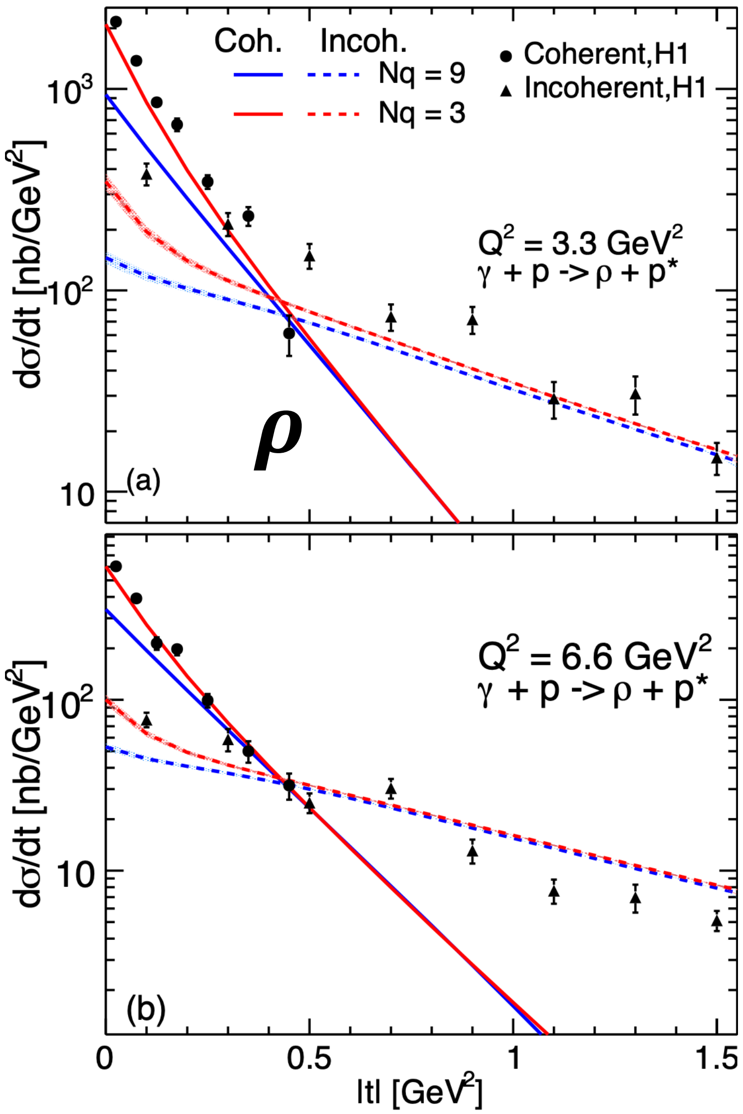

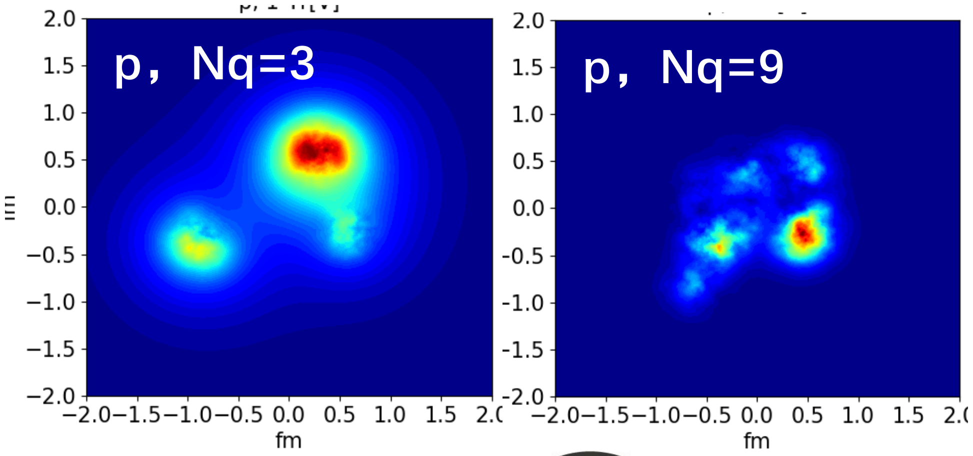

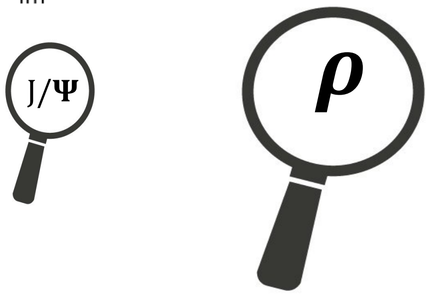

- The ρ mesons probe proton fluctuations at large length scales.
- Large differences observed for ρ productions between Nq=3 and Nq=9 MAPs.
- Larger Q^2, smaller difference.

H. Mantysaari, B.Schenke, C. Shen and W. Zhao, Phys. Lett. B 833 (2022), 137348, and in progress.

Hydrodynamics response to collision geometry in HIC

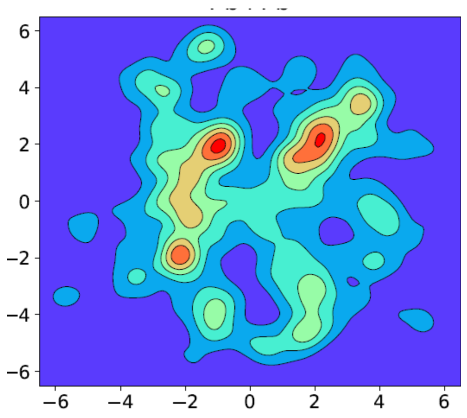

Hydrodynamics →

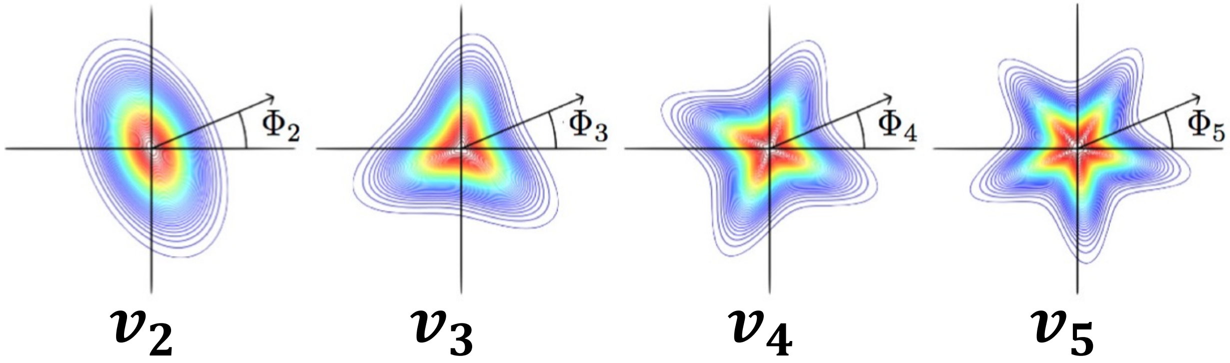

Fourier decomposition of final particle azimuthal distribution

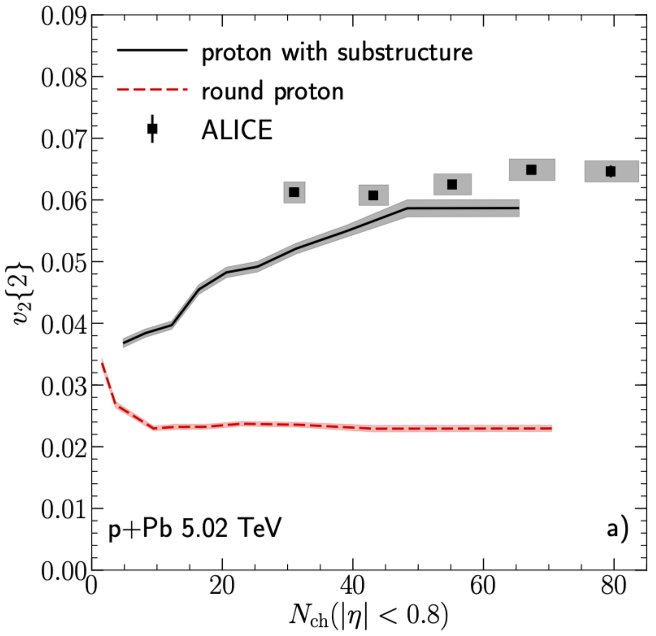

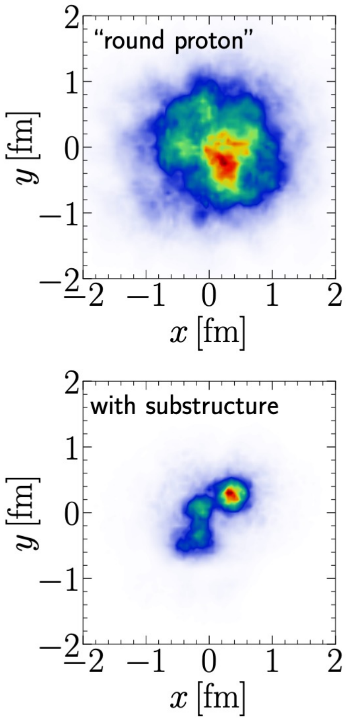

$$\frac{dN}{d\phi} = \frac{N}{2\pi}\left(1 + 2\sum_{n=1}^{\infty} v_n \cos[n(\phi - \Psi_n)]\right)$$

- Heavy-ion Collisions: Initial spatial geometry ⇒ final momentum anisotropy.
- Proton's sub-nucleonic structure is crucial to understand the collectivity in small collision systems

B. Schenke, Rept. Prog. Phys. 84, 082301 (2021).

Connecting to Relativistic Nuclear Collisions

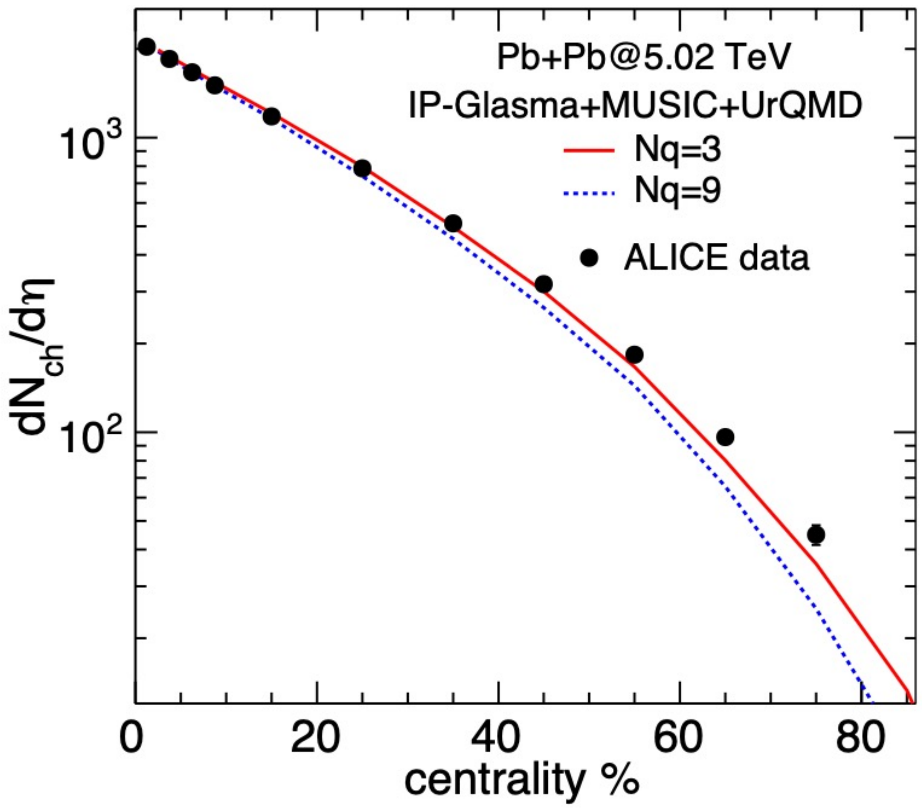

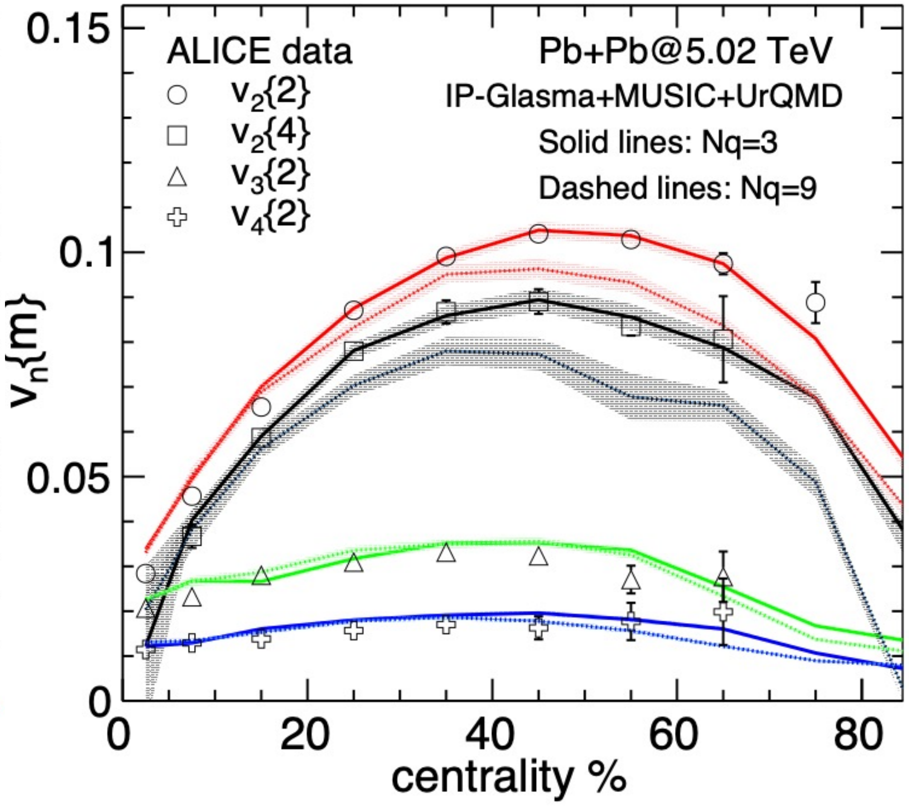

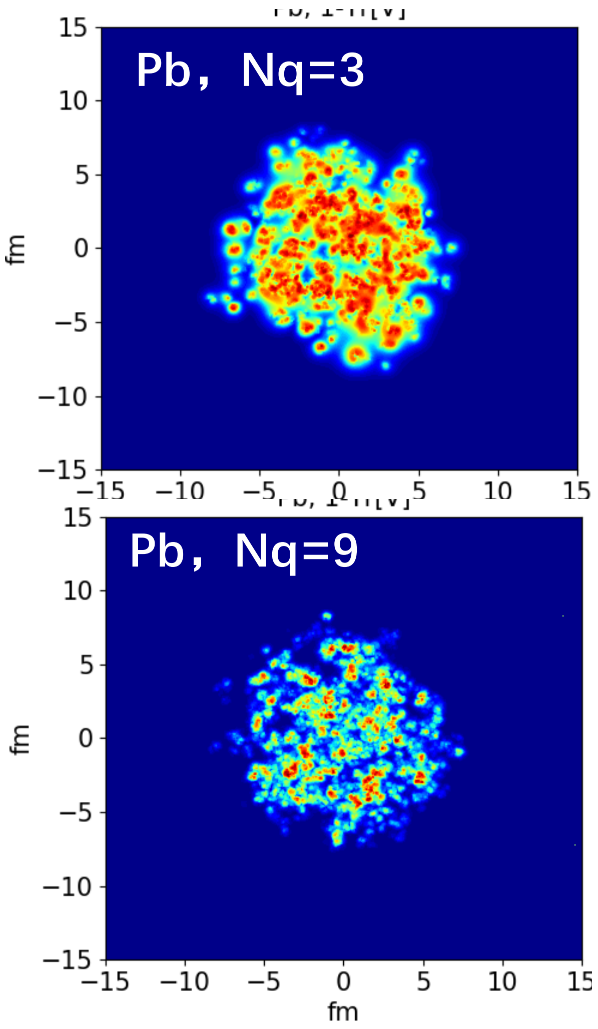

- The multiplicity distributions and elliptic flow coefficients in Pb+Pb collisions favor the small Nq case.

H.Mantysaari, B.Schenke, C. Shen and W. Zhao, Phys. Lett. B 833 (2022), 137348.
H.Mantysaari, B.Schenke, C. Shen and W. Zhao, [arXiv:2208.00396 [hep-ph]].

p + Pb Collisions

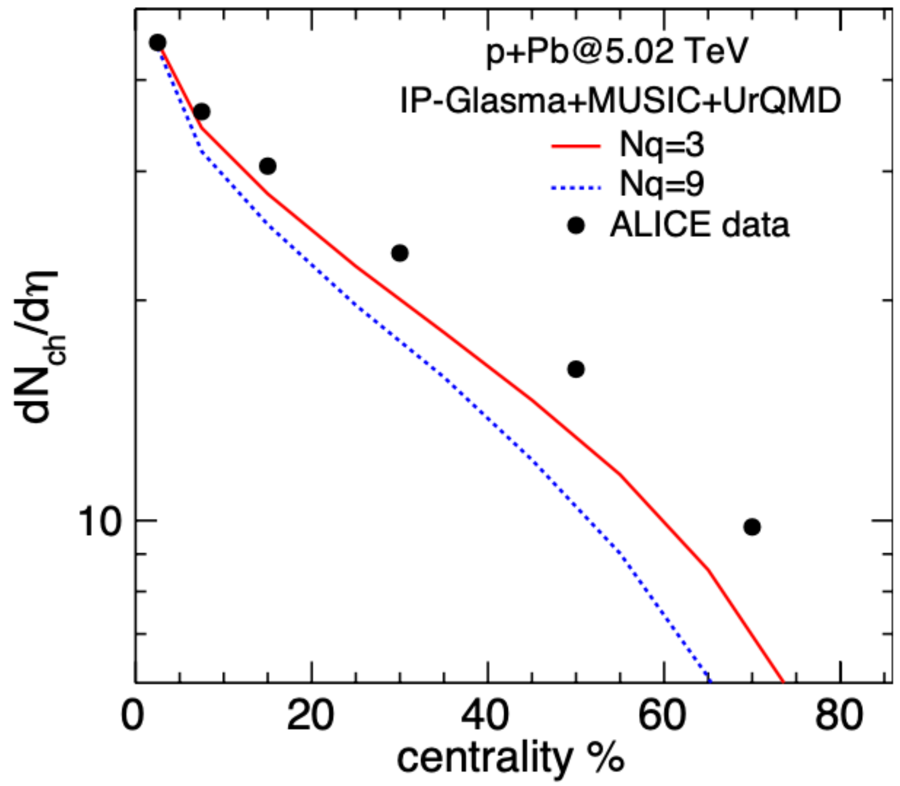

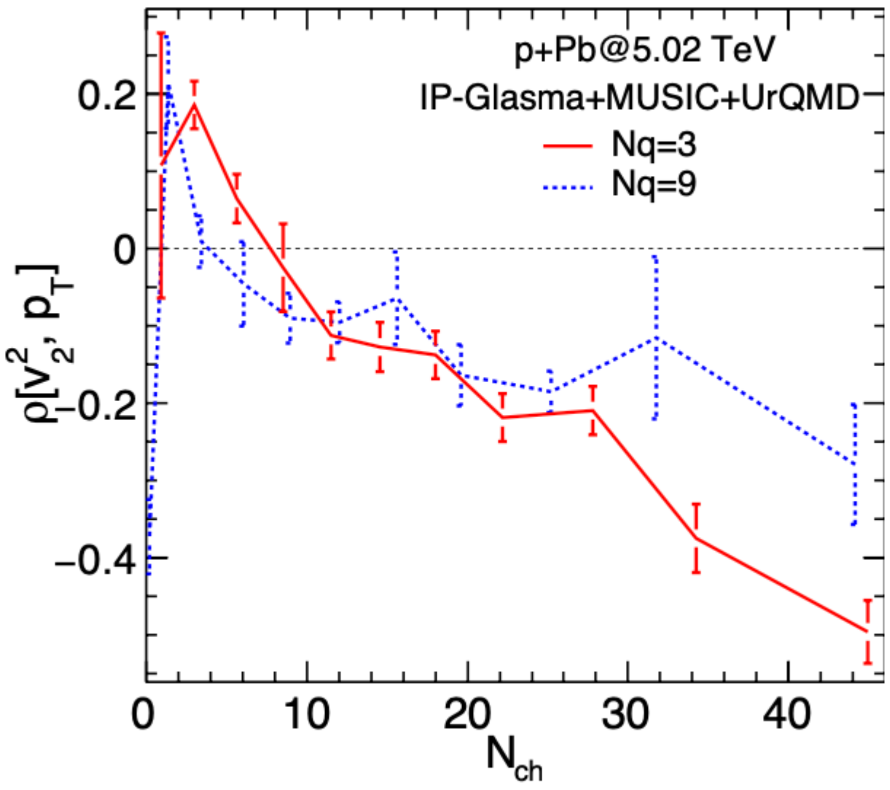

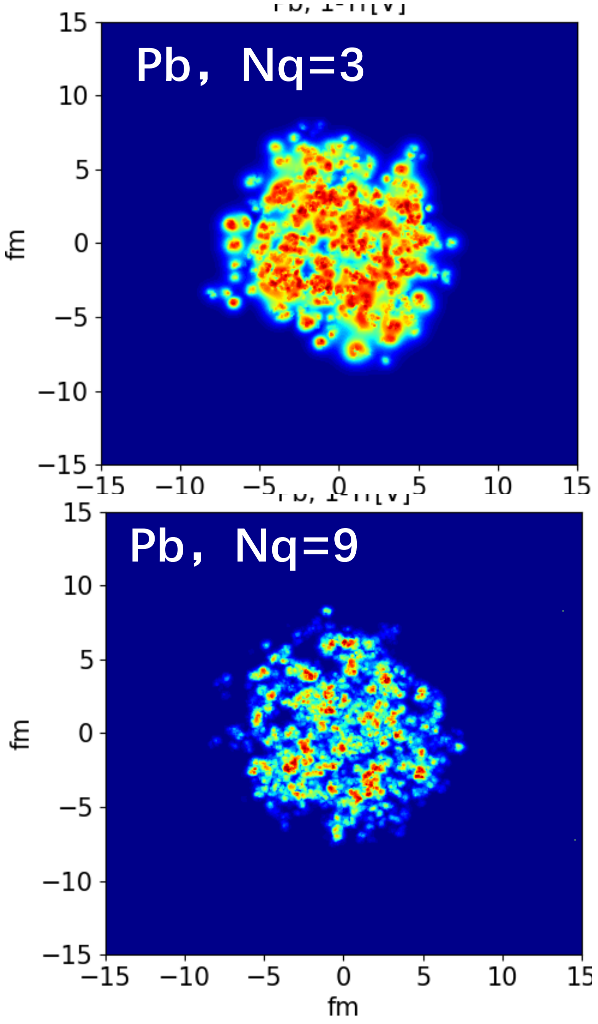

- Similar to Pb+Pb case, p+Pb favors the small Nq case as well.
- $v_2 - p_T$ correlator in p+Pb identified as a promising observable.
- We would like to explore more experimental constraints using HERA + LHC Pb+Pb and p+Pb data

H.Mantysaari, B.Schenke, C. Shen and W. Zhao, Phys. Lett. B 833 (2022), 137348.
H.Mantysaari, B.Schenke, C. Shen and W. Zhao, [arXiv:2208.00396 [hep-ph]].

Probing ^{20}Ne and ^{16}O

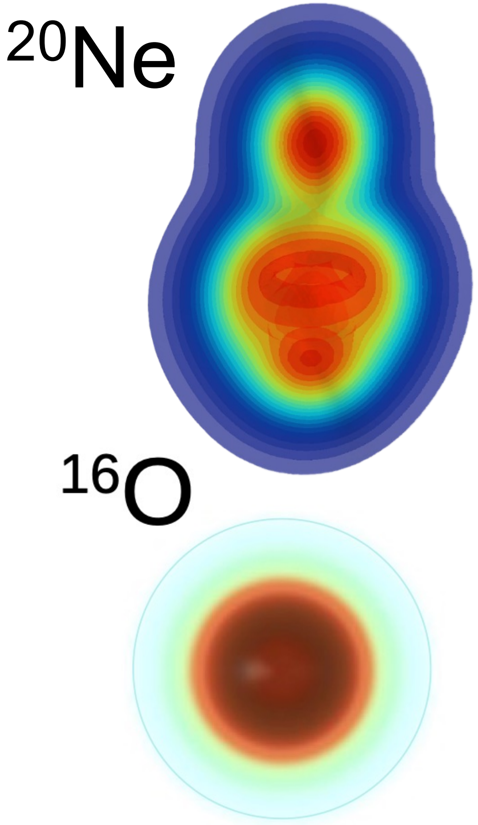

Nucleon density distribution is taken from G. Giacalone.

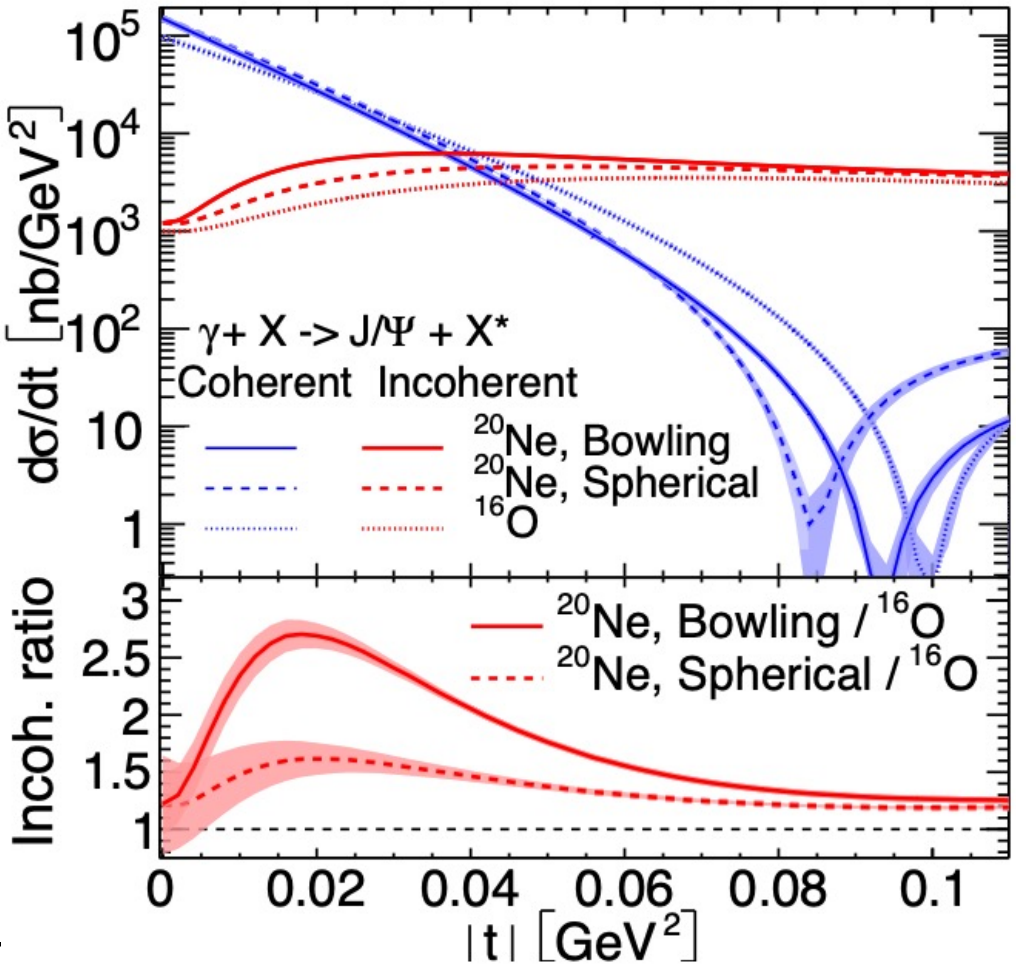

- Incoherent cross section at small |t| captures the deformation of the ^{20}Ne.
- Significant difference between ^{20}Ne and ^{16}O diffractive cross sections is observed.

H.Mantysaari, B.Schenke, C. Shen and W. Zhao, [arXiv:2303.04866] (accepted by PRL).

Bayes Theorem

Thomas Bayes

Probabilistic constraints on parameters (→ prior)

Mean value of measurements (→ D)

Experimental and theoretical **uncertainties** (→ Cov)

$$\mathbf{posterior}(p|D) \propto prior(p) \times exp\left(-\frac{1}{2}(D - Model(p))^T\ Cov^{-1}\,(D - Model(p))\right)$$

External constraints on parameters:
positivity or range of allowed values, "probabilistic theoretical constraints", …

Prediction of model for given set of parameters

Ref: Jean-Francois, APS, 2021

- Constrain the model parameters by the Bayesian analysis.

JIMWLK evolution to smaller xp

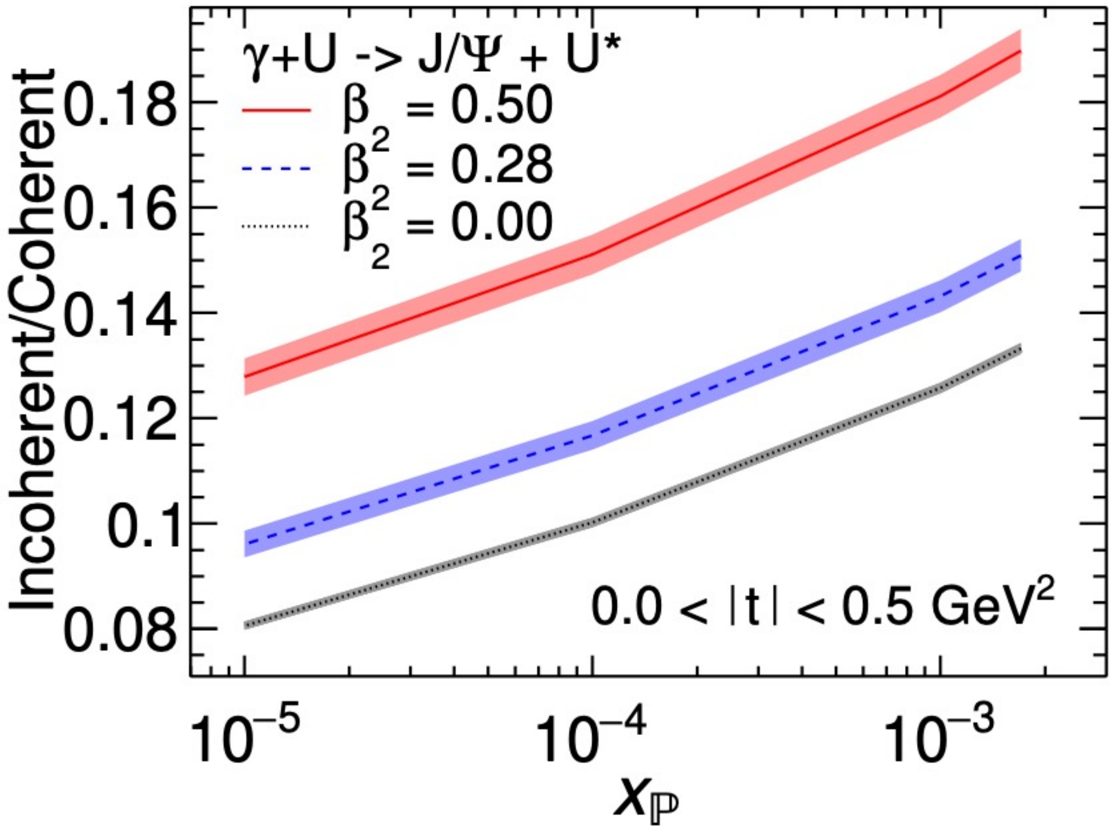

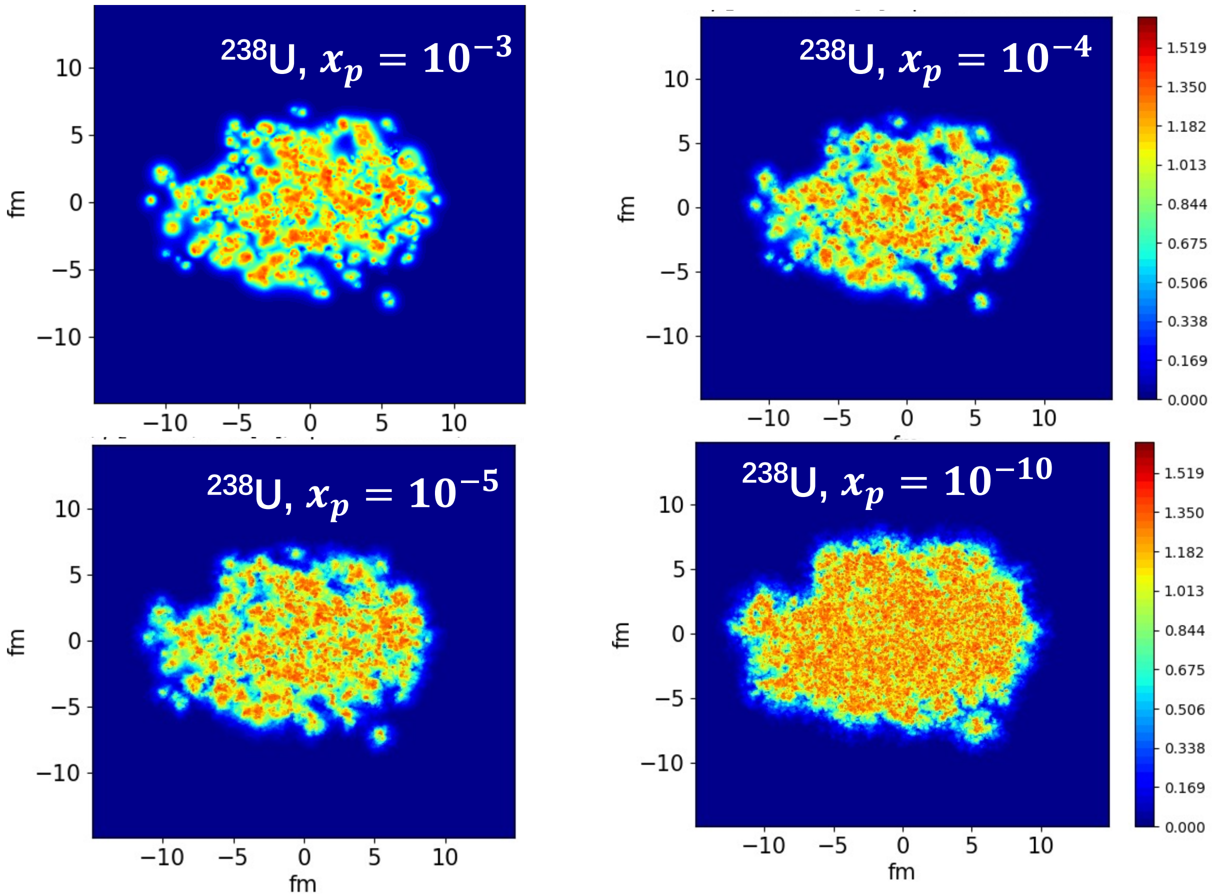

- Incoherent-to-coherent ratio effectively suppresses model uncertainties from wave functions.
- At smaller x_p, nucleon is smoother, reduces the fluctuations, decreases Incoherent-to-coherent ratio.
- JIMWLK evolution doesn't wash out difference between different β_2 (β_2 controls overall shape).

H.Mantysaari, B.Schenke, C. Shen and W. Zhao, in progress.
H.Mantysaari, B.Schenke PRD, 98, 034013.

Diffraction in optics

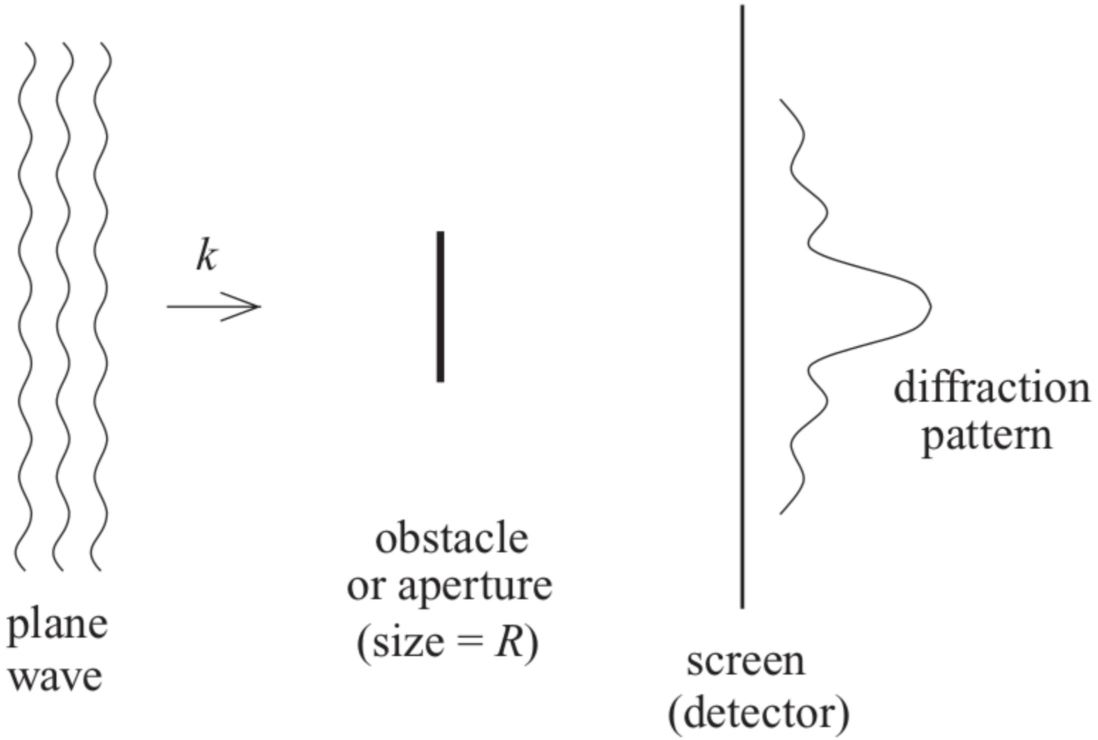

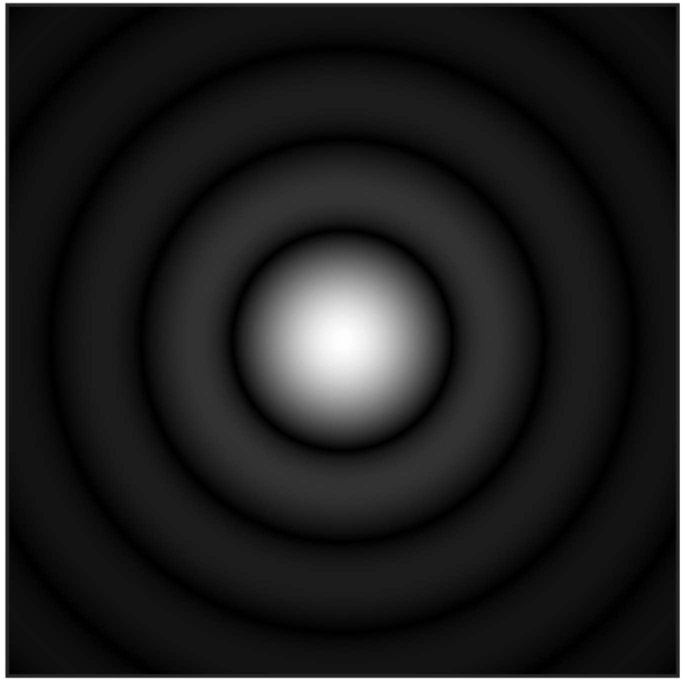

Taken from Wiki

- In momentum-space the positions of the minima and maxima of diffraction pattern are determined solely by the target size R.

Yuri V. Kovchegov, QUANTUM CHROMODYNAMICS A T HIGH ENERGY

Proton & hotspot sizes at high energy

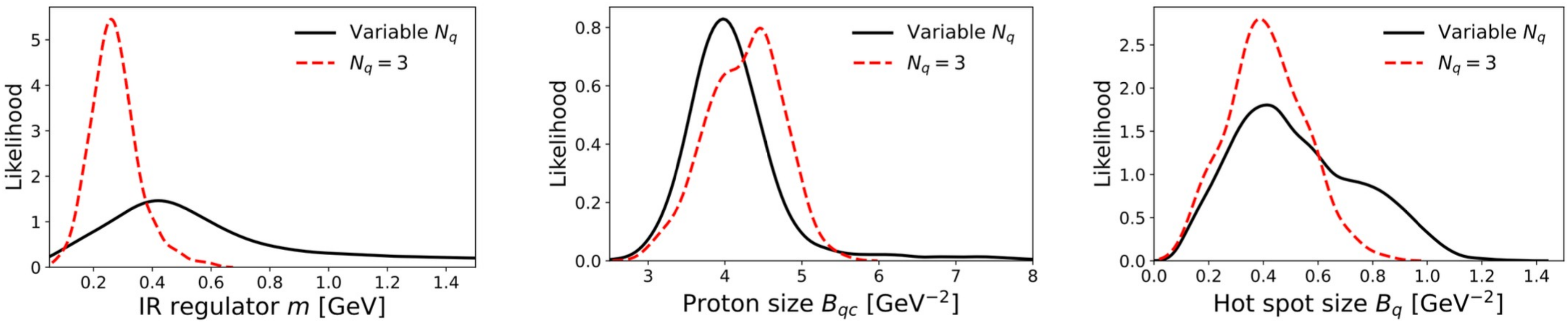

- Some parameters are well constrained .
- Wider posterior distributions for the varying Nq case.
- The 2D RMS proton radius $R_{rms} = \sqrt{2(B_{qc} + B_q)} \sim$ 0.6 fm, which is consistent with the results in heavy-ion collisions.

H.Mantysaari, B.Schenke, C. Shen and W. Zhao, Phys. Lett. B 833 (2022), 137348.
H.Mantysaari, B.Schenke, C. Shen and W. Zhao, [arXiv:2208.00396 [hep-ph]].
G. Giacalone, B. Schenke and C. Shen, Phys. Rev. Lett. 128, 042301 (2022)

Fixed Nq ≡ 1 cases

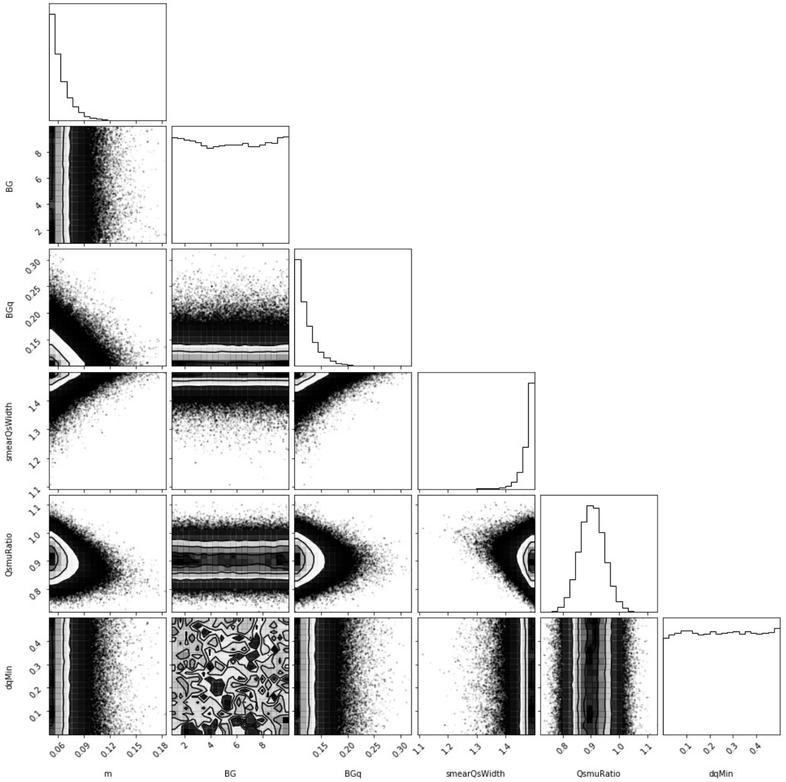

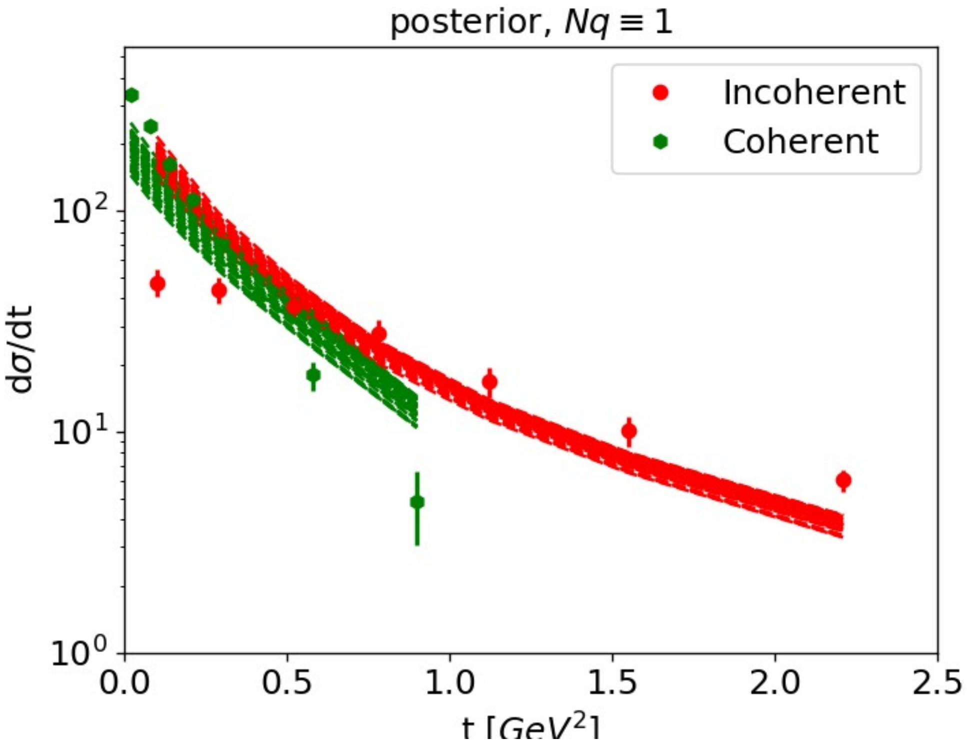

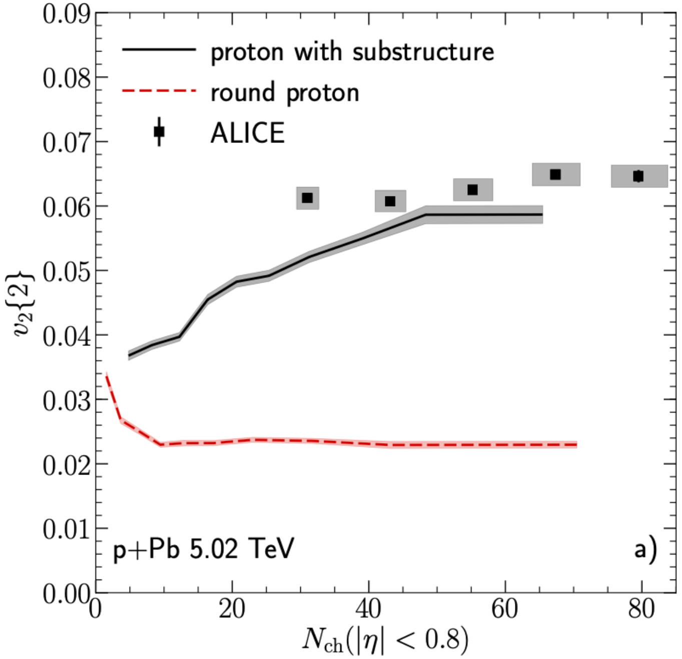

B. Schenke, Rept. Prog. Phys. 84, 082301 (2021).

- Bayesian analysis with fixed Nq≡1 can't extract the parameter set to fit the HERA data.
- It's consistent with the hydrodynamic results.

H.Mantysaari, B.Schenke, C. Shen and W. Zhao, Phys. Lett. B 833 (2022), 137348.

Closure tests

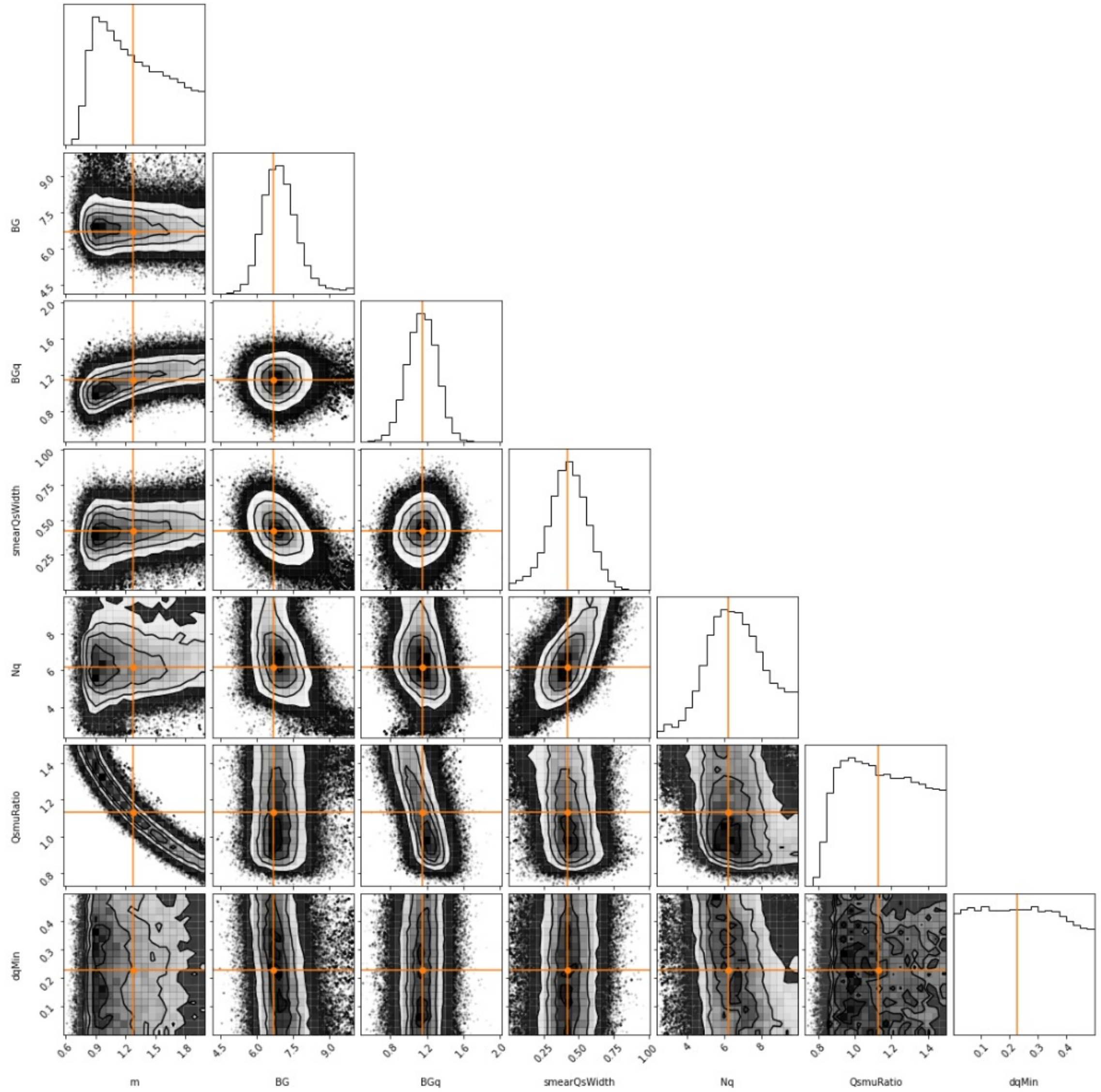

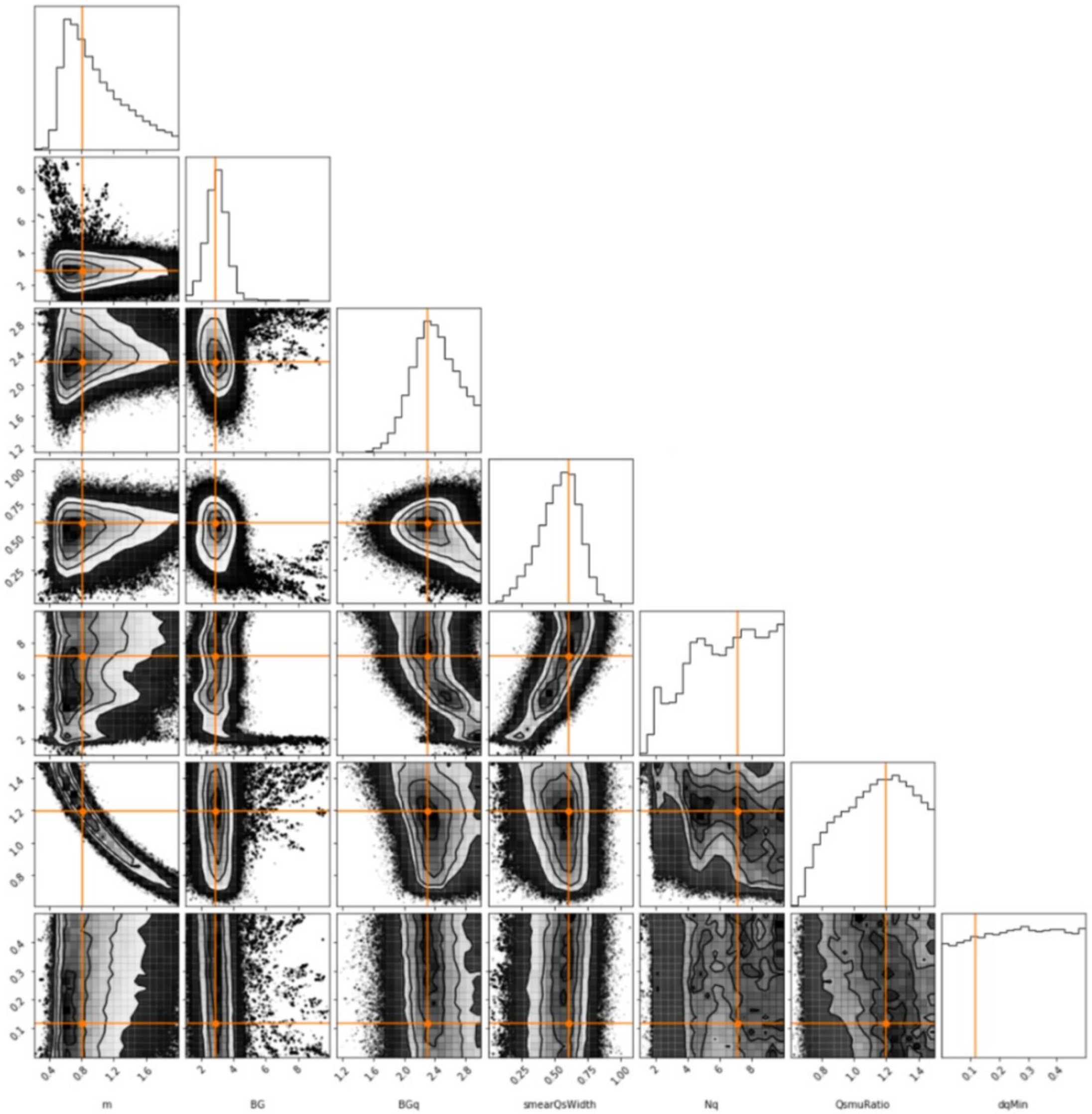

H.Mantysaari, B.Schenke, C. Shen and W. Zhao, Phys. Lett. B 833 (2022), 137348.

Building intuition for the model parameters

- Proton size:

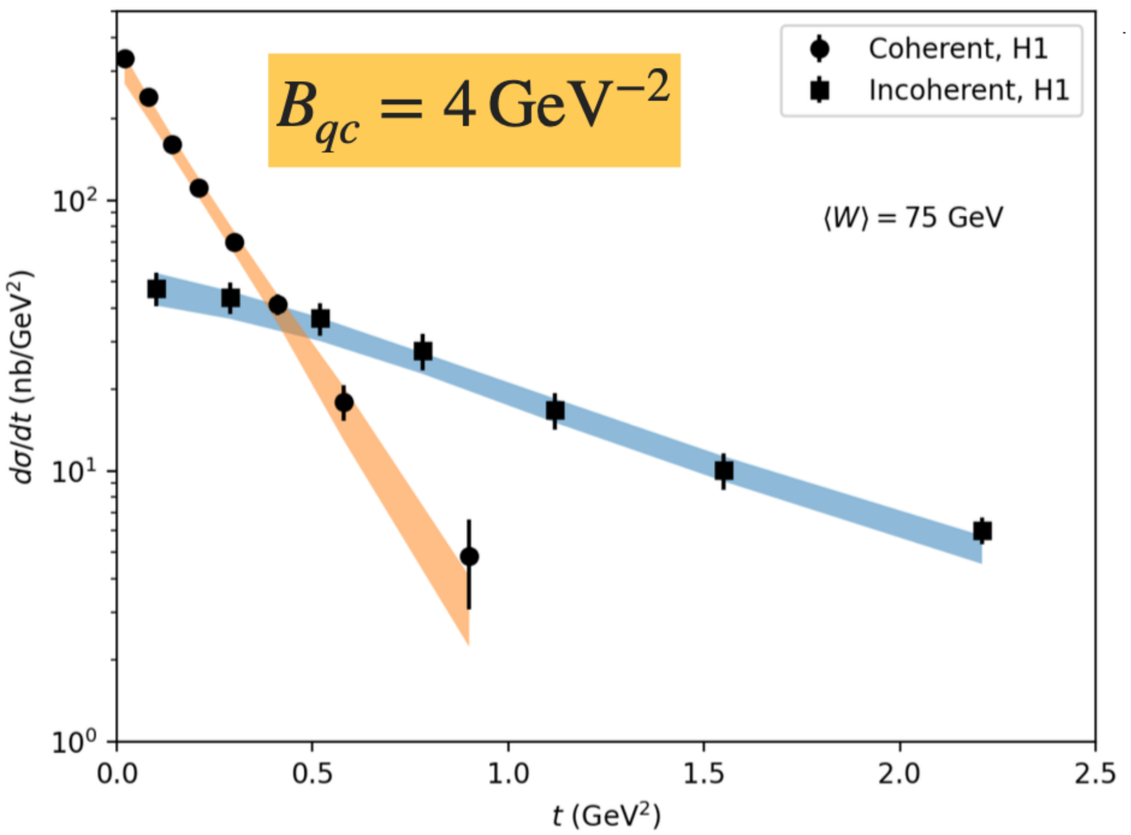

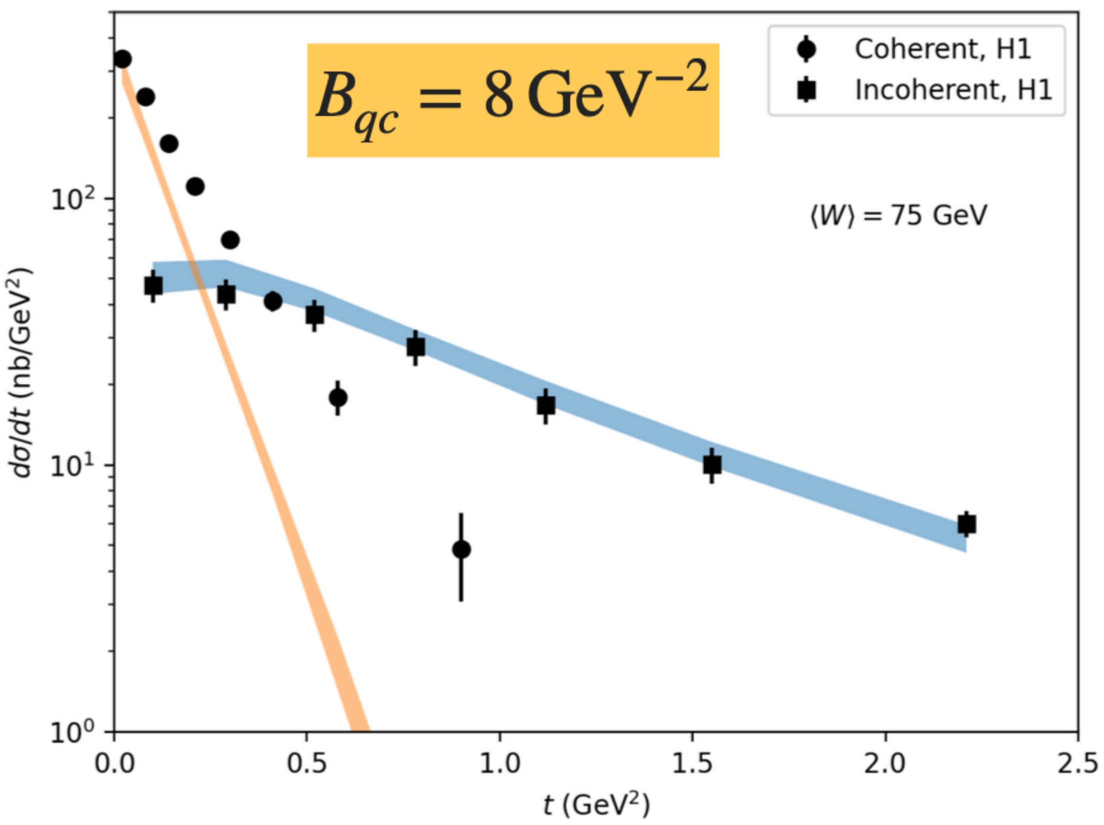

- The proton size mainly affects the coherent cross section.

H.Mantysaari, B.Schenke, C. Shen and W. Zhao, Phys. Lett. B 833 (2022), 137348.

Building intuition for the model parameters

- Hot spot size:

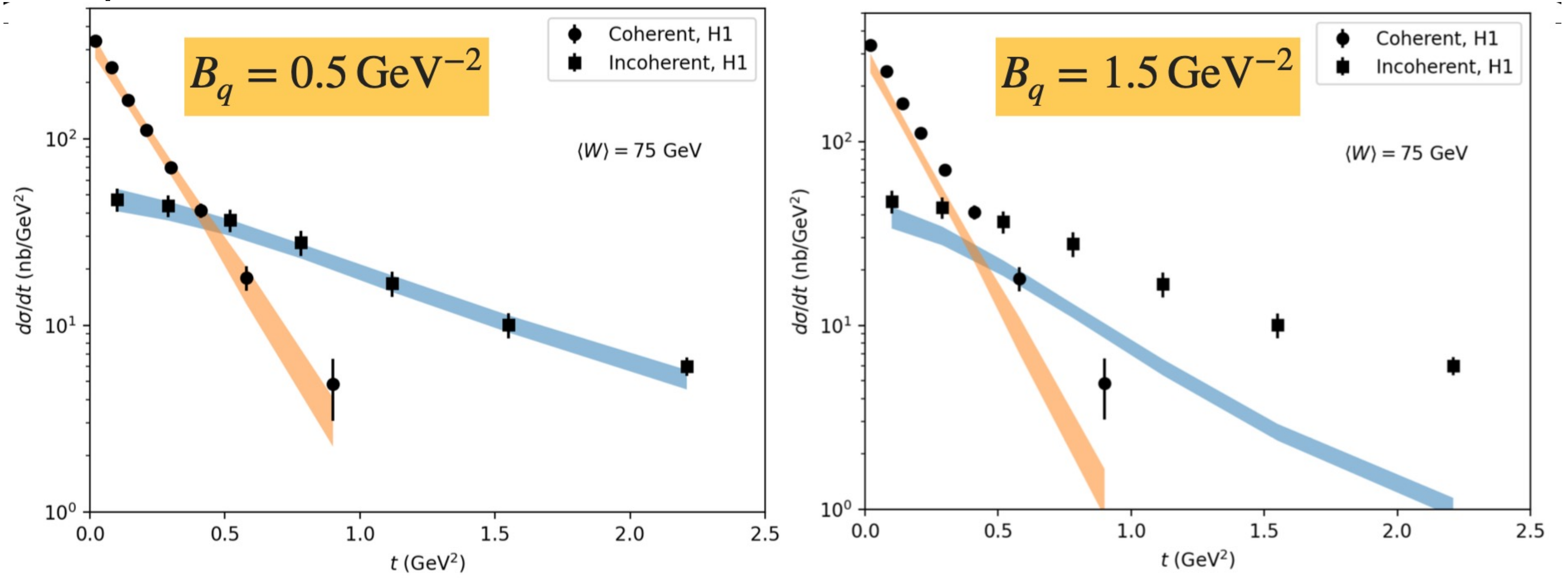

- The shape of incoherent cross-section is sensitive to the sub-nucleonic hot spot size

H.Mantysaari, B.Schenke, C. Shen and W. Zhao, Phys. Lett. B 833 (2022), 137348.

Building intuition for the model parameters

- Infrared regulator:

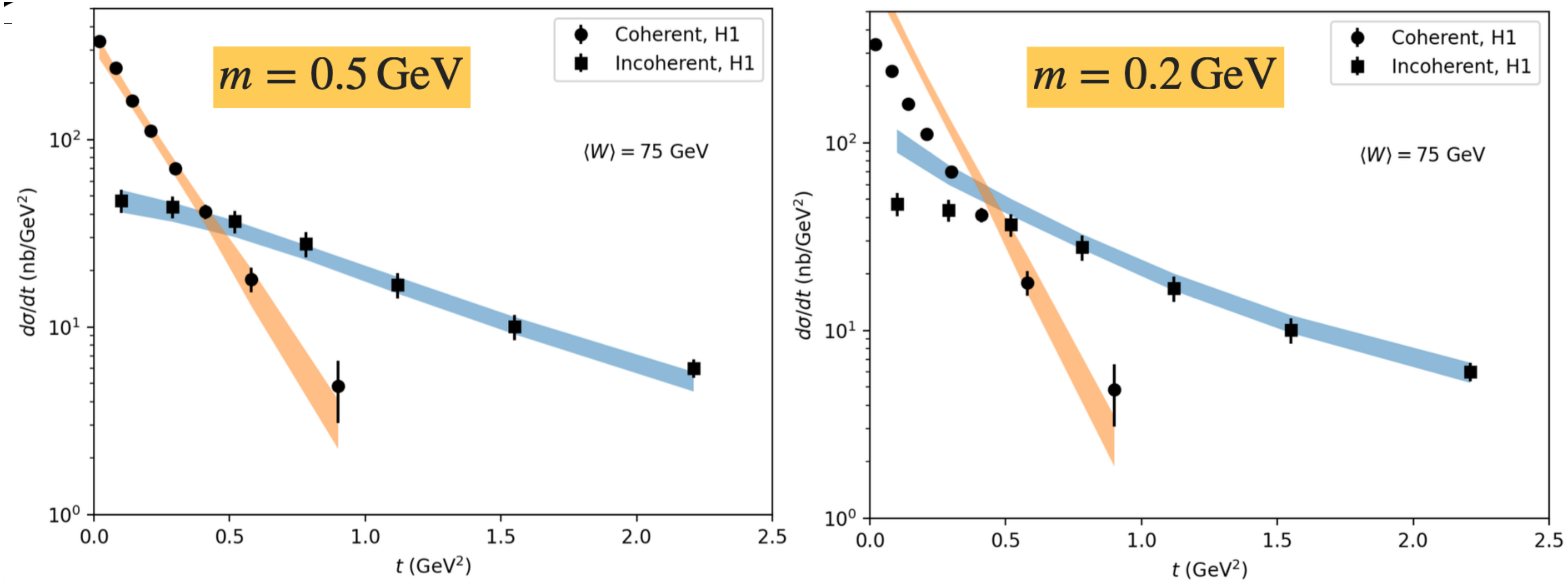

- A small infrared regulator extends density tail in the large scale region, which results in increase of coherent and incoherent cross-section at low |t|.

H.Mantysaari, B.Schenke, C. Shen and W. Zhao, Phys. Lett. B 833 (2022), 137348.

Building intuition for the model parameters

- Overall color charge density:

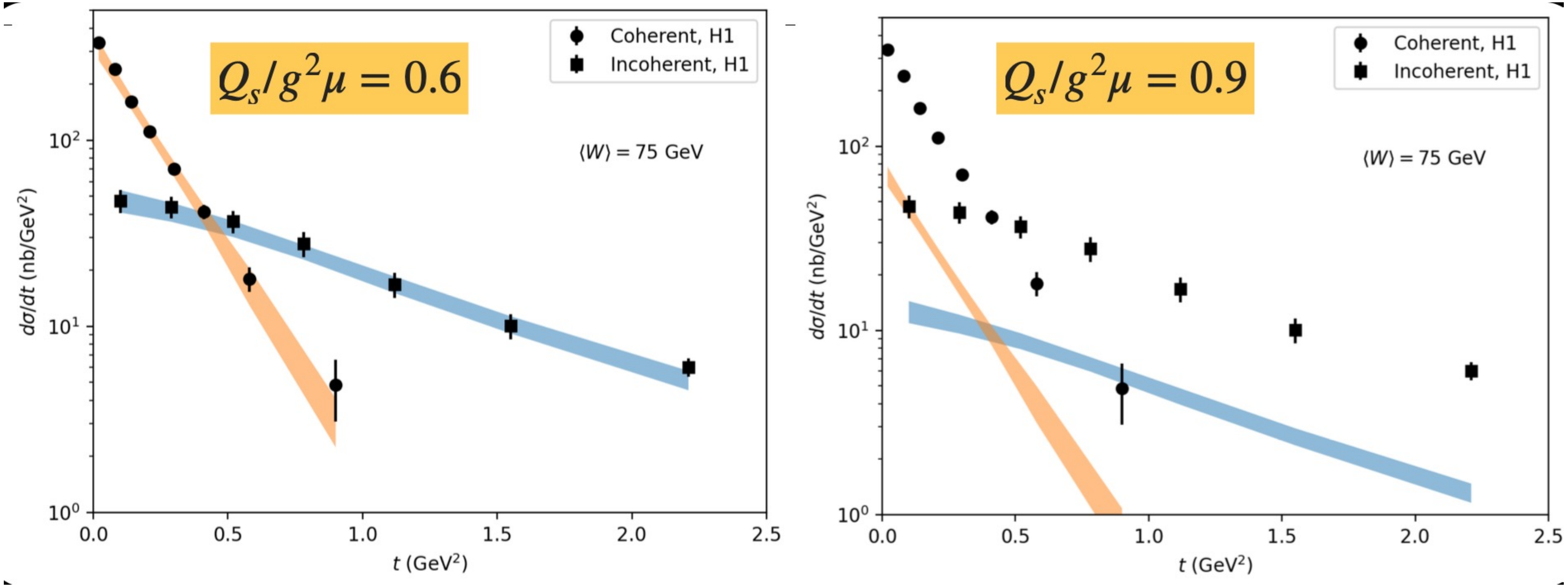

- A large $Q_s/g^2\mu$ ratio gives small color charge density, which reduces the magnitudes of both coherent and incoherent cross-sections.

H.Mantysaari, B.Schenke, C. Shen and W. Zhao, Phys. Lett. B 833 (2022), 137348.

Building intuition for the model parameters

- Hot spot density fluctuations:

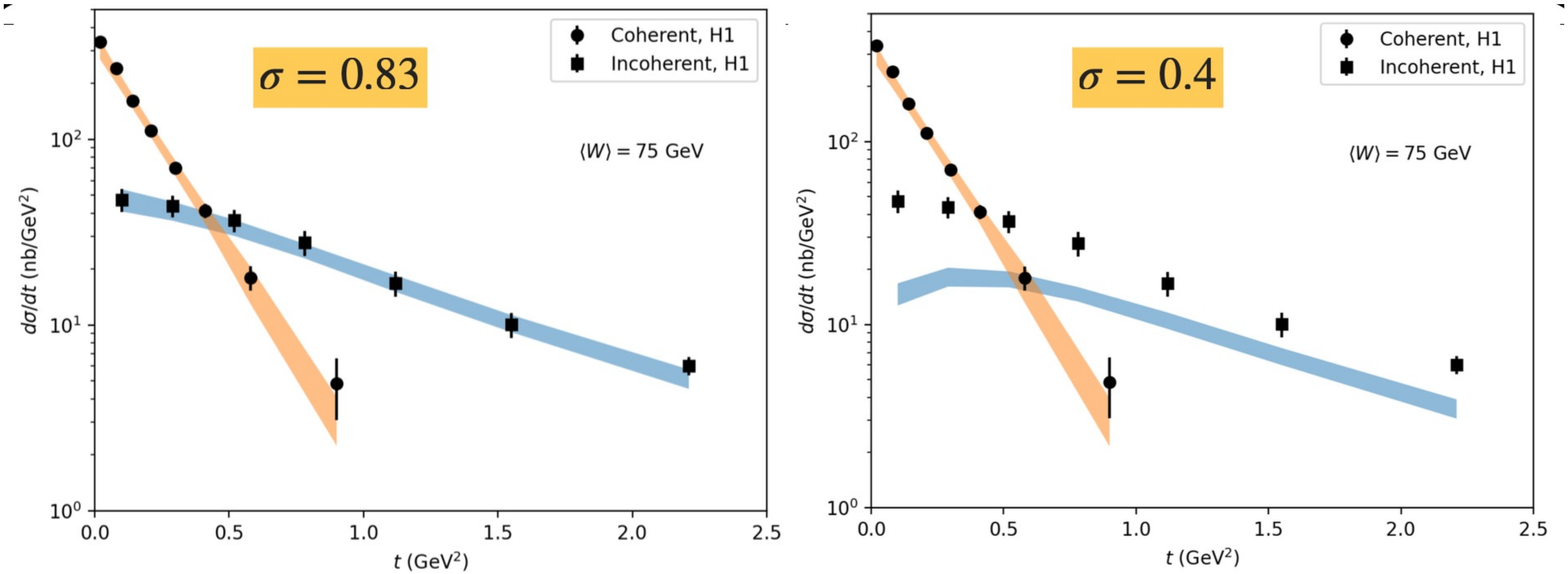

- A small variance of the density fluctuations reduces the magnitude of incoherent cross-section

H.Mantysaari, B.Schenke, C. Shen and W. Zhao, Phys. Lett. B 833 (2022), 137348.

Building intuition for the model parameters

- Number of hot spots:

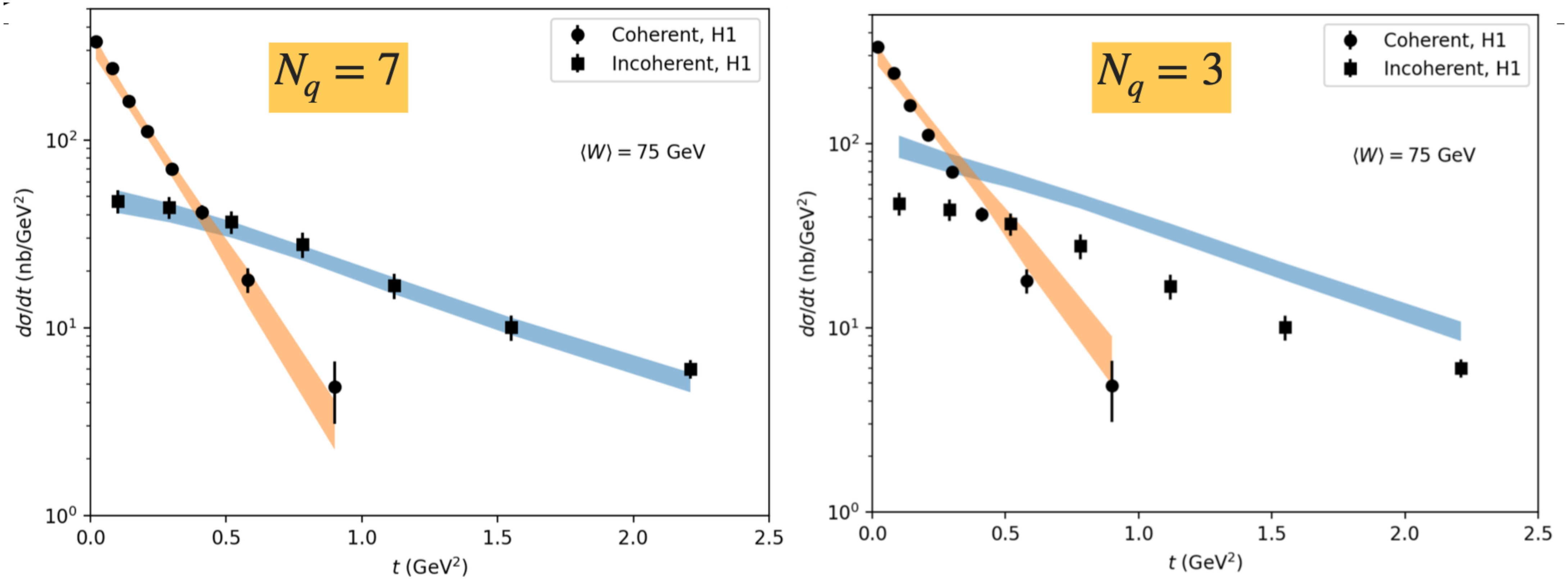

- Small number of hot spots increases fluctuations, which results in large incoherent cross-sections

H.Mantysaari, B.Schenke, C. Shen and W. Zhao, Phys. Lett. B 833 (2022), 137348.

Building intuition for the model parameters

- Minimum distance between hot spots

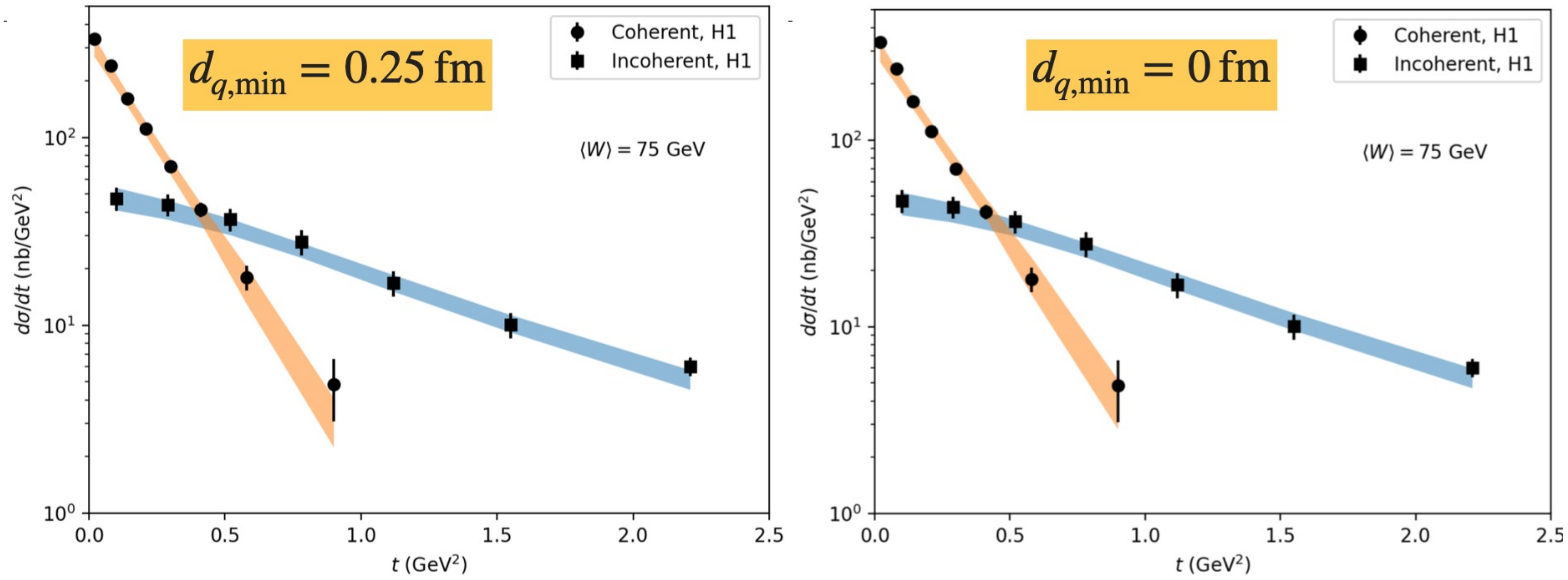

- No clear sensitivity on the intra distance between hot spots.

H.Mantysaari, B.Schenke, C. Shen and W. Zhao, Phys. Lett. B 833 (2022), 137348.

JIMWLK

The JIMWLK equations are determined by going to next-to-leading order (computing loop diagrams) and resumming large logarithms that appear

$$\sim \alpha_s \ln \frac{\text{separation scale}}{\text{observation scale}} \sim \alpha_s \ln \frac{x_0}{x_1} = \mathcal{O}(1)$$ (contribute at leading order; need to be resummed)

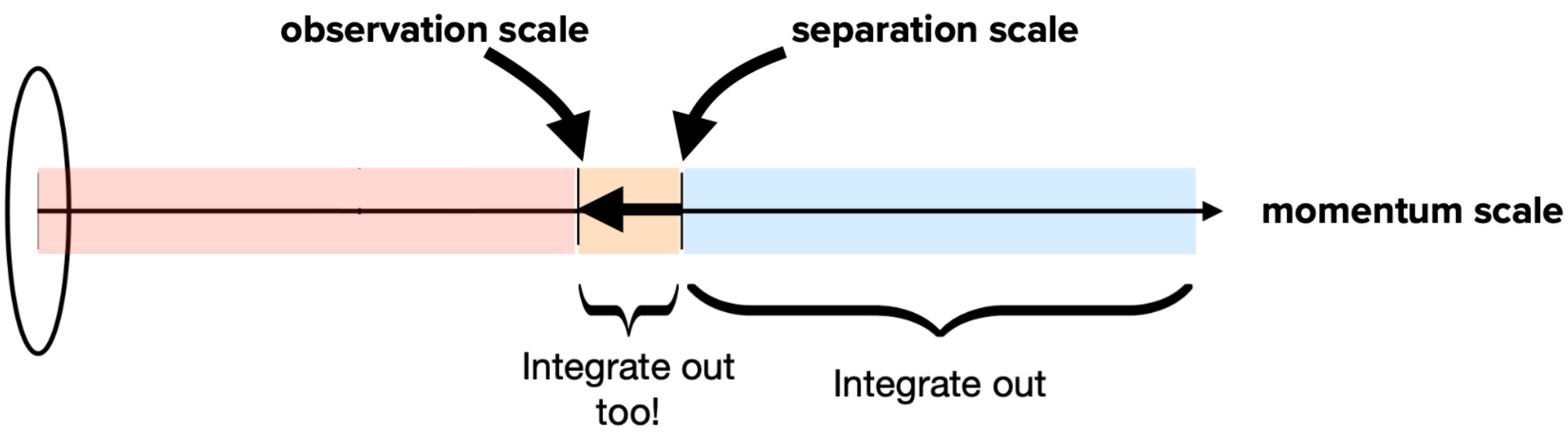

Leading logarithms can be absorbed into redefinition of $W_{x_0}[\rho] \to W_{x_1}[\rho]$

40

H.Mäntysaari, B.Schenke PRD, 98, 034013.

JIMWLK

$$V_{ij}(\vec{x}_T) = \mathscr{P}\left(ig \int_{-\infty}^{\infty} A^{+,c}(z^-, \vec{x}_T)\, t^c_{ij}\, dz^- \right)$$

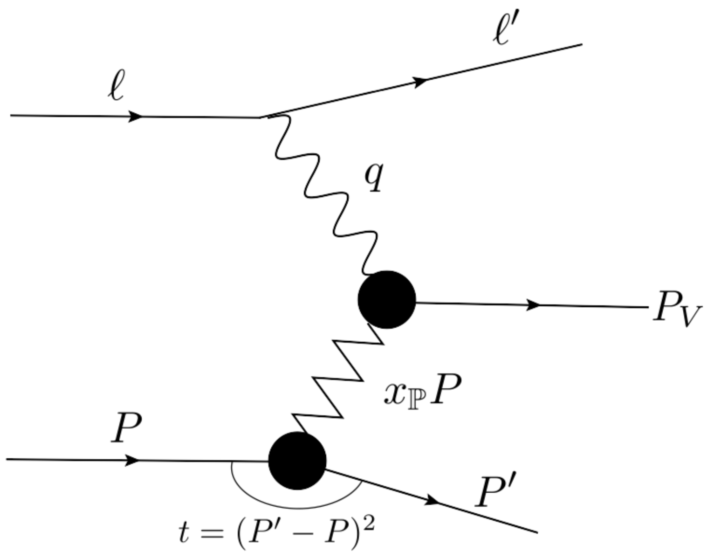

Evolve the Wilson lines according to the Langevin equation

$$\frac{\mathrm{d}}{\mathrm{d}y} V_{\mathbf{x}} = V_{\mathbf{x}}(it^a)\left[\int \mathrm{d}^2\mathbf{z}\, \varepsilon^{ab,i}_{\mathbf{x},\mathbf{z}} \xi_{\mathbf{z}}(y)^b_i + \sigma^a_{\mathbf{x}}\right].$$

The deterministic drift term is

$$\sigma^a_{\mathbf{x}} = -i\frac{\alpha_s}{2\pi^2}\int \mathrm{d}^2\mathbf{z} S_{\mathbf{x}-\mathbf{z}} \mathrm{Tr}[T^a U^\dagger_{\mathbf{x}} U_{\mathbf{z}}], \quad S_{\mathbf{x}} = 1/\mathbf{x}^2$$

The random noise is Gaussian and local in coordinates, color, and rapidity with expectation value zero and

$$\langle \xi^a_{\mathbf{x},i}(y)\xi^b_{\mathbf{y},j}(y')\rangle = \delta^{ab}\delta^{ij}\delta^{(2)}_{\mathbf{xy}}\delta(y-y').$$

The coefficient of the noise in the stochastic term is

$$\varepsilon^{ab,i}_{\mathbf{x},\mathbf{z}} = \left(\frac{\alpha_s}{\pi}\right)^{1/2} K^i_{\mathbf{x}-\mathbf{z}}[1 - U^\dagger_{\mathbf{x}} U_{\mathbf{z}}]^{ab}, \qquad K^i_{\mathbf{x}} = \frac{x^i}{\mathbf{x}^2}.$$

H.Mantysaari, B.Schenke PRD, 98, 034013.

JIMWLK

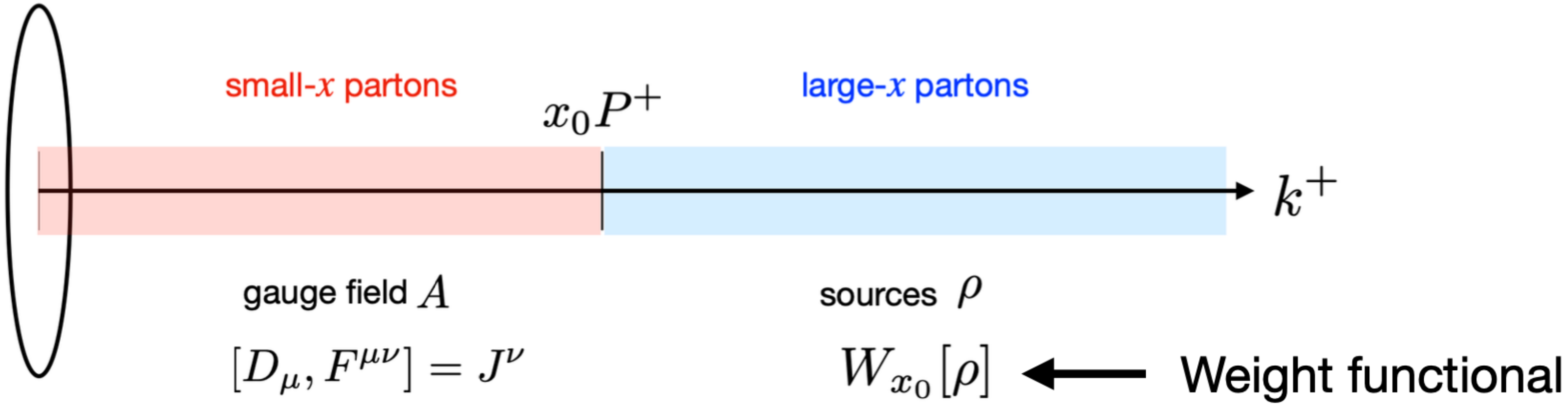

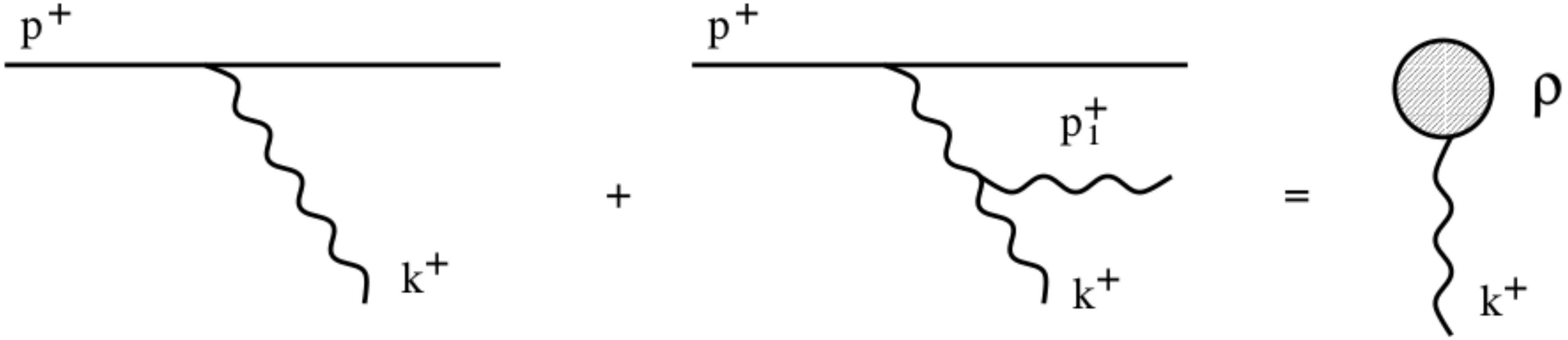

$$\frac{\partial W_\tau[\alpha]}{\partial \tau} = \frac{1}{2}\int_{\boldsymbol{x},\boldsymbol{y}} \frac{\delta^2}{\delta\alpha_\tau^a(\boldsymbol{x})\delta\alpha_\tau^b(\boldsymbol{y})}\left[W_\tau \chi_{xy}^{ab}\right] - \int_{\boldsymbol{x}} \frac{\delta}{\delta\alpha_\tau^a(\boldsymbol{x})}\left[W_\tau \sigma_x^a\right],$$

Wilson lines

$$V_{ij}(\vec{x}_T) = \mathcal{P}\left(ig \int_{-\infty}^{\infty} A^{+,c}(z^-, \vec{x}_T)\, t^c_{ij}\, dz^- \right)$$

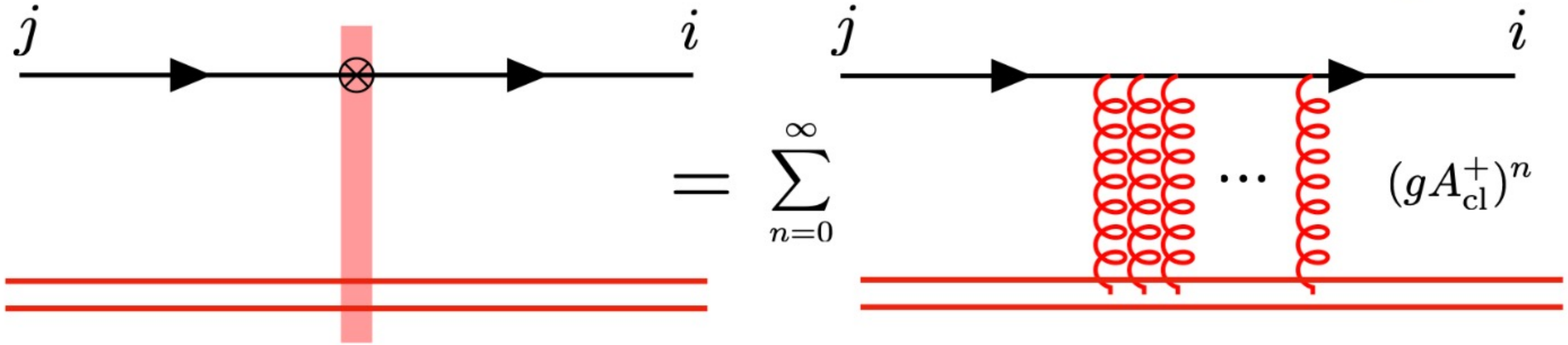

MULTIPLE INTERACTIONS NEED TO BE RESUMMED, BECAUSE $A^+ \sim 1/g$

Universality: from proton-nucleus to electron-nucleus

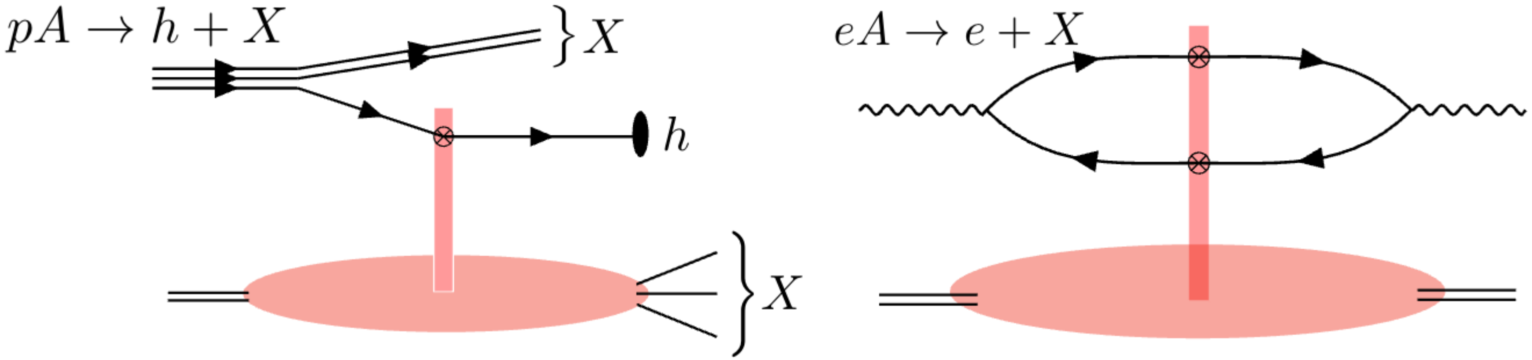

Both processes depend on the "dipole" $S(\boldsymbol{x}_\perp, \boldsymbol{y}_\perp) = \langle \mathrm{Tr}[V(\boldsymbol{x}_\perp) V^\dagger(\boldsymbol{y}_\perp)] \rangle$

Jalilian-Marian, Gelis (PRD 2003)

Wilson lines

Interaction of high energy color-charged particle with a classical field of a nucleus can be described in the eikonal approximation:

The scattering rotates the color, but keeps longitudinal momentum, transverse position, and any other quantum numbers the same

MULTIPLE INTERACTIONS NEEDED TO BE RESUMMED, BECAUSE GLUON FIELDS ARE HIGHLY OCCUPIED

$A \sim 1/g$

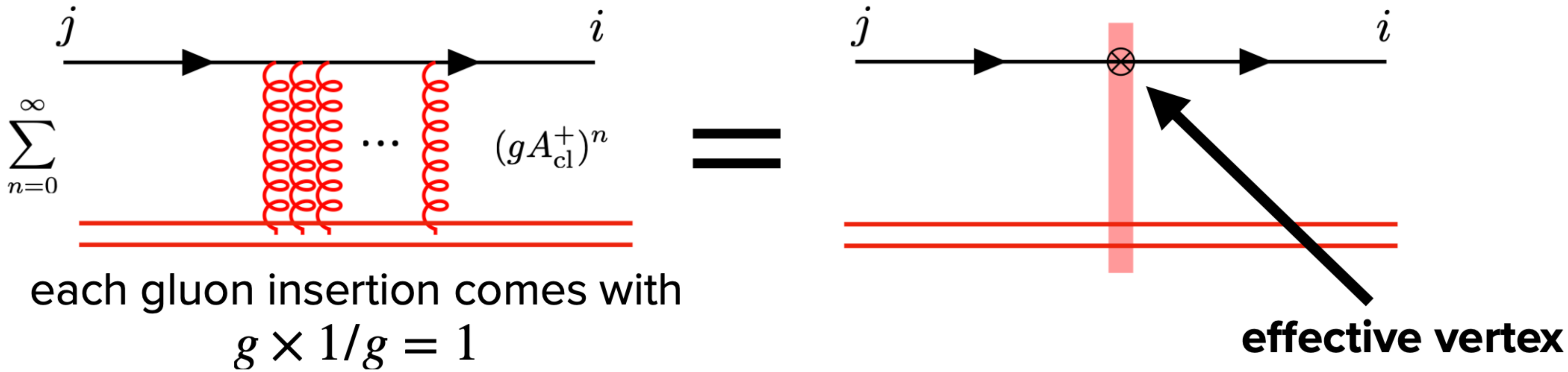

each gluon insertion comes with

$g \times 1/g = 1$

The effective vertex is expressed by a *Wilson line* V:

The resummed multiple interaction with the gluon fields of the target

Wilson lines

$$\mathcal{A}^{\gamma^* p \to Vp} \sim \int \mathrm{d}^2 b \mathrm{d}z \mathrm{d}^2 r \Psi^{\gamma^*} \Psi^{V}(r, z, Q^2) \mathbf{e}^{-i\mathbf{b}\cdot\boldsymbol{\Delta}} N(r, x, b)$$

$$N_\Omega(\mathbf{r}_\perp, \mathbf{b}_\perp, x_\mathbb{P}) = 1 - \frac{1}{N_c} \mathrm{tr}\left[V\left(\mathbf{b}_\perp + \frac{\mathbf{r}_\perp}{2}\right) V^\dagger\left(\mathbf{b}_\perp - \frac{\mathbf{r}_\perp}{2}\right)\right].$$

$$V(\mathbf{x}_\perp) = \mathrm{P}_- \left\{\exp\left(-ig \int_{-\infty}^{\infty} \mathrm{d}z^- \frac{\rho^a(x^-, \mathbf{x}_\perp) t^a}{\boldsymbol{\nabla}^2 - m^2}\right)\right\}$$

$$g^2 \langle \rho^a(x^-, \mathbf{x}_\perp) \rho^b(y^-, \mathbf{y}_\perp)\rangle = g^4 \lambda_A(x^-) \delta^{ab} \times \delta^{(2)}(\mathbf{x}_\perp - \mathbf{y}_\perp) \delta(x^- - y^-).$$

From the dipole amplitude $\mathcal{N}(x, \mathbf{r}_\perp, \mathbf{b}_\perp) = (d\sigma^p_{\mathrm{dip}}/d^2\mathbf{b}_\perp)(x, \mathbf{r}_\perp, \mathbf{b}_\perp)/2$ given by Eq. (1), we can extract a saturation scale $Q_s(x)$ by using the definition that $Q_s^2 = 2/R_s^2$, with R_s defined via $\mathcal{N}(x, R_s) = 1 - \exp(-1/2)$. Note that $\mathcal{N}$ and Q_s also depend on the thickness function T_A

$$\mu^2 = \int \mathrm{d}x^- \lambda_A(x^-), \qquad \frac{Q_s(\mathbf{x}_\perp)}{g^2\mu},$$ is a free parameter

B. Schenke, C. Shen and P. Tribedy, Phys. Rev. C 102 (2020) no.4, 044905.
H.Mantysaari, B.Schenke, C. Shen and **W. Zhao**, Phys. Lett. B 833 (2022), 137348.

Universal Wilson lines

We use one framework to
compute Wilson lines
for a nucleus at a given energy.

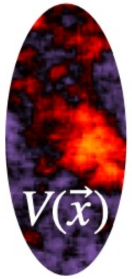

This allows to directly constrain
parameters (like hot spot sizes)
using one process (e.g. in e+A or e+p)
and employ the model for another
(e.g. in A+A or p+A)

e+A or UPC

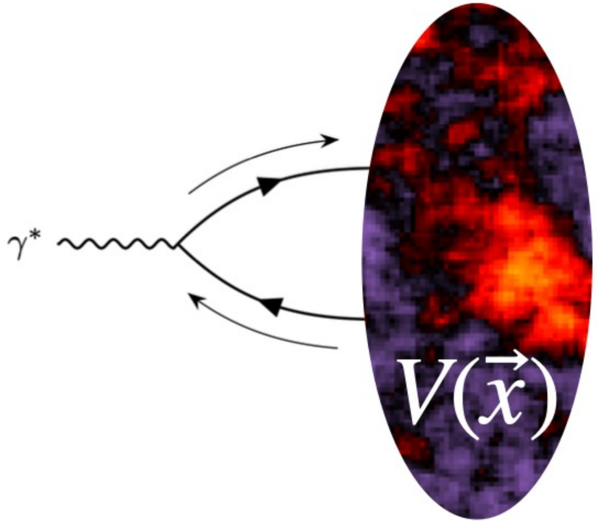

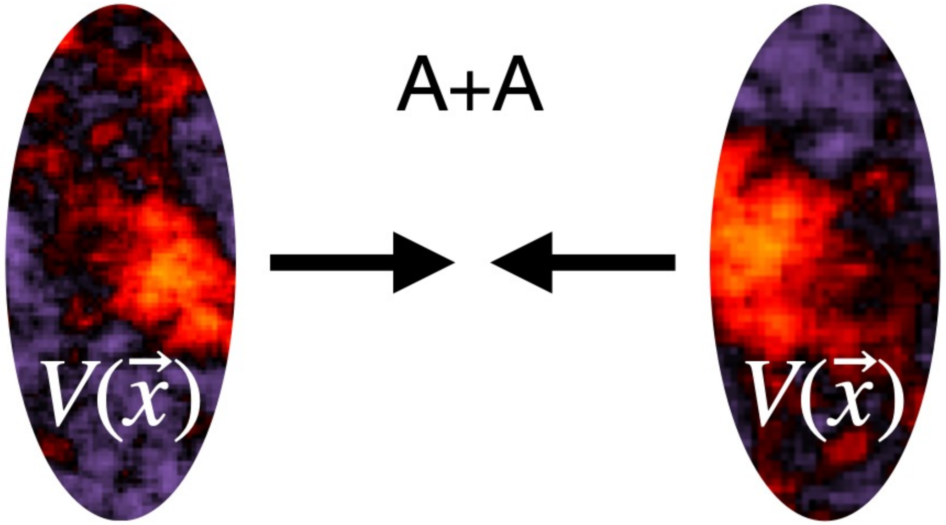

From Bjorn's slide

Color Glass Condensate (CGC): Sources and fields

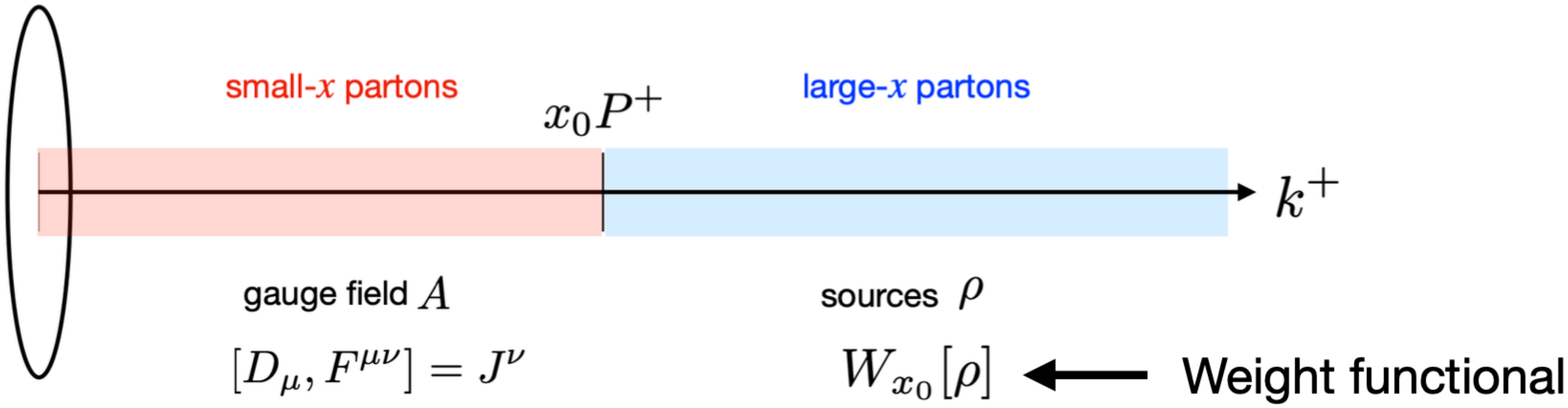

Two steps to compute expectation value of an observable $\mathcal{O}$:

1) Compute quantum expectation value $\mathcal{O}[\rho] = \langle \mathcal{O} \rangle_\rho$ for sources drawn from a given $W_{x_o}[\rho]$

2) Average over all possible configurations given the appropriate gauge invariant weight functional $W_{x_o}[\rho]$ (e.g. from McLerran Venugopalan model)

When $x \lesssim x_0$ the path integral $\langle \mathcal{O} \rangle_\rho$ is dominated by classical solution and we are done

For smaller x we need to do quantum evolution

4

From Bjorn's slide

Wave functions

Forward photon wave functions (QED)

$$\Psi_{h\bar{h},\lambda=0}(r,z,Q) = e_f e \sqrt{N_c}\,\delta_{h,-\bar{h}}\,2Qz(1-z)\,\frac{K_0(\epsilon r)}{2\pi},$$

$$\Psi_{h\bar{h},\lambda=\pm1}(r,z,Q) = \pm e_f e \sqrt{2N_c}\,\{\mathrm{i}e^{\pm \mathrm{i}\theta_r}[z\delta_{h,\pm}\delta_{\bar{h},\mp} - (1-z)\delta_{h,\mp}\delta_{\bar{h},\pm}]\partial_r + m_f\delta_{h,\pm}\delta_{\bar{h},\pm}\}\,\frac{K_0(\epsilon r)}{2\pi},$$

Vector meson: Boosted Gaussian (Non-perturbative)

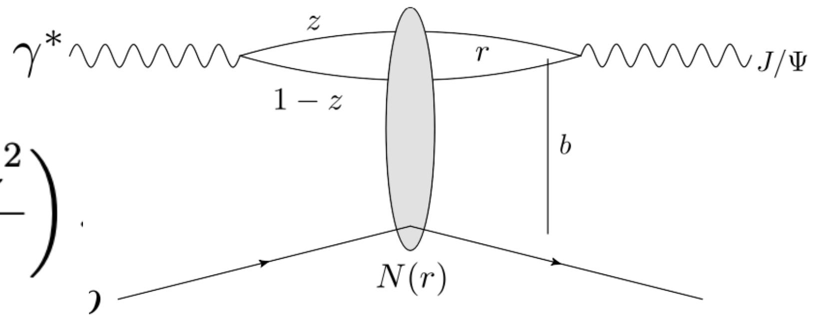

$$\phi_{T,L}(r,z) = \mathcal{N}_{T,L}\,z(1-z)\exp\left(-\frac{m_f^2\mathcal{R}^2}{8z(1-z)} - \frac{2z(1-z)r^2}{\mathcal{R}^2} + \frac{m_f^2\mathcal{R}^2}{2}\right).$$

Meson	M_V/GeV	f_V	m_f/GeV	$\mathcal{N}_T$	$\mathcal{N}_L$	$\mathcal{R}^2$/GeV^{-2}	$f_{V,T}$
J/ψ	3.097	0.274	1.4	0.578	0.575	2.3	0.307
ϕ	1.019	0.076	0.14	0.919	0.825	11.2	0.075
ρ	0.776	0.156	0.14	0.911	0.853	12.9	0.182

H. Kowalski, L. Motyka and G. Watt, Phys. Rev. D 74 (2006), 074016.

Different vector meson's wave functions

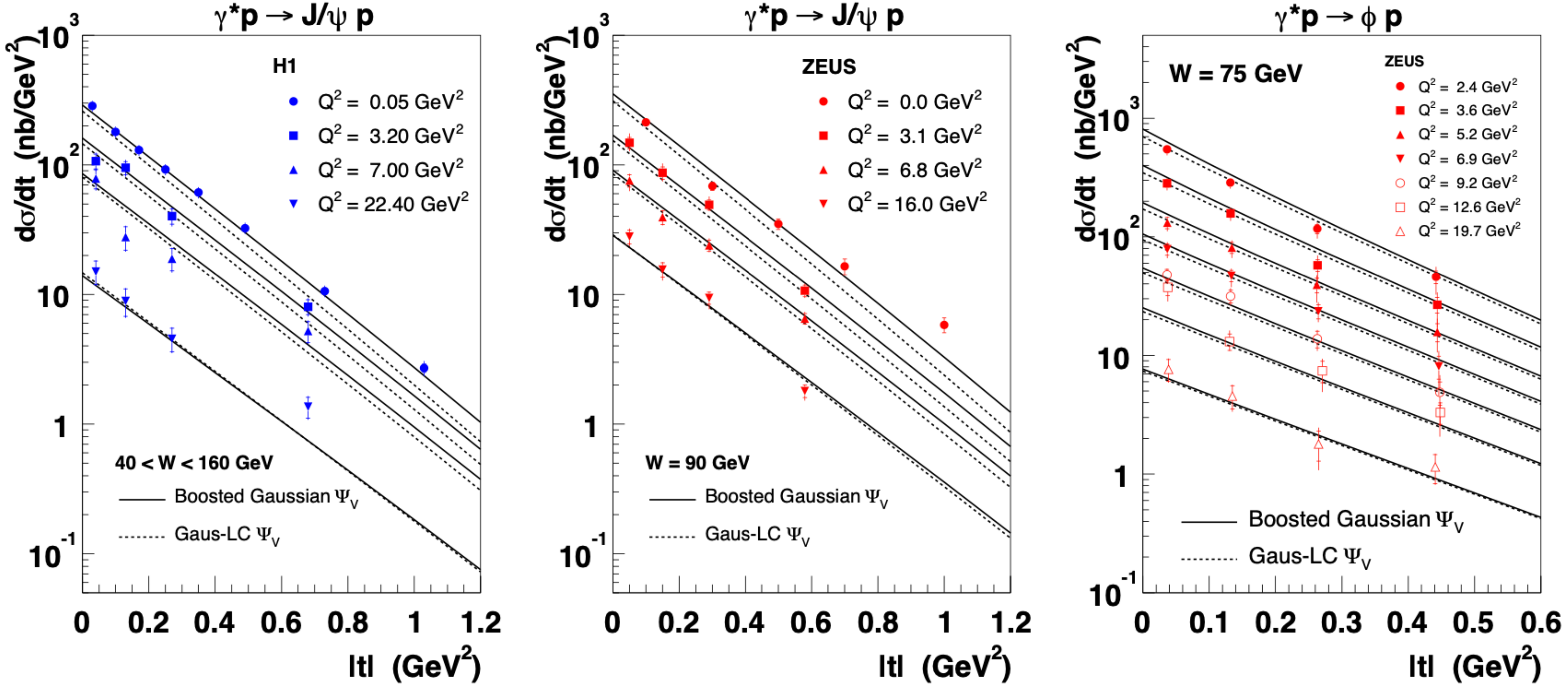

H. Kowalski, L. Motyka and G. Watt, Phys. Rev. D 74, (2006), 074016.

Virtuality dependent PDF

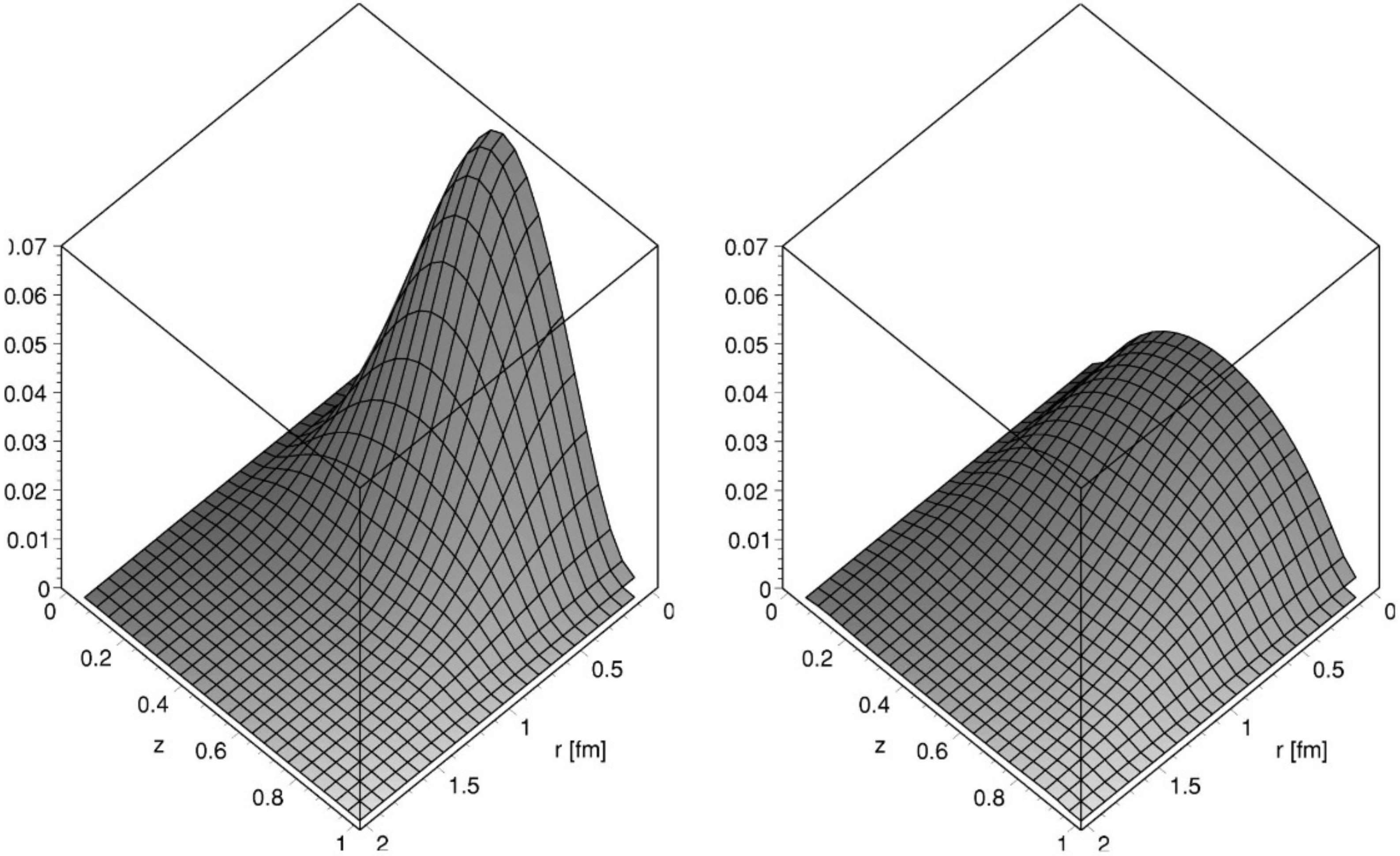

FIG. 6. The ρ wave functions $|\Psi^L|^2$ (left) and $|\Psi^T|^2$ (right) in the boosted Gaussian model with the quark mass used in the FKS dipole model.

J. R. Forshaw, R. Sandapen and G. Shaw, Phys. Rev. D 69, 094013 (2004).